Journal of Shellfish Research, Vol. 41, No. 1, 1–59, 2022.

SEASONAL CHANGES IN SHELL MICROSTRUCTURE OF SOME COMMON BIVALVE MOLLUSCS IN THE MID-ATLANTIC REGION

LOWELL W. FRITZ,[1]* LISA M. CALVO,[1] LISA WARGO[1] AND RICHARD A. LUTZ[2]

[1]*Haskin Shellfish Research Laboratory, Rutgers University, 6959 Miller Avenue, Port Norris, NJ 08349;* [2]*Department of Marine and Coastal Sciences, Rutgers University, 71 Dudley Road, New Brunswick, NJ 08901*

ABSTRACT Bivalve molluscs record histories of individual growth as alternating periods of activity (shell deposition) and inactivity (growth cessation marks) within their multilayered shells, and in some species, as alternating sublayers with different morphology. Shell growth patterns reflect tidal, daily, and seasonal cycles of key environmental parameters, such as submergence and temperature, which influence physiology (e.g., feeding, respiration, metabolic rates, and reproductive cycles). Knowledge of the periodicity of formation of various structures within the shell enables researchers to place a calendar across the growth history of an animal knowing only the date of collection. In turn, this enables both the determination of age (essential in studies of population dynamics) and the assessment of how bivalve populations responded to known environmental events, be they anthropogenic or natural, after the event has occurred. Seasonal microstructural shell growth patterns of six common bivalve species living in fresh (*Corbicula fluminea* O. F. Müller, 1774), brackish (*Rangia cuneata* G. B. Sowerby I, 1832), lower estuarine (*Geukensia demissa* Dillwyn, 1817), coastal (*Mytilus edulis* Linnaeus, 1758 and *Mya arenaria* Linnaeus, 1758), and continental shelf (*Spisula solidissima* Dillwyn, 1817) habitats in the mid-Atlantic region of the United States are documented using optical and scanning electron microscopy based on collections in the late 1980s. Some of the works have been published previously, but the results for each of the six species are combined and summarized in one volume as a guide to the seasonal shell microstructure for some common bivalves in New Jersey waters. The utility of shell growth pattern analysis in environmental impact assessments and population dynamics studies is evaluated within each habitat and example applications are provided. Although the results reported here were from studies conducted over 30 y ago, they represent collectively a contribution to our knowledge of molluscan shell microstructure that remain relevant today and are published as a coherent monograph before they are lost as so many other important unpublished works have been as time ran out on aging authors before they could relay the precious secrets they uncovered over the years.

KEY WORDS: bivalve, shell, microstructure, environmental assessment, population dynamics

INTRODUCTION

Studies of environmental stress in aquatic and marine environments are frequently based on expensive faunal surveys, bioassay work, or a combination of approaches. Such a research program can be instructive, but may be compromised if baseline data are not available. Shells of bivalve molluscs contain a wealth of information about present and past environments stored as structural and morphological changes in the organism's exoskeleton (for an extensive review, see Rhoads & Lutz 1980). Research into these relationships in the past has been largely for the purpose of reconstructing paleoenvironments (Barker 1964, Berry & Barker 1968, 1975, Pannella et al. 1968, Rhoads & Pannella 1970, Koike 1975, Pannella 1975, 1976, Clark 1979). The implications of this approach for ecological work, and specifically for fisheries and population dynamics studies, has interested many neontologists (Saloman & Taylor 1969, Farrow 1971, Evans 1972, Lutz 1977, Gordon & Carriker 1978, Jones et al. 1978, Lutz & Rhoads 1978, 1980, Lutz & Castagna 1980, Jones 1981, Fritz & Haven 1983).

Ecologists are frequently concerned with reconstructing the impacts of environmental events, such as major storms, salinity fluctuations, temperature changes, or pollutant discharges on organisms after the event has occurred. In the absence of information on predisturbance rates of growth, reproduction, and mortality, the ecologist, like the paleoecologist, is confronted with the problem of after-the-fact data acquisition.

Several studies have shown the usefulness of shell growth analytical techniques for the reconstruction of environmental events. Kennish and Olsson (1975) provided one of the first illustrations of this in studies of microstructural shell growth of hard clams, *Mercenaria mercenaria* (Linnaeus, 1758), exposed to thermal discharges from a nuclear power plant. Crossed-lamellar microstructure (Carter 1980) replaced prisms in the outer shell layer of this species throughout the duration of the high-temperature stress period. The pattern or relative spacing of these growth disruption marks within known periods of shell deposition provided evidence for periodic microgrowth increment formation within the outer shell layer that permitted relatively accurate determination of the dates of mark formation. From the standpoint of environmental monitoring, this finding had profound implications, because it showed that the time of formation of specific regions of the shell could be accurately determined, almost to the point of overlaying a calendar across the outer shell layer.

Fritz (1982) and Fritz and Haven (1983) documented the annual formation of translucent and opaque bands in the middle homogenous layer of *Mercenaria mercenaria* shells and daily formation of microgrowth increments in the outer prismatic shell layer of this species. From the analysis of shells from a 13-y growth monitoring experiment, it was found that the decrease in salinity in the York and James Rivers (Virginia, USA) in the summer of 1972 caused by large amounts of rain from tropical storm Agnes decreased (1) the annual increment

*Corresponding author. E-mail: lowellfritz@yahoo.com
DOI: 10.2983/035.041.0101

of shell deposited in 1972; (2) the number of microgrowth increments deposited in that year; and (3) the average microgrowth increment width. Consequently, the decline in growth rate in 1972 was a result of not only decreased daily growth rate, but also from fewer days of growth.

Fritz and Lutz (1986) documented the natural shell growth patterns of *Corbicula fluminea* (O. F. Müller, 1774) and how both natural and anthropogenic perturbations were reflected in its shell structure. A rainfall event of 10 cm in the upper watershed of the Raritan River increased flow rates over 50-fold in a 24-h span. This was reflected in shell microstructure as a distinct growth cessation mark (gcm) in all 1-y-old specimens analyzed. Also, clams exposed to the combined effluents of an organic chemical plant and a sewage treatment plant grew at significantly slower rates than those at control locations. The decrease in growth rate was observed in 6-mo growth experiments and would not have been discernable through serial length measurements. Thus, the quality of growth information recorded in molluscan shells permitted the documentation of the effects of sublethal alterations in water quality that would not have been possible by traditional means.

Two examples of after-the-fact data acquisition using shell growth pattern analyses are described by MacDonald and Thomas (1982) and Fritz (1984). In the former study, annual growth rates of *Mya arenaria* (Linnaeus, 1758) were determined from three samples; the first taken in an area shortly after a large oil spill in 1970, the second in the same area but 9 y later, and the third in a control area with a long-term growth record for this species. Growth rates of clams in the control area in 1970 and 1979 were not significantly different from growth rates of clams in the impacted area in 1970. It was found, however, that persistent changes in the environment caused by the spill significantly reduced the growth rates of clams in the impacted area between 1971 and 1979. All information on clam growth rates obtained during this study were back-calculated using the annual growth patterns observed in shell microstructure of clams collected after the spill occurred. A similar study was also conducted using shells of *Spisula solidissima* (Dillwyn, 1817) that were living at two locations, one that was directly affected by an ocean outfall from an organic chemical plant and another (control) that was not (Fritz 1984). Growth rates of surf clams near the outfall were significantly lower than those at the control site during three consecutive years.

In this monograph, analyses conducted to define and assess the utility of structural and morphological patterns within the bivalve shell in sublethal environmental impact assessments are summarized. The primary objective was to identify a suite of organisms in freshwater, brackish, and marine habitats that were common and had regular shell growth patterns that would be suitable for such studies. Furthermore, because of differences in the growth rate and longevity among species as well as rates of environmental change in their habitats, the suite of species was chosen so that a range of time scales (from daily cycles to multiyear records) was represented in their shell growth patterns. For instance, rates of environmental change on the continental shelf are much slower and have smaller amplitudes than those in lakes, rivers, or shallow coastal bays. The rate at which information is recorded in the shells of each species reflects both the species' life history and ambient rates of environmental change.

MATERIALS AND METHODS

Six bivalve species were collected throughout the year in New Jersey and Delaware from freshwater (the Maurice and Delaware Rivers, and Union Lake), brackish (lower Delaware River), lower estuarine (lower Delaware Bay), oceanic coastal (Atlantic coast from Newark to Great Bay), and continental shelf habitats. The six species were golden clams (*Corbicula fluminea*) from freshwaters; wedge clams (*Rangia cuneata* G. B. Sowerby I, 1832) from brackish waters; epifaunal ribbed (*Geukensia demissa* Dillwyn, 1817); blue mussels (*Mytilus edulis* Linnaeus, 1758) from lower estuarine and oceanic coastal habitats; infaunal softshell clams (*Mya arenaria*) from the oceanic coast; and surf clams (*Spisula solidissima*) from the continental shelf (Fig. 1).

Golden clams were collected by hand from three freshwater locations, two within the Union Lake-Maurice River system and one in the Delaware River. The Union Lake collection site was on the upper eastern shore near where the Maurice River enters the lake in Millville, NJ (39° 25′46″ N, 75° 03′47″ W). Clams were common near the shore in 1–2 feet of water in sandy, silty areas and less common in the rhizome mats of aquatic vegetation. There was a small downlake current at this location and water flow was primarily wind-driven. In the Maurice River, *Corbicula* were collected in the riffle area on the eastern bank at the base of the Union Lake dam in Millville, NJ (39° 24′04″ N, 75° 03′13″ W). Clams were located in the rock/shell rubble in the lee of large boulders. Water flow at this site was generally vigorous in winter and spring, and moderate to vigorous (depending on recent precipitation) in summer and fall. The site is also within reach of spring high tides in the Maurice River, but at no time was a salinity >0.02‰ measured. The Delaware River site was located near Scudder's Falls, NJ (40° 15′56″ N, 74° 50′56″ W). Clams were collected in the riffle area near the downstream end of a small island located about 20 yards offshore. Flow was always vigorous at this site, but water depth varied from 6 to 12 inches in summer and fall to approximately 3 feet in winter and spring with proportional increases in flow.

Wedge clams were collected by hand and with a clam rake from the Delaware River south of Newcastle, DE (39° 39′00″ N, 75° 36′08″ W). Wedge clams were located in approximately 3–4 feet of water at low tide in muddy-sand offshore from submerged rhizome-peat mats. Salinities at this location ranged from 0.2‰ in winter and spring to 5.5‰ in fall.

Ribbed mussels were collected by hand at four intertidal sites: two lower estuarine locations in lower Delaware Bay and two along New Jersey's Atlantic coast. The Delaware Bay-Maurice River mouth site (39° 13′42″ N, 75° 02′12″ W) was located in Bivalve, NJ, 0.5 miles south of the Rutgers University Haskin Shellfish Research Laboratory. Mussels were attached to pilings and bulkheads on the riverside of a marina at approximately mean water level. Temperature and salinity were highly variable at this location and dependent on the amounts of insolation and recent precipitation. Monthly means of high-water salinity for the years 1975 to 1986 at the laboratory pier ranged between 12‰ and 22‰. At the Delaware Bay-Cape May site, ribbed mussels were collected off a rock jetty north of the western inlet

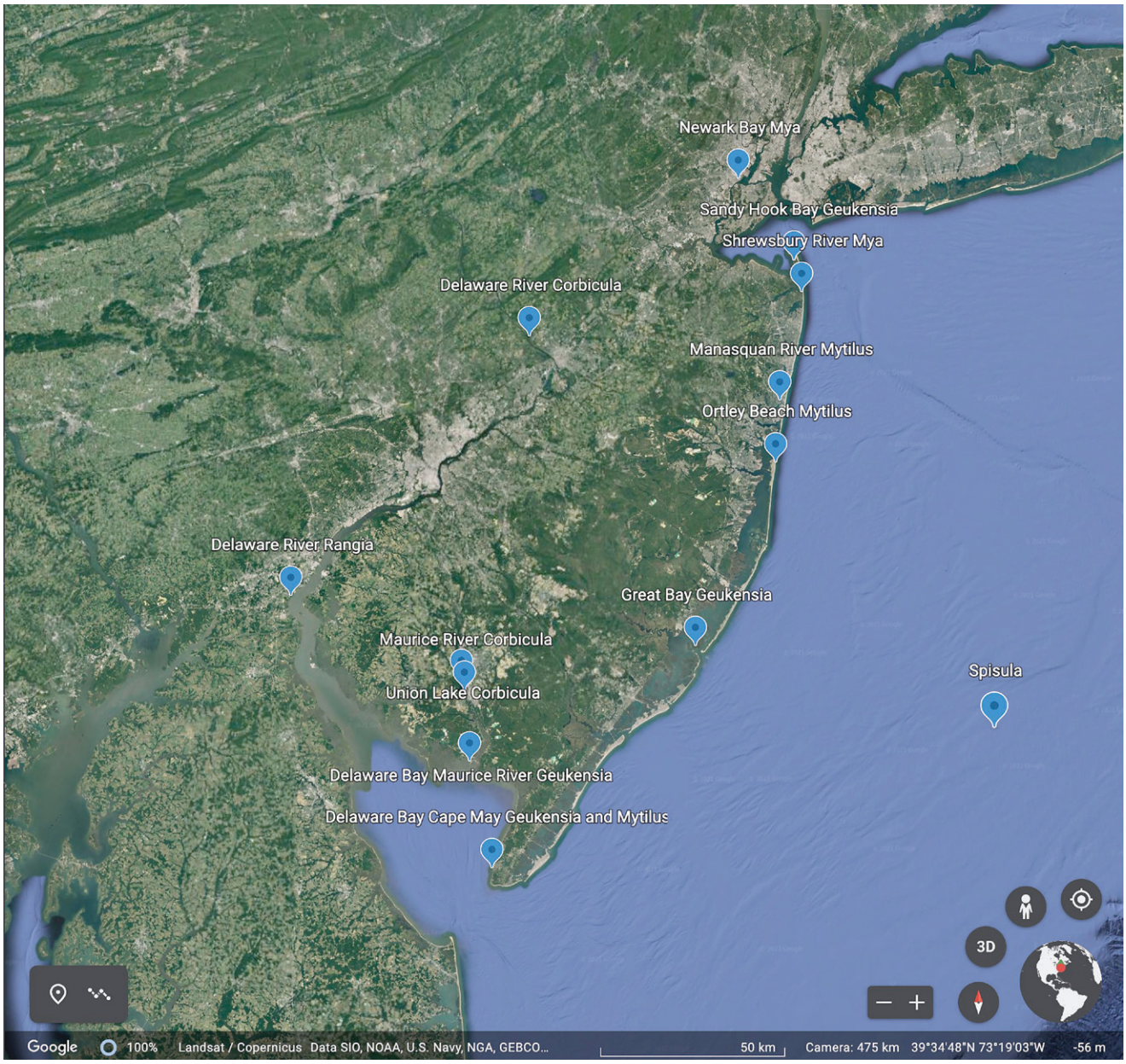

Figure 1. Sampling locations in New Jersey and Delaware of six bivalve species for analysis of shell microstructural growth. The Rutgers University Haskin Shellfish Research Laboratory is located in Bivalve, NJ, 0.5 mile from the Delaware Bay—Maurice River collection site for *Geukensia demissa*.

to the Cape May Canal at approximately 3 feet above mean low water (38° 58′05″ N, 74° 57′57″ W). The temperature regime at this site was similar to that at the Maurice River mouth site, but salinities were between 5‰ and 10‰ greater and monthly ranges were smaller. The Atlantic Coast-Sandy Hook Bay site (40° 27′03″ N, 73° 59′50″ W) was located at Horseshoe Cove in the Sandy Hook National Seashore, 3.8 miles north of the Atlantic Highlands bridge. Ribbed mussels were collected from the base of intertidal vegetation along the edge of a small tidal creek that drains a marsh. At the Atlantic Coast-Great Bay site, ribbed mussels were also collected from the base of intertidal plants along the edge of a tidal creek on the grounds of the Rutgers University Marine Field Station at Tuckerton, NJ (39° 30′35″ N, 74° 19′26″ W).

Blue mussels were collected at three locations, one lower estuarine intertidal site in lower Delaware Bay and two subtidal sites along the Atlantic coast. The Delaware Bay-Cape May blue mussel collection site was the same as that for ribbed mussels, and both species lived in the same intertidal zone. Along the Atlantic Coast, one site was located near the mouth of the Manasquan River in Brielle, NJ (40° 06′27″ N, 74° 03′00″ W). Mussels were collected by hand at low tide from the river bottom near the north end of the railroad bridge. This population was never observed exposed to the air at low tide, but during spring tides or with a strong westerly wind, they could have been. The second Atlantic Coast blue mussel collection site was located off Ortley Beach, NJ (39° 57′23″ N, 74° 03′55″ W), and consisted of a series of suspended subtidal

cages at various distances offshore from the end of the effluent discharge pipe from the Ciba-Geigy chemical plant in Toms River, NJ. The Ortley Beach mussels were part of a study of the effects of the plant effluent on growth of *Mytilus edulis* conducted by the New Jersey Department of Environmental Protection (Cooper et al. 1987). Ortley Beach mussels were originally collected on September 10, 1986, from an intertidal population on Cape Cod, MA, held in a flow-through seawater tank (receiving ambient Narragansett Bay water) for either 8 or 20 days and transferred to growth cages on September 18 and 30, 1986.

Softshell clams were collected from two locations along the Atlantic Coast. One was in Newark Bay in Elizabeth, NJ, on an intertidal mudflat near the offshore edge of a marsh in Marciante-Jackson-Millet Park. Clams were collected at low tide by hand using a shovel approximately 200 yards south of the park (40° 38′58″ N, 74° 10′36″ W). The second collection site was in the Shrewsbury River. Softshell clams were purchased from a seafood dealer who bought clams from fisherman in the area; specific collection locations are not known. Clams were kept refrigerated until received.

Surf clams were obtained from Snow Foods, Wildwood, NJ, from commercial catches on the continental shelf east of New Jersey; specific collection locations are not known. Clams were obtained within 2 days of the ship's return to port and were refrigerated until received.

Specimens of each species were collected from each location every 4–12 wk for approximately 1 y beginning in May 1985 through May 1989. The number of sampling dates at each site ranged from five to seven for all species except *Rangia cuneata* (12 sampling dates). The number of specimens collected per site and date ranged between 8 and 38 (mean = 19; total number collected and analyzed = 1,745). Clams and mussels were kept on ice in transit to the Haskin Shellfish Research Laboratory in Bivalve, NJ, where animals were sacrificed, usually within 4 h of collection, but occasionally the next day. Shell morphometric measurements were obtained, and shells were thoroughly cleaned, rinsed in fresh tap water, air-dried, and individually numbered. One of the two valves of each specimen collected was imbedded in liquid casting plastic for sectioning, whereas the remaining valves were kept intact or fractured for analysis.

Acetate peel replicas and thin shell sections were prepared according to the methods outlined in Stewart and Taylor (1965), Clark (1980), Kennish et al. (1980), and Fritz (1982). For an acetate peel, the imbedded valve was sectioned from the umbo to the ventral (or posterior) margin along the height axis using either a Buehler Isomet low-speed saw (for small specimens) or a Raytech 10-inch circular rock saw (for large specimens). One of the exposed cross-sectional surfaces was ground and polished smooth using 180, 400, and 600 grit carborundum papers sequentially on a lapidary wheel, and polished with 15, 9, and 6 μM diamond pastes on rotating cloth mats. Care was taken to avoid transfer of grit between polishing steps by ultrasonic cleaning. The polished surface was etched in 1% HCl (by volume) for between 20 and 60 sec (depending on the size of the shell), thoroughly rinsed in deionized water, and air-dried for at least 24 h. An acetate peel replica of the polished and etched surface was prepared by flooding the surface with acetone and carefully rolling a piece of acetate (0.005 inches thick) up the inclined surface, pushing a bead of acetone. This method reduces the amount of air trapped between the shell and acetate surfaces. Acetate sheets were allowed to dry for at least 1 h after which they were removed, labeled, trimmed, and sandwiched between two glass microscope slides or thick acetate sheets for analysis using light microscopy.

Thin shell sections were obtained only on those specimens 30 mm shell height and smaller. This was a limitation imposed by the specimen holder for the Buehler Isomet saw used to prepare thin shell sections. The imbedded and sectioned surface was ground flat with 400 or 600 grit carborundum paper and air-dried overnight. The sectioned sanded surface was affixed to a clean (with acetone) glass petrographic slide with quick set glass cement and allowed to dry overnight. The valve was resectioned parallel to the glass slide leaving a 500 μM thick section attached to the slide, which was then ground and polished until it was translucent and microgrowth patterns were visible under light microscopy (approximately 30–50 μM thick).

Fracture sections were prepared by the general methods outlined by Kennish et al. (1980). Unimbedded valves were fractured using gloved hands along the radial surface (or as close as possible to it). Shell fragments were glued to aluminum scanning electron microscopic stubs with cyanoacrylate cement and carbon paint, and coated with gold-palladium in a sputter coater. Specimens were analyzed at 15 and 20 kV accelerating voltages in a Hitachi S-450 scanning electron microscope (SEM).

To prepare polished and etched sections for analysis in the SEM, imbedded and sectioned shells were polished, etched in a 0.1 M EDTA solution for between ¾ and 1.5 min and air-dried. Sectioned shells were mounted on SEM stubs with cyanoacrylate cement and carbon paint, and coated with gold-palladium in a sputter coater.

Elemental analyses, using an energy dispersive X-ray spectrometer (EDS) at Yale University's Peabody Museum of Natural History, were conducted on *Corbicula* shells to determine the composition of crystals and associated organic pedestals found on specimens collected in September 1986. Preparation of *Corbicula* shells with attached mantle tissue was conducted to analyze the outer structure of the mantle and its connection to the shell near the umbo. Clams were relaxed in an Epsom salts (magnesium sulfate) solution and carefully opened so that the mantle and shell remained attached to each other. Mantle/shell preparations were fixed in 2% glutaraldehyde (in 0.05 M phosphate buffer) for 2 h, rinsed three times (10 min each) in 0.05 M phosphate buffer, postfixed in an air-tight container with (not in) 4% aqueous osmium (OsO_4 in 0.05 M phosphate buffer) for 1 h, rinsed three times (10 min each) in distilled water, and decalcified in 0.1 M EDTA for 2 wk (with repeated changes of EDTA). Preparations were dehydrated, critically-point dried, and sputter-coated with gold-palladium for SEM analysis.

Dry tissue weights (DTW) of *Rangia*, *Mytilus*, and *Mya* specimens were obtained by placing all tissue from each individual on labeled filter paper and drying in a 50°C oven until a constant weight was measured (between 1 and 4 days depending on the size of the specimen).

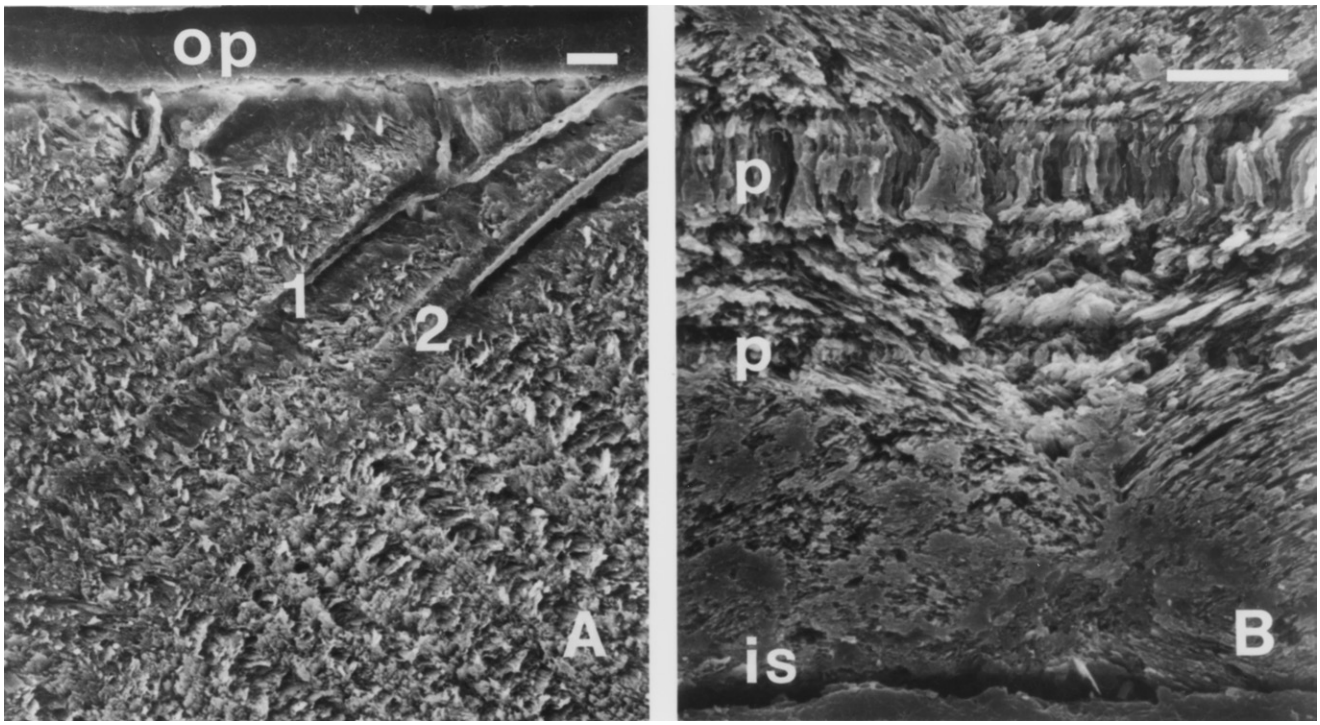

Figure 2. Scanning electron micrographs of a polished and etched radial shell section of *Corbicula fluminea* collected in September 1986 from Union Lake. Growth is to the right and outer shell surface is up. Scale bars = 10 μM. (A) Outer fine crossed-lamellar layer with organic periostracum (op) and two (labeled 1 and 2) prismatic bands formed in winter 1985 to 1986. (B) Inner complex crossed-lamellar layer with two prismatic bands (p). Inner shell surface (is) is at the bottom.

RESULTS AND DISCUSSION

Corbicula fluminea, the Golden Clam

The golden clam, *Corbicula fluminea*, was introduced accidentally into North America from southeast Asia in the early 1900s. The first record of a collection of *C. fluminea* on this continent was in Nanaimo, Vancouver Island, British Colombia, Canada, in 1924, and the species has spread quickly throughout the United States (Britton & Morton 1979, 1982). Along the Atlantic seaboard, the northernmost extent of its range is believed to be the Raritan River, NJ (Trama 1982).

The golden clam is well-adapted in both its reproductive and behavioral ecology to rapid colonization of freshwater lakes and rivers. The species is hermaphroditic (with self-fertilization possible) and also broods its fertilized eggs in specialized pouches within the gills (Britton & Morton 1982). After approximately 1 wk of development, the pediveliger larvae are released. Dispersal is facilitated by both active movements of the larvae and mucous nets extended from the exhalent siphon into the water column for downstream transport (Prezant & Chalermwat 1984).

The shell of *Corbicula fluminea* is composed of three aragonitic layers when viewed in radial section: (1) an outer fine crossed-lamellar layer; (2) a pallial myostracum (to which the mantle is attached) composed of small prisms; and (3) an inner complex crossed-lamellar (CCL) layer (Taylor et al. 1973, Counts & Prezant 1982, Prezant & Tan-Tiu 1985, Tan-Tiu 1987, Tan-Tiu & Prezant 1989; Fig. 2). The outer layer is composed of both first- and second-order lamellae, with the second-order lamellae organized as shingles on a roof within the first-order lamellae (Fig. 2A). The orientation of the second-order lamellae alternates at approximately 90 deg in adjacent first-order lamellae. The outer layer is also composed of microgrowth increments that represent alternating periods of shell deposition and growth cessation (Lutz & Rhoads 1977). In Raritan River populations, microgrowth increments were deposited at the rate of approximately one per day during the spring, summer, and fall and were used to determine the time of formation of gcm (Fritz & Lutz 1986). Long periods of little or no shell growth are reflected in outer layer microstructure by gcm, or bands with a prismatic microstructure, that may also have granular inclusions (Fig. 2A).

The inner layer is composed of a CCL microstructure, which when viewed in polished and etched radial section, appears as crisscrossing first- and second-order lamellae (Fig. 2B). The lamellae terminate on the inner shell surface in various patterns from tightly organized rosettes to a loose pattern of lamella tips. Within the inner layer, bands or horizons of prisms are frequently present that range in thickness from 1 to 10 μM. Prism bands, as well as the appearance of the inner surface of the inner shell layer, will be discussed further in relation to seasonal changes in its microstructure.

Seasonal Changes in Outer Layer Microstructure

The fine crossed-lamellar microstructure of the outer shell layer of *Corbicula fluminea* is elaborated into microgrowth increments that are visible in acetate peel replicas of polished and etched radial (Figs. 3 and 4) and in thin shell sections. At all three sites, a gcm was formed during the winter. This appeared in scanning electron micrographs of polished and etched

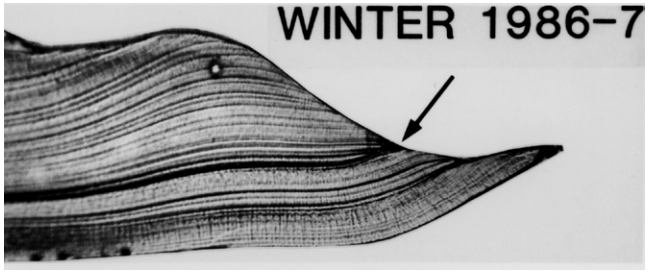

Figure 3. Light micrograph of an acetate peel replica of the polished and etched radial shell section of *Corbicula fluminea* collected in May 1987 from the Delaware River Ventral shell margin is at the right and horizontal field width = 4.85 mm.

sections as either a single, or more often, paired set of prismatic bands (Fig. 2A). In acetate peels, the winter gcm was also either a single or double dark line in outer layer microstructure (Figs. 3 and 4), in which, at 400× magnification, the prismatic structure was evident.

In spring (May through June) at all stations, microgrowth increment boundaries were generally poorly defined and far apart, suggesting relatively rapid shell growth. By summer (July through September), increment boundaries were generally easier to distinguish and closer together, suggesting that the shell growth rates during summer had slowed. This observation is supported by the work of Tan-Tiu (1987), who had studied the growth of *Corbicula fluminea* in the Leaf River, MS. During summer, growth appears to be frequently interrupted, and many gcm are formed in the outer layer microstructure (Fig. 4). This was evident at all sites, but more common at the Union Lake and Maurice River sites than at Scudder's Falls in the Delaware River. Preliminary observations of gonadal development and larval brooding in histological sections suggest that populations at all three sites were gravid during an extended period in summer, with each individual potentially having more than one brood of larvae per year. Thus, the discontinuous nature and slow shell growth rates of clams in summer may reflect: (1) energy diversion to both gonadal and larval development and (2) a decline in adult feeding rates during larval brooding in gill pouches.

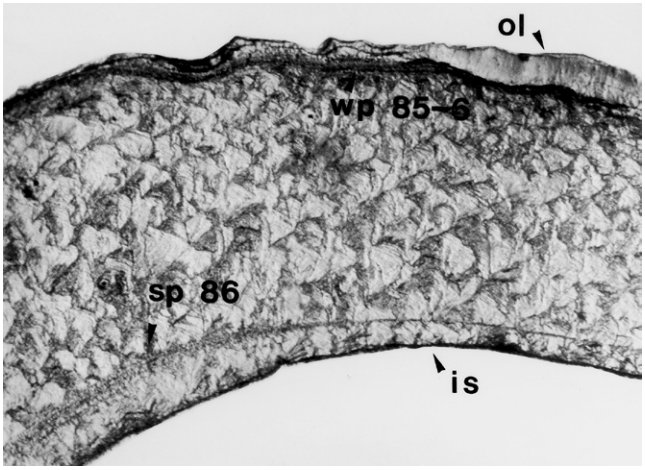

Figure 5. Light micrograph of an acetate peel replica of the polished and etched radial shell section of *Corbicula fluminea* collected in September 1986 from the Maurice River. Micrograph taken in the umbonal region; prismatic band in the inner shell layer formed during winter 1985 to 1986 (wp 85–6), and a series of prismatic bands in the inner shell layer formed during summer 1986 (sp 86) are shown. Growth is to the right; is = inner shell surface; ol = outer shell layer; HFW = 0.85 mm.

In fall (October through December), there was a considerable variability in microgrowth increment deposition and clarity as well as growth rates at all three sites. Smaller (younger) individuals had a greater tendency to have a period of relatively rapid shell growth, whereas in larger (older) individuals, the slow growth rates of summer continued through fall. Shell growth ceased at all locations during winter (January until mid-April), and resulted in the single or double prismatic bands noted earlier. The prismatic bands could be a result of both dissolution and extremely slow rates of shell deposition during winter, because granular shell material was usually present within the prismatic bands and the inner shell surface of the outer layer was often etched. By mid-April in both 1986 and 1987, shell growth had begun in some specimens at all sites, coinciding with an increase in water temperatures (Rodgers et al. 1979, Fritz & Lutz 1986).

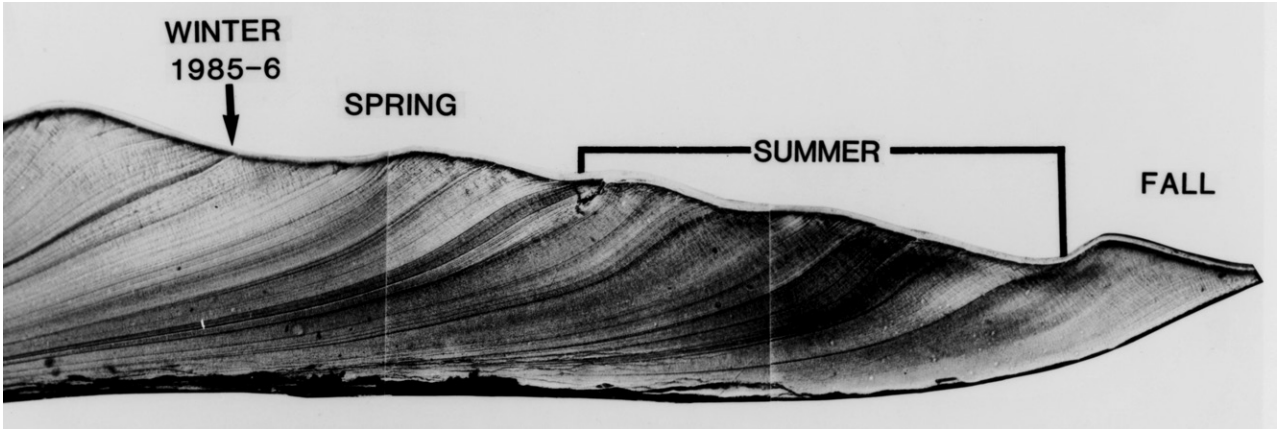

Figure 4. Light micrograph of an acetate peel replica of the polished and etched radial shell section of *Corbicula fluminea* collected in October 1986 from the Maurice River. Ventral margin is at the right and HFW = 1.4 mm.

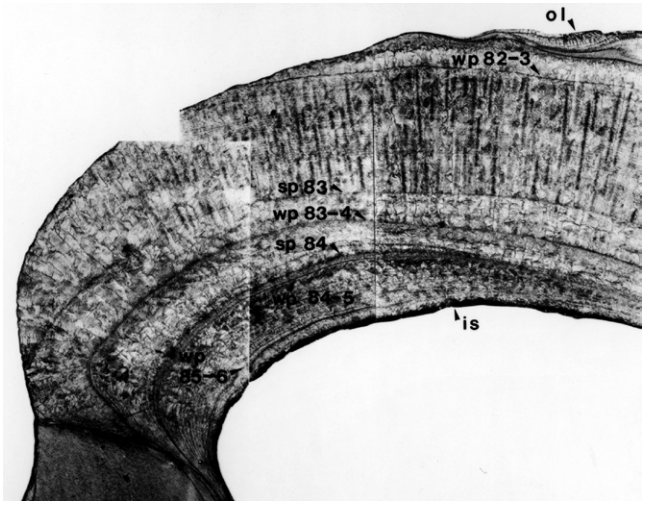

Figure 6. Light micrograph of an acetate peel replica of the polished and etched radial shell section of *Corbicula fluminea* collected in December 1986 from Union Lake. Micrograph taken in umbonal region; prismatic bands in the inner shell layer formed each winter (wp 82–3, wp 83–4, wp 84–5, and wp 85–6) and its first and second summer (sp 83 and sp 84). Summer 1985 and 1986 prismatic bands merged with bands formed in subsequent winters due to dissolution along the inner shell surface and reduced growth rates with age. Growth is to the right; is = inner shell surface; ol = outer shell layer; HFW = 3.3 mm.

Seasonal Changes in Inner Layer Microstructure and Age Determination

The inner shell layer of *Corbicula fluminea* is composed primarily of a complex series of crossed lamellae. These are usually oriented in cone or rosette-shaped patterns, which, when viewed in radial fracture or polished and etched sections, appear as a diagonal (with respect to the inner shell surface) series of parallel and interwoven crystalline lamellae (Figs. 2B and 5–9). At all sites at all sampling times, there was considerable variability in the appearance (visual and in SEM) of the inner shell layer along both the fracture and inner surfaces from the umbo to the pallial line. Tan-Tiu (1987) and Tan-Tiu and Prezant (1989) also reported a similar finding in their studies of temporal variation in microstructure of the inner shell layer of *C. fluminea* from the Leaf River, MS.

Growth cessations in both winter (because of low water temperatures) and summer (possibly because of periods of larval brooding) were reflected in inner shell layer microstructure by prismatic bands (Figs. 2B, 5, and 6). At all three sites, there were generally two sets of prismatic bands formed in the inner layer each year: (1) the winter band(s): one or two distinct and relatively wide (up to 10 μM) prismatic band, often with granular inclusions either on its outer edge (toward the outer shell surface) or within it and (2) the summer band(s): a series of thin (approximately 1–5 μM) prismatic bands ranging in number between one and five and separated from each other by thin zones of CCL microstructure. During spring, relatively wide zones of CCL microstructure were deposited, and usually thinner zones of this microstructural type were deposited in fall. Figures 5 and 6 show this sequence in 1+- and 3+-y-old specimens collected from the Maurice River and Union Lake locations, respectively. Both light micrographs are of acetate peel replicas and were taken in the umbo area. The younger specimen (Fig. 5), a member of the 1985 y-class (YC) was collected in September 1986. The series of prismatic bands deposited in summer 1986 is evident near the inner shell surface and is separated from it by a thin zone of CCL. In the upper (toward the outer shell surface) portion of the inner layer, the winter 1985 to 1986 prismatic band is evident. This specimen had a shell length (SL) of only 4.2 mm in late 1985, which accounted for the very thin inner shell layer at this time. Growth during spring and early summer 1986, however, was relatively rapid, as evidenced by the wide zone of CCL and the increase in SL to 10.2 mm by September 1986. The series of prismatic bands deposited in summer previous to capture could have resulted from period(s) of larval brooding, because *Corbicula fluminea* have been reported to become mature at approximately 7 mm in SL (Prezant & Chalermwat 1984).

Figure 6 shows a series of prismatic bands and zones of CCL microstructure in a 1982 YC specimen collected in December 1986. As in all multilayered bivalve shells, deposition rates of the inner shell layer were greatest near the umbo and decreased with decreasing distance from the pallial line. This became increasingly apparent with age (note the relatively uniform thickness of the inner layer between the winter prismatic bands of 1982 to 1983 and 1983 to 1984 compared with that between the winter prismatic bands of 1984 to 1985 and the inner shell surface). With increasing age, there was also a tendency for the fall zone of CCL to be lost, with the result being the merging of summer and winter prismatic bands into a single band. This occurred in this specimen during both its third (1984) and fourth (1985) growing seasons. During its fifth season (1986), rates of shell deposition were so reduced as to barely separate the previous winter prismatic band from the inner shell surface; this specimen grew only 1.5 mm in SL in 1986. Merging of summer and winter prismatic bands could also result from dissolution during winter of the zone of CCL deposited in fall.

The general sequence of inner layer microstructural growth outlined previously and shown in Figures 5 and 6 occurred at all three collection sites. At Scudder's Falls in the Delaware River, most of the specimens collected were members of either the 1985 or 1986 YC (only 7 of 76 specimens analyzed were of the 1984 YC and none were older). At both the Union Lake and Maurice River sites, specimens 4+ y old (1982 YC, the oldest clams analyzed) were not uncommon, and all younger YC were represented. Erosion of the outer surface near the umbo was much more common in clams at the Maurice River site than at either of the other two locations. Often, only the inner layer bands formed in the year of collection and portions of the previous year remained intact, and all older annual inner layer bands were eroded away. This limited the availability of size-at-age data from Maurice River clams.

A series of scanning electron micrographs of radial fracture and inner shell surface microstructure at each site during May (1986 or 1987), September 1986, and March 1987 is shown in Figures 7–9. Because of the variability and differential rates of deposition across the inner shell surface, these micrographs are meant only as examples of the types of microstructures encountered. Figure 7A, B (May 1986) shows the radial fracture and inner surface microstructure of a 1983 YC specimen that had not begun to grow in early spring. At the inner shell surface in

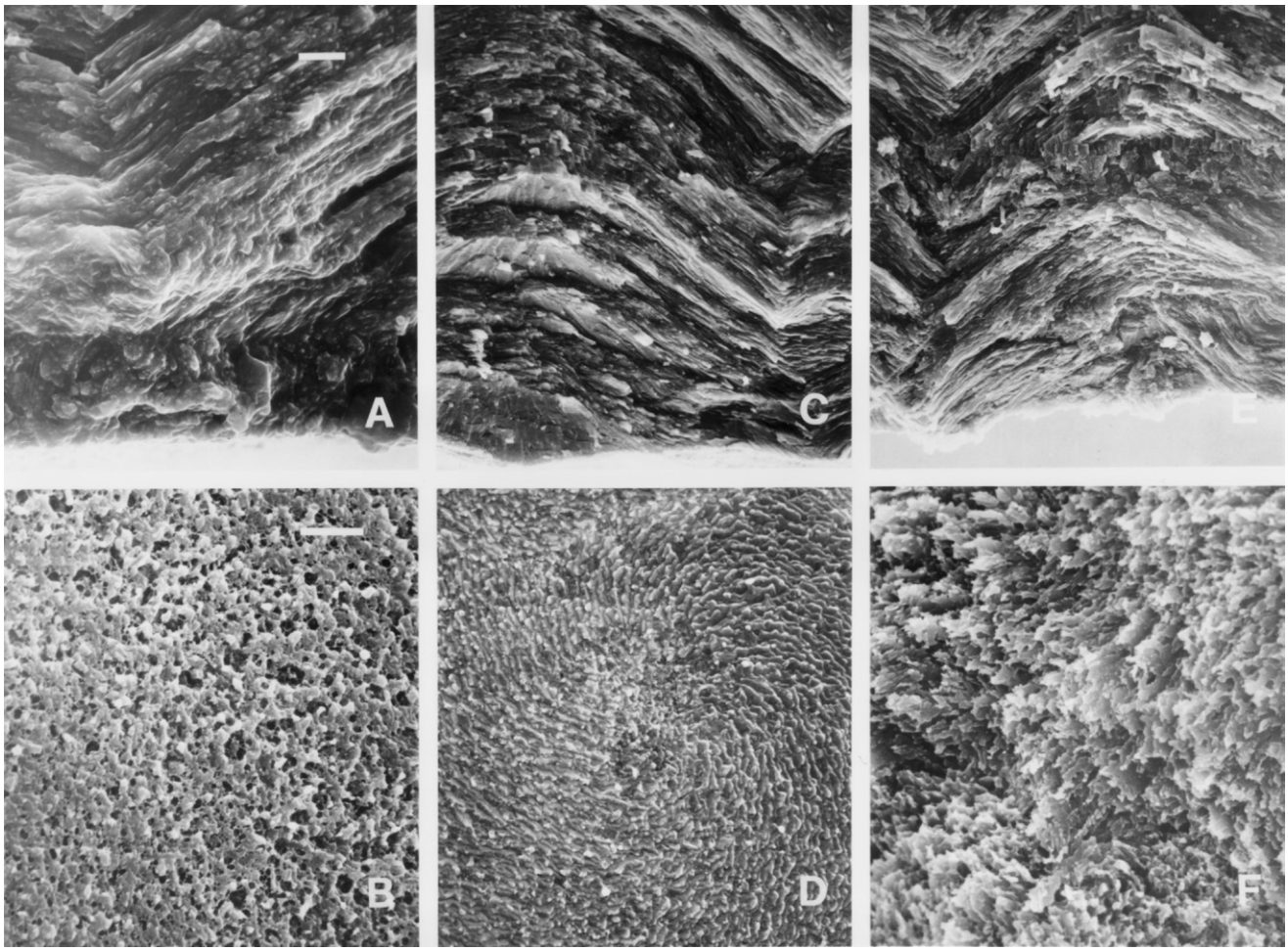

Figure 7. Scanning electron micrographs of radial fracture (A, C, and E; same scale; inner shell surface is at the bottom) and inner surfaces (B, D, and F; same scale) of the inner complex crossed-lamellar shell layer of *Corbicula fluminea* collected from Union Lake in May 1986 (A and B), September 1986 (C and D) and March 1987 (E and F). Scale bars = 4 µM; growth to the right.

fracture, there was a granular and modified prismatic microstructure present while the inner shell surface also showed little sign of recent growth and some evidence of dissolution. Other specimens at both locations, however, had begun to deposit shell by May 1986, and appeared similar to Figure 8A, B, in which new lamellae in fracture and the crisp rosette pattern of freshly deposited lamellae tips along the inner shell surface were evident.

Figure 7C, D are micrographs of a 1985 YC (1+-y-old) specimen collected in September 1986 showing a zone of CCL and their rosette pattern along the inner shell surface. This specimen had deposited prismatic bands earlier in summer 1986, but had a zone of CCL microstructure along the inner shell surface, evidence of growth in early fall. Older specimens collected in September 1986 (Fig. 8C, D; a 1983 YC specimen) showed little evidence of CCL deposition in early fall, and more often had a thin band of prisms along the inner surface of the inner shell layer (note: the gill pouches of the specimen shown in Fig. 8C, D were filled with brooded larvae when sampled in September 1986, at the same time as a thin prismatic band was being formed along the inner shell surface).

In March 1987, all specimens sampled showed evidence of dissolution along the inner shell surface (Figs. 7E, F and 8E, F). In the umbonal regions of some specimens, the zone of CCL deposited in fall was present (Fig. 7E) and the eroded lamella tips along the inner shell surface (Fig. 7F) were the evidence of dissolution during winter. Closer to the pallial line, the fall zone of CCL was no longer present along the inner shell surface, because of low deposition rates of the inner shell surface in this area and dissolution in winter (Fig. 8E, F). This resulted in a granular, acicular microstructure (Fig. 8F, left) that was often coated by an organic material (Fig. 8F, right). It should be noted that the prismatic band shown in Figure 8E is most probably composed of several smaller prismatic bands from more than 1 y that have merged together near the pallial line.

The sequence of inner-layer seasonal changes described for Maurice River and Union Lake populations also occurred in clams collected at Scudder's Falls in the Delaware River. A zone of CCL elaborated in rosette patterns along the inner shell surface was formed in May (Fig. 9A, B), whereas in September (Fig. 9C, D), there was evidence of slowed growth (lamellae tips were slightly eroded along the inner shell surface). In March,

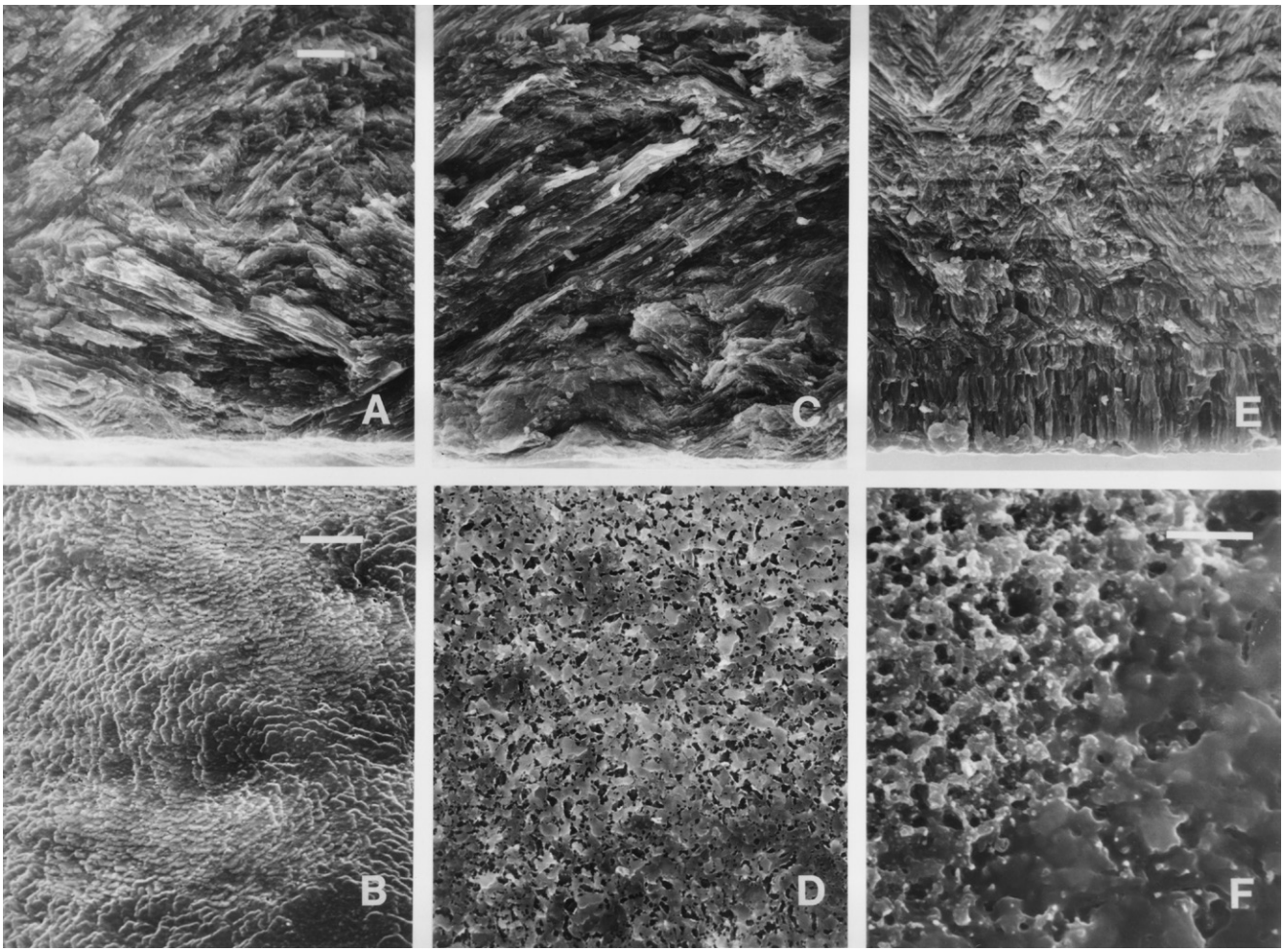

Figure 8. Scanning electron micrographs of radial fracture (A, C, and E; same scale; inner shell surface is at the bottom) and inner surfaces (B, D, and F; same scale) of the inner complex crossed-lamellar shell layer of *Corbicula fluminea* collected from the Maurice River in May 1986 (A and B), September 1986 (C and D) and March 1987 (E and F). Scale bars = 4 μM; growth to the right.

there was evidence of extensive shell dissolution, with a thin granular and modified prismatic band present along the inner shell surface (Fig. 9E, F).

Shell Growth Rates

The number of winter prismatic bands in both the inner and outer shell layers were used to estimate the age of each specimen sectioned. The outer layer prismatic band(s) were accompanied by a large growth disruption visible along the external shell surface, permitting the measurement of the SL of each specimen at the end of each growing season. The SL at each age and site (Table 1) revealed that *Corbicula fluminea* shell growth rates were greater at Scudder's Falls in the Delaware River than at both sites in the Maurice River system. At the end of their second growing season, the mean SL of the Delaware River population was almost 20 mm, a SL that was not attained by clams at the Union Lake and Maurice River locations until the end of their third growing season.

It is not known why growth rates are lower in the Maurice than in the Delaware River. Certainly, the water chemistry is quite different in the two systems, because the Maurice River, which drains the Pine Barrens, has a relatively low pH and larger amounts of dissolved organic material compared with the Delaware River. These differences could affect both the quality and quantity of planktonic food organisms. Certainly, another major difference between the two systems is the presence of large amounts of arsenic in Union Lake sediments, although it is not known how much this would affect growth rates. Stunted populations have also been described from other areas [such in Mississippi (Tan-Tiu 1987) and California (Britton & Morton 1982)], and growth rates are usually lower in lentic than in lotic waters (Britton & Morton 1982). This latter observation could partially explain the slower growth of clams in Union Lake than in the Delaware River, but does not explain the slower growth of clams at the Maurice River location.

To quantify seasonal shell growth, shell deposited along the height axis from the winter 1985 to 1986 prismatic band in the outer layer to the ventral shell margin was measured off acetate peels (at 40× magnification) in clams sectioned from each sampling date and site (Fig. 10). The natural logs of growth measurements in 1986 were regressed against the SL of each clam at the winter 1985 to 1986 growth cessation separately for each sampling date and site. This yielded separate growth models for each site relating initial SL and growth increment in 1986

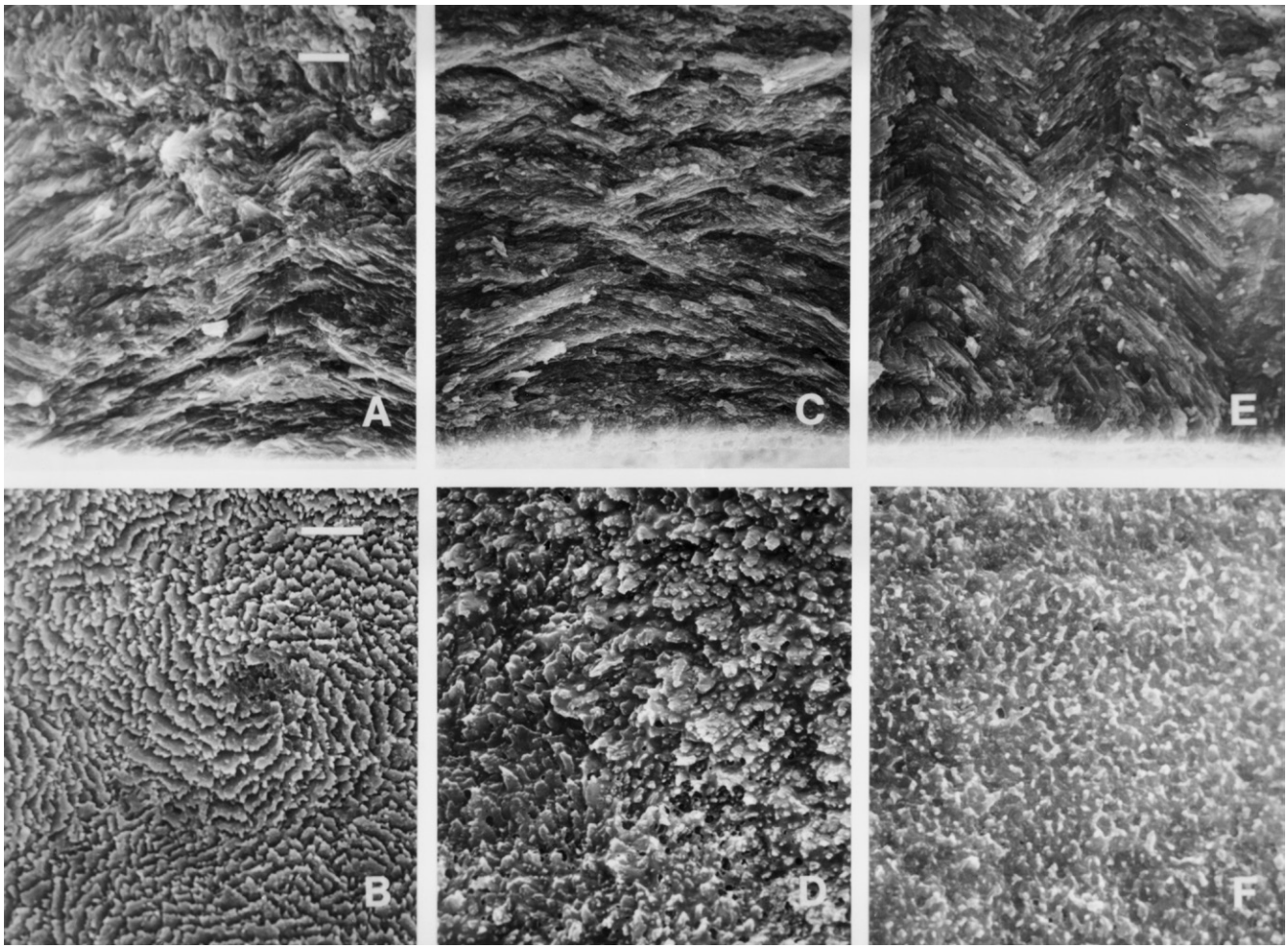

Figure 9. Scanning electron micrographs of radial fracture (A, C, and E; same scale; inner shell surface is at the bottom) and inner surfaces (B, D, and F; same scale) of the inner complex crossed-lamellar shell layer of *Corbicula fluminea* collected from the Delaware River in May 1987 (A and B), September 1986 (C and D) and March 1987 (E and F). Scale bars = 4 µM; growth to the right.

for each sampling date. The growth increment of a standard 15-mm specimen was estimated from each equation and plotted against sampling date in 1986 and 1987. For the Union Lake population, a 15-mm specimen grew approximately 1.3 mm along the height axis from the winter 1985 to 1986 to May 1986 (with a very wide confidence band), 2.5 mm by July 1986, and then varied between 3.1 and 5.4 mm from September 1986 to March 1987. The mean 1986 annual increment in the groups sampled between September 1986 and March 1987 was 4.2 mm, suggesting that most of the annual growth increment

TABLE 1.

Shell length (mean and range in mm; N = number of measurements) of *Corbicula fluminea* at the end of each growing season (GS) in Union Lake, Maurice River and Delaware River.

	Union Lake			Maurice River			Delaware River		
GS	Mean	Range	N	Mean	Range	N	Mean	Range	N
1	8.3	2.5–14.0	91	8.6	4.2–12.0	46	7.2	4.3–12.5	66
2	16.0	12.1–22.3	73	14.4	11.8–18.4	63	19.8	14.3–22.3	8
3	20.1	17.3–23.2	22	19.2	15.5–23.7	51	24.0	21.4–27.3	4
4	22.6	21.6–25.4	8	23.2	19.5–25.2	24	–	–	–

Clams are approximately 0.5-y-old at the end of the first growing season, approximately 1.5-y-old at the end of the second, and so on, assuming midsummer larval release.

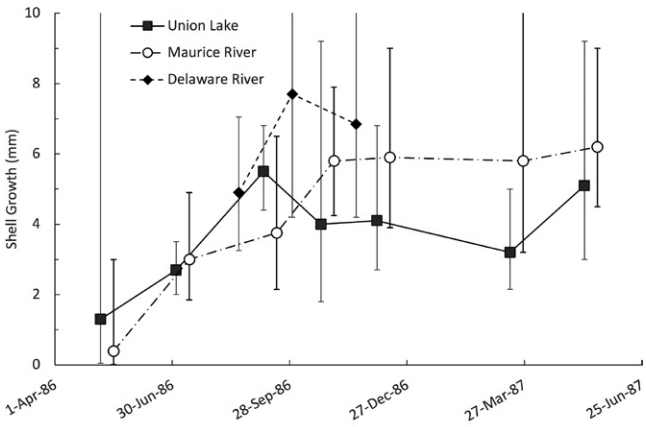

Figure 10. Estimated (±95% confidence intervals) shell growth along the height axis of a standard 15 mm *Corbicula fluminea* from the winter 1985 to 1986 growth cessation mark in the outer shell layer to the ventral margin through May 1987 in Union Lake and the Maurice River, or through November 1986 in the Delaware River. Ten days were added to the collection date of *C. fluminea* in the Maurice River for graphical display purposes only.

in 1986 was deposited by midsummer (60% of the increment was deposited by July) at Union Lake. There is little evidence of an increase in growth rate in fall.

At the Maurice River location, there was relatively rapid growth in spring and early summer (between May and July 1986), slower rates in mid and late summer (between July and September 1986), relatively rapid rates again in early fall (between September and October 1986), and little or no shell growth in late fall and winter (between October 1986 and March 1987). The mean 1986 annual increment in the Maurice River population obtained from the groups sampled in October 1986 through March 1987 was 5.7 mm, or 1.5 mm greater than the Union Lake population. This difference could be a result of the greater water flow, and hence food supply, at the Maurice River site than at the Union Lake site (Britton & Morton 1982).

Data are limited for the Delaware River site because of the few 1985 YC and older clams present at the site in March and May 1987. Growth rates in late summer (between August and September 1986) were rapid at this site and then appeared to decline through the fall. As with the Union Lake population, there was evidence on acetate peels and in fracture sections of a short period of relatively rapid shell growth in fall, but this is not reflected in the shell increment data in Figure 10. The 1986 increment at the Delaware River site averaged (mean of September and November 1986 computed values) 7.2 mm, or 1.5 mm greater than in the Maurice River and 3.0 mm greater than in Union Lake.

Shell Microtubules and Outer Mantle Epithelial Processes

Microtubules have been observed in the shells of numerous taxonomic groups of bivalves, including the Arcoida, Carditidae, Pisidiidae, Spaeriidae, and Corbiculidae (Collins 1967, Wise 1971, Taylor et al. 1973, Waller 1980, Tan-Tiu & Prezant 1989, Araujo et al. 1993, 1994, Araujo & Korniushin 1998, Malchus 2006, 2010). In the marine epibenthic Arcoida, tubules were 2–10 μM in diameter, traversed the entire calcified portion of the shell (terminating beneath the periostracum), and were located just inside the pallial line (Wise 1971, Waller 1980). In the freshwater and estuarine infaunal Sphaeralcea (which includes *Corbicula*), tubule diameters were similar to those in arks, but they were found in the umbonal region rather than in more ventral locations (Collins 1967, Tan-Tiu & Prezant 1989, Araujo et al. 1993, 1994, Isaji 1995). In all taxa, projections of the outer epithelium of the mantle were observed within the tubules. In the arks, mantle projections have been attributed to function in photoreception or in secretion of chemicals to prevent boring by other organisms (Waller, 1980). In the Corbiculidae, microtubules and mantle projections may be involved in respiration (for the exchange of gases during periods of valve closure; Collins 1967, McMahon & Williams 1984, Araujo et al. 1994), adhesion (to keep the mantle and shell tightly bound; Tan-Tiu & Prezant 1989), and secretion of chemical deterrents to boring organisms (Waller 1980) or carbonates and organic compounds for shell maintenance (Oberling 1964, Araujo et al. 1994, Isaji 1995).

Microtubules (4–10 μM in diameter) were observed in the shells of *Corbicula fluminea* collected from each of the three locations in this study. There were macroscopic differences in the shells from each site, with much more outer shell erosion in the umbonal area of Maurice River specimens than those collected from Union Lake or the Delaware River. Along the inner shell surface near the umbo, there were also differences in the density of tubules between specimens collected at the three sites. At the Maurice River site (Fig. 11A), the density of tubule openings in the umbo area was much greater than at either of the other two sites (Fig. 11B, C). At the Union Lake and Maurice River sites, tubule openings were common and evenly distributed along the inner surface near the umbo, but their density was much greater and they were observed farther from the umbo in specimens collected from the Maurice River.

Tubule openings were first (and exclusively) observed on the inner surface of the inner layer, and were never observed terminating on the inner surface of the outer layer (Fig. 12). There was no evidence of shell repair along the inner shell surface surrounding the tubule openings. The appearance of the inner tubule openings varied throughout the year and was dependent on the seasonal depositional sequence of the inner shell layer. In May, tubule openings at the three sites reflected no recent growth (Fig. 12A), a small amount of recent inner CCL deposition (Fig. 12B), and a larger amount of recent growth with the rosette pattern of lamellae tips clearly evident surrounding the tubule openings (Fig. 12C). In September (Fig. 12D), recent prismatic band deposition was evident (this is the same specimen as in Fig. 9C, D). Bifurcated tubules were not uncommon along the inner shell surface (Fig. 12D) or along the fracture surface. In late winter (Fig. 12E, F), there was evidence of dissolution, in which the zone of CCL deposited in fall was partially dissolved away, leaving "trails" of tubule walls along the inner shell surface. These "trails" were parallel to each other and always "pointed" (on the inner surface) to the ventral shell margin. As observed in fracture and thin sections, tubules located away from the umbo usually traversed diagonally through the shell (from inner to outer surfaces) in a ventral-dorsal orientation, and they were rarely straight, even channels. This orientation suggests that individual tubule openings slowly migrate ventrally with growth along the inner shell surface. Nearer to

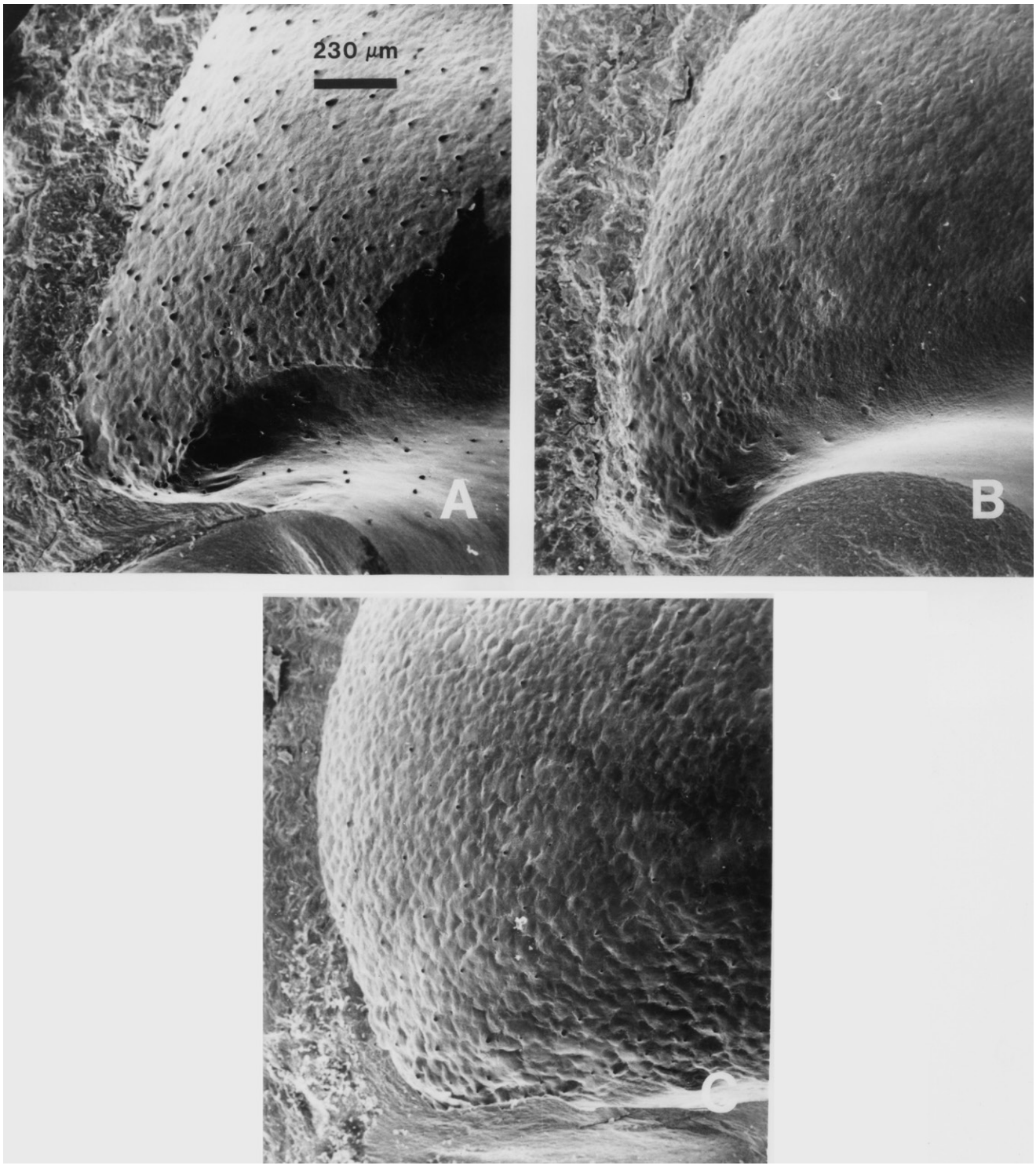

Figure 11. Scanning electron micrographs of fracture (left side of each) and inner shell surfaces of *Corbicula fluminea* collected in September 1986 from the (A) Maurice River, (B) Union Lake, and (C) Delaware River. Each micrograph was taken in the umbo area (note the chondrophore at the bottom of each micrograph) and shows the distribution and density of microtubule openings along the inner shell surface. Note the greater density of tubules in the Maurice River specimen (A). Scale in each micrograph is the same as in A.

the umbo, tubules were more often perpendicular to both the inner and outer shell surfaces, and inner surface "trails" were not observed.

Some tubules traversed through the entire thickness of the shell from interior to exterior surfaces. This only occurred in areas where the periostracum was eroded away, and where either the outer or inner layers of the shell formed the shell exterior surface. Tubule openings on the shell exterior were more common in areas where the inner shell layer formed the outer shell surface (where both the periostracum and outer shell

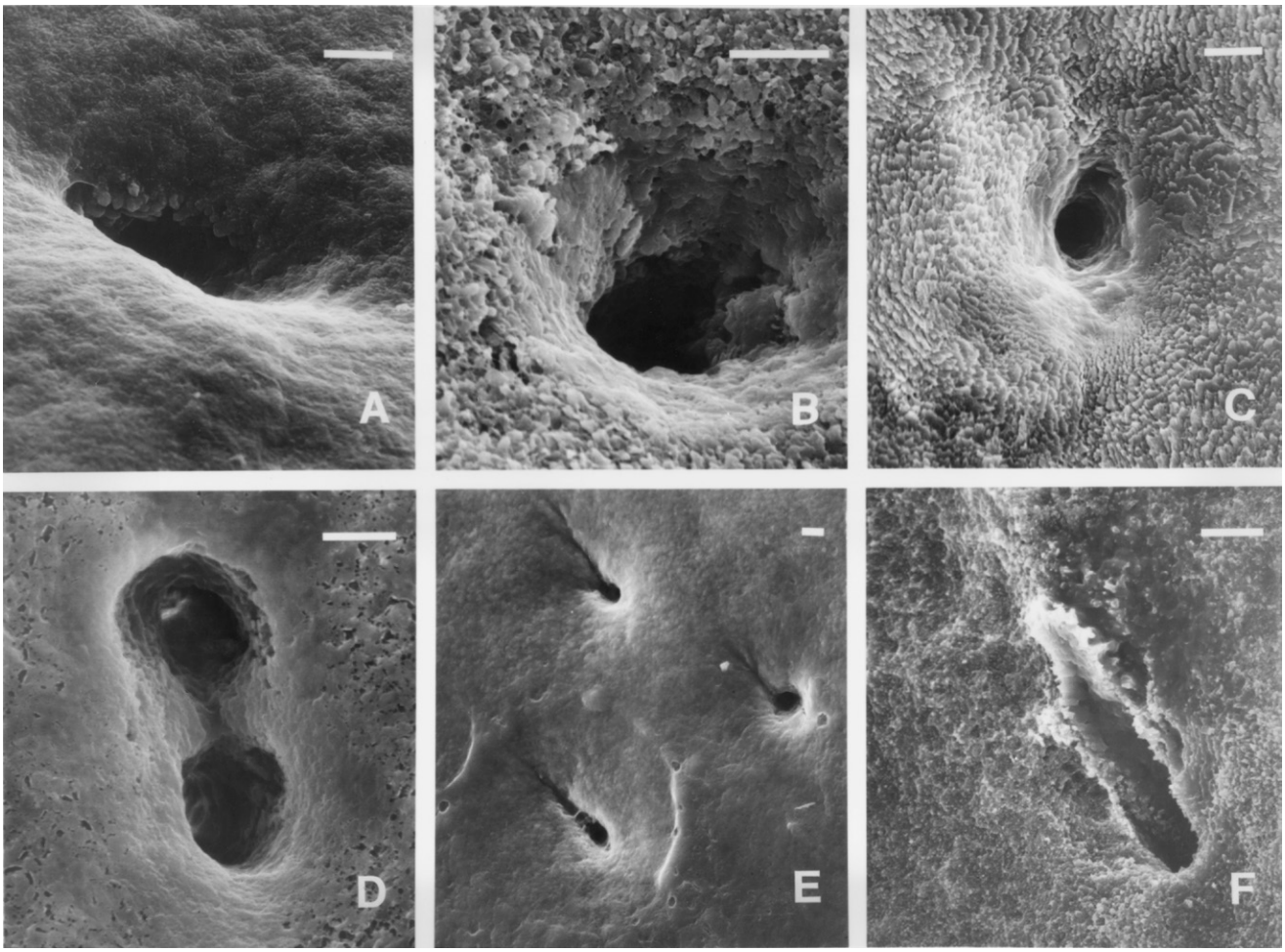

Figure 12. Scanning electron micrographs of tubule openings along the inner shell surface of *Corbicula fluminea* collected in the Maurice River (A. May 1986; D. September 1986; E. March 1987; F. February 1988), Union Lake (B. May 1986), and Delaware River (C. May 1987). All scale bars = 4 μM.

layers were eroded away). In areas where the outer shell layer was still intact and the periostracum was gone, some tubules opened to the outside, whereas others appeared to only partially penetrate the outer shell layer and did not reach the outer shell surface. In fracture section, it is apparent that the tubule wall structure is different from either the inner or outer layer microstructures (Fig. 13). The tubule walls were composed not of fine or CCL, but of short 1–2 μM long columnar prisms, the long axes of which are generally inclined toward the inner shell surface, suggestive of wall maintenance and crystal growth as the shell is thickened.

The appearances of tubule openings on the outside of the shell varied considerably from one another. This variation appeared to depend more on the collection site than on the time of sampling. Outer tubule openings in specimens collected from Union Lake and the Delaware River (which had relatively little erosion in the umbo area) were often located within small "dimples" on the shell exterior (Fig. 14A, B) and were located atop cylindrical projections from the outer surface (Fig. 14B, C). In thin shell sections, the cylindrical projections were amber-colored much like that of the periostracum. Furthermore, in scanning electron micrographs, the cylindrical projections did not appear to be composed of the same material as the crystalline prismatic tubule walls (Fig. 13), but instead were constructed of a consolidated organic material (Fig. 14C, F). This organic material was also observed to be coating the edges of the "dimples" in some specimens. At the Maurice River site, all large specimens (greater than approximately 15 mm SL) had extensive erosion in the umbo area, and the cylindrical "organic" projections, as well as the shell "dimples" were much less common. Along the outer surface of clams collected from the Maurice River site, tubule openings showed evidence of the prismatic tubule wall structure (Fig. 14D, E). It is possible that the shell erosion at this site was so extensive that "dimples" and projections were eroded away. Tubule openings were also found farther from the umbo in specimens collected from this site than at either the Union Lake or Delaware River sites, with the farthest being 8 mm from the umbo on the outer shell surface.

The morphology of the outer surface of the mantle was investigated using scanning electron microscopy to see whether there were any structures that entered or exited the tubules. A large number of epithelial processes were found in the dorsal portions of the mantle; these also had diameters similar to the tubules (4–10 μM; Fig. 15A). The density of the processes was greatest in the dorsal portions of the mantle and decreased with increasing distance from the umbo (Fig. 15A). This distribution

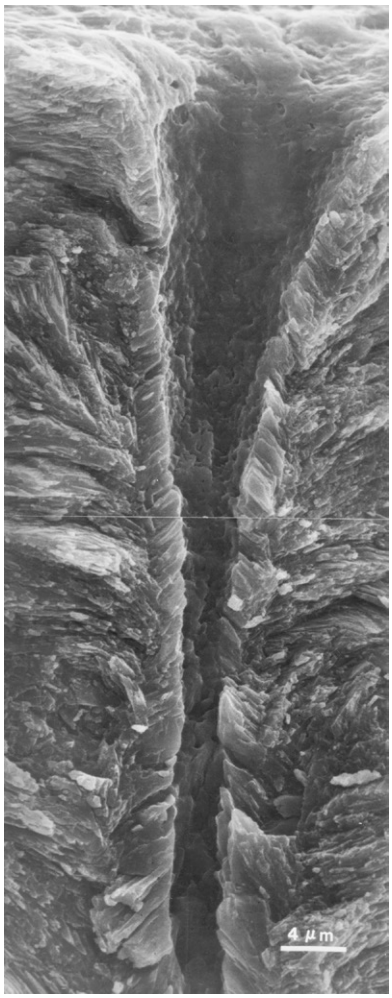

Figure 13. Scanning electron micrograph of a tubule opening along the inner shell surface (top) and the tubule along the fracture surface going through the shell to the exterior (beyond the bottom of the micrograph) in a *Corbicula fluminea* collected September 1986 from the Maurice River. The tubule wall is composed of 1–2 µM long columnar prisms angled toward the inner shell surface. The tubule diameter increases toward the inner shell surface, which mirrors the morphology of the outer mantle epithelial processes (see Figure 15).

is the same as that of the tubules themselves. The mantle processes were also observed to stick out of the tubule openings on the outer shell surface of one specimen (Fig. 14B). Some of the mantle processes bifurcated (Fig. 15B), as did some of the tubules (Fig. 12D). The processes and the mantle itself appeared to be encased in a mucoid sheet in this preparation (Fig. 15B).

Other investigators of tubules and mantle projections in Sphaerids thought that each projection, or process, was formed by a single differentiated pyramidal cell in the outer mantle epithelium (Collins 1967, McMahon & Williams 1984). There is preliminary evidence from *Corbicula fluminea* that supports this conclusion from histological sections that revealed the presence of both the processes and the pyramidal cells that form them. In histological sections, the processes were observed to bifurcate, and they often contained a substance that stains dark purple-red in our preparations (hematoxylin, aniline blue, and acid fuchsin stains). The cells that line the periostracal groove at the mantle margin stain this same color, which suggests that the pyramidal cells are secreting a periostracal-like substance to the shell exterior through the epithelial processes inside the tubules. It is this material that may be lining the distal ends of the tubules and may also be elaborated into the tubule projections seen on the outer shell surface. This periostracal-like material may be conferring some resistance to shell dissolution and erosion. By secreting organic material through the mantle projections, golden freshwater clams may be increasing the stability of its shell exterior in the relatively corrosive freshwater environments in which they live. The larger number of tubules in specimens collected from the Maurice River site, as well as the more extensive erosion at this site, suggests that individuals may be able to form these processes, and hence convert a "normal" mantle epithelial cell into a pyramidal cell, in response to an environmental cue. The observations also suggest that the processes, once they are formed by a differentiated outer mantle epithelial cell, "tunnel" their way through the calcified shell layers to the outer surface of the shell; mechanisms behind this process, however, are not known. Such secondary production of mantle processes is known to occur in the Arcoida (Waller 1980).

Biomineralization of Barite

The shells of molluscs are composed primarily of calcium carbonate in one or both of its common mineral forms, aragonite and calcite (Wilbur 1964, Taylor et al. 1969). Two other minerals have also been reported in molluscan shells: dahllite, a form of hydroxyapatite or calcium phosphate, in the larval shell of the pearl oyster (Watabe 1956), but this observation has not been duplicated; and vaterite, an unstable form of calcium carbonate, in regenerated shell of *Elliptio complanate* (Lightfoot, 1786) and *Viviparus intertextus* (Say, 1829) (Wilbur & Watabe 1963). Molluscan shells also contain trace amounts of a wide variety of other elements (see Carell et al. 1987). The arrangement of atoms in the structure of aragonite and calcite allows for substitution of some divalent (e.g., Mg, Sr, Ba, Mn, Fe, Cu, Zn, and Pb) and small (ionic radius) monovalent cations (e.g., Li) directly into their crystal lattices (Masuda & Hirano 1980, Masuda 1981). Large monovalent cations (e.g., Na, K, and Rb), trivalent cations (e.g., Al, Cr, and Sc), and anions (e.g., Cl and Br) can also be incorporated into shells: (1) as separate mineral phases entrapped as impurities during calcification at the ventral shell margin (or ventral to the region of mantle-shell attachment, the pallial line) or (2) as contaminants of the shell's organic matrix that provides nucleation sites for carbonate crystallization and coats each crystalline unit (Carriker et al. 1980). Only in the cases of substitution into crystal lattices or contamination of organic matrix have trace elements been reported to be incorporated directly into shells as a result of secretions from the outer mantle epithelium into the extrapallial fluid.

Fritz et al. (1990b) documented the biomineralization of barium sulfate ($BaSO_4$; barite) by wild *Corbicula fluminea* along the inner surface of the inner shell layer, whereas Fritz et al. (1992) showed that barite crystal formation could be induced along the inner surfaces of both the inner and outer shell layers in the laboratory. These were the first reports of the presence of a noncalcium-based mineral in the shell of any molluscs and the

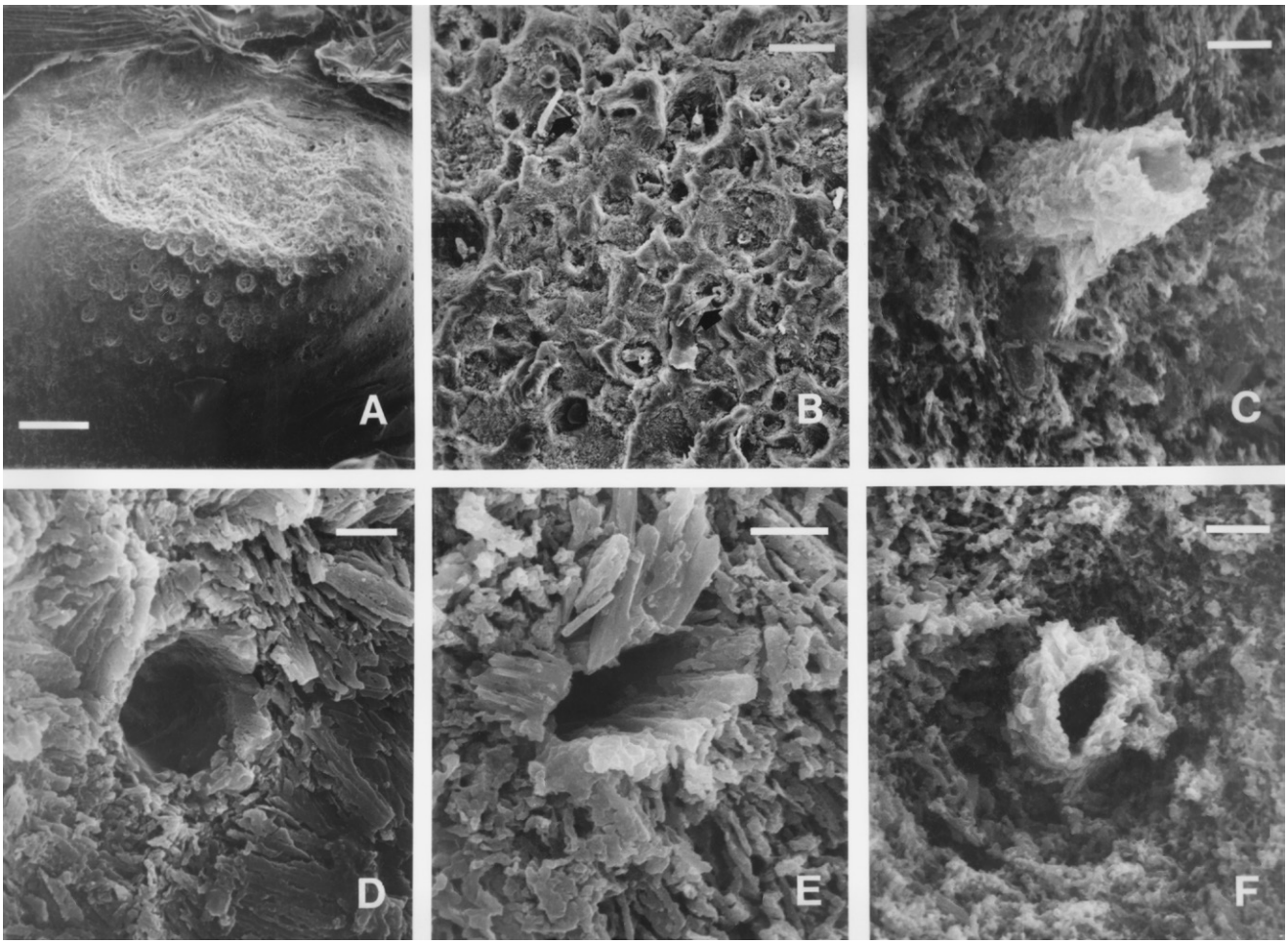

Figure 14. Scanning electron micrographs of tubule openings along the outer shell surface of *Corbicula fluminea* collected in the James River, VA (A and D. April 1986), Delaware River (B. March 1986; black arrows indicate mantle epithelial processes sticking out of tubule openings), Union Lake (C and F; September 1986), and the Maurice River (E. September 1986). Scale bars: A—300 µM; B—40 µM; C-F—4 µM.

biomineralization of barium sulfate by an animal other than a protozoan (Arrhenius & Bonatti 1965, Riley & Chester 1971).

Barite crystals were first observed on the inner shell surfaces of *Corbicula fluminea* collected in September 1986 from the Maurice River. These appeared as rosette-shaped crystals in a band 2–3 mm wide running antero-posteriorly approximately two-thirds of the distance from the umbo to the pallial line (Fig. 16). The crystals were loosely arranged in rows parallel to the pallial line within this band (Fig. 16A). Some of the crystals, each of which was composed of many thin orthorhombic tablets (*c*-axes between 1 and 6 µM long) assembled rosette fashion, were attached to what appeared to be organic pedestals atop the inner shell surface (Fig. 16B). The individual tablets were usually arranged with either their *a* (Fig. 16B) or *c* (Fig. 16C) axes perpendicular to the inner shell surface. In specimens collected from the same location in March 1987, similar rosette-shaped crystals were observed: (1) partially buried in the inner shell layer (or reexposed after carbonate dissolution in winter; Fig. 16D, E) and (2) in fracture sections, completely surrounded by shell aragonite (Fig. 16F). Crystals were also present in specimens collected in November 1987 and February 1988 from this location, suggesting that the conditions that led to their formation were not limited to 1986, but persisted at least through 1987.

In the crystals, EDS analyses revealed the presence of (1) barium, with definitive separation of five peaks in the Ba *L* family ($L\alpha$ = 4.47, $L\beta_1$ = 4.83, $L\beta_2$ = 5.16, $L\gamma_1$ = 5.53, and. $L\gamma_2$ = 5.82 keV); (2) sulfur (a single S *K* family peak, 78% the height of the Ba $L\alpha$ peak, at 2.29 keV); and (3) strontium (a single Sr *L* family peak, 16% the height of the Ba $L\alpha$ peak, at 1.74 keV). Energy dispersive X-ray spectrometer analyses of the pedestals revealed the presence of sulfur [S *K* family peak as a shoulder 75% the height of the Au (from sputter-coating) *M* family peak] and calcium, but no barium. Pedestals deteriorated rapidly under the electron beam in these unfixed specimens, which probably accounted for the high calcium peaks. These results, along with their appearance in secondary electron images, strongly suggested that the pedestals were organic in composition and not crystalline, inorganic material. Energy dispersive X-ray spectrometer analyses conducted on several crystals partially buried in the inner shell layer of specimens collected in March 1987 (Fig. 16D, E) as well as on a single crystal found in fracture section (Fig. 16F) yielded the same elemental composition (barium, sulfur, and strontium) as those

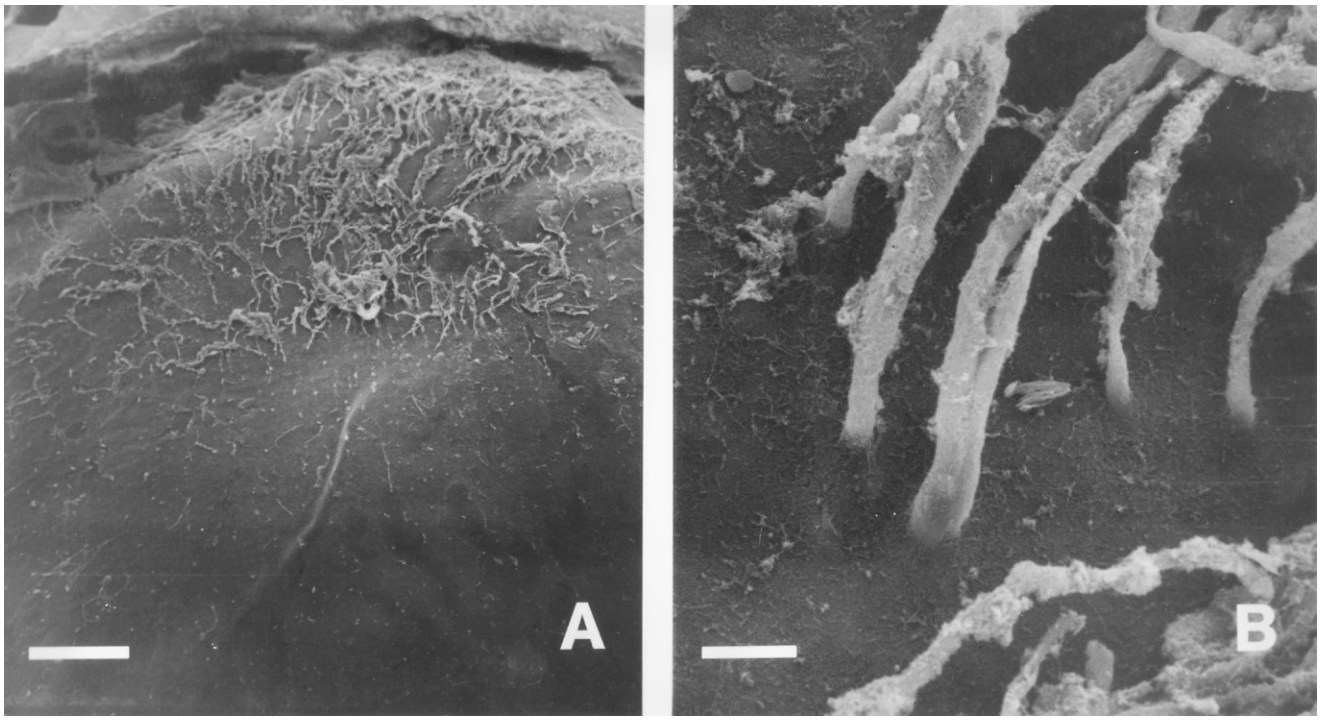

Figure 15. Scanning electron micrographs of the outer mantle epithelium of *Corbicula fluminea* collected from the Maurice River. (A) View is dorsal, with the umbo and remnants of the shell at the top (scale bar = 550 μM). Note the large number of mantle processes in the umbo area and decrease in numbers ventrally. (B) Several processes are attached to the outer mantle surface, one of which is bifurcated (scale bar = 20 μM). Clams were relaxed in Epsom salts (magnesium sulfate), and carefully opened so that the mantle and shell remained attached to each other. Mantle/shell preparations were fixed in 2% glutaraldehyde (in 0.05 M phosphate buffer) for 2 h, rinsed three times (10 min each) in 0.05 M phosphate buffer, postfixed in an air-tight container with (not in) 4% aqueous osmium (OsO_4 in 0.05 M phosphate buffer) for 1 h, rinsed three times (10 min each) in distilled water, and decalcified in 0.1 M EDTA for 2 wk (with repeated changes of EDTA). Preparations were dehydrated, critically point dried and sputter-coated with gold-palladium for scanning electron microscope analysis.

observed on the inner shell surfaces of specimens collected in September 1986 (Fig. 16B, C). The high concentration of barium in the crystals is shown in Figure 17.

Incorporation of a foreign element in the shell of a bivalve depends on its concentration in the ambient water as well as the size of its ionic radius, which for a divalent cation, governs its ability to substitute in the crystal lattices of aragonite and calcite (Dodd 1965, Carriker et al. 1980, Masuda & Hirano 1980, Masuda 1981). Changes in the absolute and relative amounts of elements in shells have been used in analyses of bivalve growth history with respect to both natural (e.g., temperature and salinity; Dodd 1965) and anthropogenic (e.g., pollution; Nelson 1962, Ferrell et al. 1973, Carell et al. 1987) environmental variation. It is thought that bivalves rid themselves of high tissue concentrations of certain elements, divalent cations in particular, by secreting them into the extrapallial fluid for incorporation into the shell.

Barium concentrations in shells have not been studied extensively, most probably because barium is a common element in surface waters (National Academy of Sciences 1977) and is not listed as a priority pollutant in water quality criteria established by the US Environmental Protection Agency (US EPA 1986). In two studies, barium concentrations in shells reflected environmental barium levels and were greater than predicted based on ionic size considerations. In the first study (Carell et al. 1987), barium concentrations increased along the growth record (with increasing distance from the umbo) in the outer shell layer of a 125-y-old specimen of *Margaritifera margaritifera* (Linnaeus, 1758), the freshwater pearl mussel. The increase in shell barium concentrations, along with other elements, was attributed to stream acidification that increased barium solubility during the lifetime of this individual. Barium was also present in higher-than-expected concentrations (based on its ionic radius) in shells of *Anadara satowi* (Dunker, 1882) and *Mizuhopecten yessoensis* (Jay, 1857) (Masuda 1981), which was attributed to incorporation of barium into the organic matrix rather than to an increase in its substitution rate into the calcite crystal lattice. In neither case, however, was barium present as a separate mineral phase in the shells of the studied bivalves.

It is clear that barite crystallized directly from extrapallial fluid along the inner depositional surface of *Corbicula fluminea*. The edges of each orthorhombic tablet in the barite rosettes were crisp, with no evidence of environmental exposure. Their alignment in loose rows within a band parallel to the pallial line also strongly supports *in situ* crystallization. Barite crystals developed in summer along the inner surface and were buried by shell aragonite in fall. Examination of thin radial shell sections revealed the presence of crystals within the inner shell layer of specimens collected in October and December. Dissolution of shell carbonates in winter reexposed some crystals along the inner shell surface. Close investigation of the barite crystals in Figure 16D, E reveals that not all the inner shell layer was dissolved from some

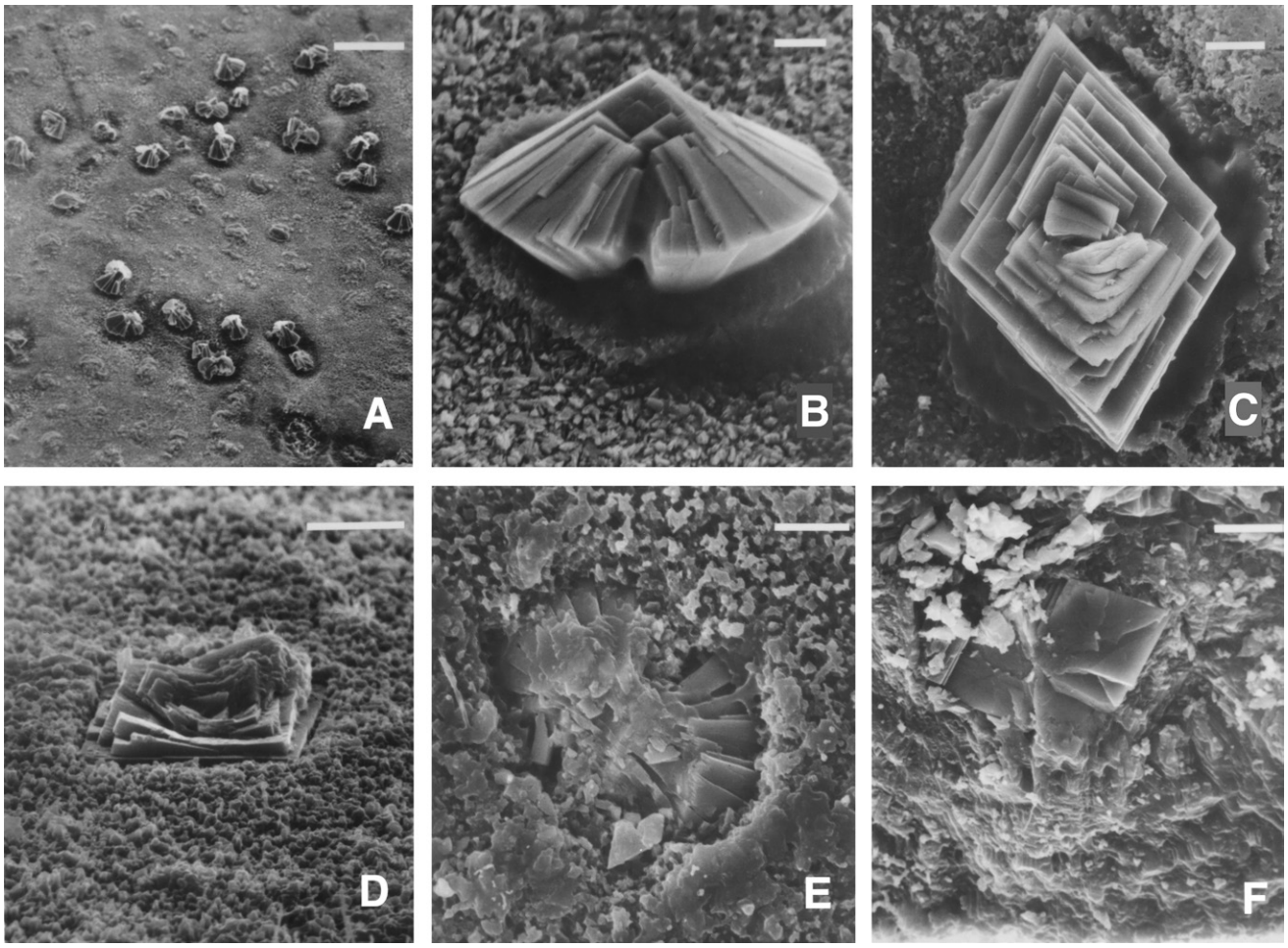

Figure 16. Scanning electron micrographs of barite crystals on the inner shell surface and embedded within the inner shell layer of *Corbicula fluminea* collected from the Maurice River. Scale bars: in A—50 μM; in B–F—5 μM A. Barite crystals in loose rows on the inner shell surface parallel to the pallial line (which is parallel to and beyond the top of the micrograph). Specimen collected in February 1988. (B and C) Two barite crystals (oblique and top views, respectively) on the inner shell surface. Specimen collected in September 1986. (D and E) Two barite crystals (oblique and top views, respectively) partially buried in the inner shell layer with partially dissolved aragonitic material remaining on the crystals. Specimen was collected in March 1987. (F) Barite crystal (in radial fracture section completely embedded within the inner shell layer. Inner shell surface is at the bottom. Specimen is the same as D and E. Modified from Figure 1 of Fritz et al. (1990b).

crystals, leaving behind a residue of granular aragonitic material. No barite crystals were found on the inner surfaces of specimens collected at the Union Lake and Delaware River sites.

Fritz et al. (1992) reported that soluble barium concentrations in the Maurice River (40–59 μg l^{-1}) were approximately twice those of the Delaware River (24–32 μg l^{-1}; Bauersfeld et al. 1987, 1988, 1990), but no data on barium concentrations in Maurice River or Union Lake waters or sediments were collected concurrently with the shell deposited by clams collected in this study. Based on the absence of barite crystals in clams collected from Union Lake (and the Delaware River), levels of soluble barium in Union Lake may be lower than those in the Maurice River downstream from the dam, and may have been similar to those observed in the Delaware River. Elevated barium levels in fresh surface waters are generally associated with industrial activity, and in particular, the manufacture of glass and ceramics (National Academy of Sciences 1977); there are several glass manufacturing plants in Millville, NJ. Barite itself is highly insoluble in water. It is possible that some soluble

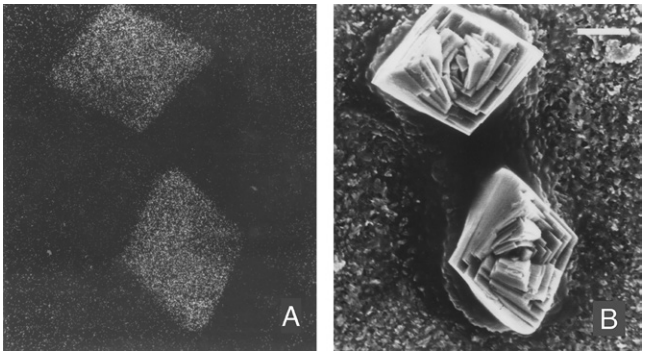

Figure 17. Scanning electron micrographs of two barite crystals on the inner shell surface of *Corbicula fluminea* collected in September 1986 from the Maurice River. Both micrographs were taken in exactly the same field. (A) X-ray detection with most frequently produced energies in the barium L family ($L\alpha$, $L\beta_1$, and $L\beta_2$). (B) Secondary electron detection. Scale bar = 10 μM; scale is the same in both micrographs. Modified from Figure 2 of Fritz et al. (1990b).

barium species (such as barium carbonate or fluorosilicate) is present in high concentrations in the lower Maurice River and is further bioconcentrated by clams located downstream from the dam. During summer, shell growth and aragonite deposition rates of *Corbicula fluminea* were slower than during spring or fall. Thus, there were fewer opportunities for barium substitution into the aragonite crystal lattice or incorporation into the organic matrix in summer than during spring or fall. Elevated barium concentrations in the extrapallial fluid apparently result in the direct crystallization of barite along the inner shell surface. Organic pedestals observed underneath the crystals may contain the individual barite crystal nucleation sites. Direct barite crystallization from extrapallial fluid would contribute to both the lowering of barium tissue levels and the deposition of it in a relatively stable, nonbiologically active form (Fritz et al. 1990b, 1992).

Rangia cuneata, the Wedge Clam

The wedge clam, *Rangia cuneata*, is a common inhabitant of brackish waters in coastal areas of the Gulf of Mexico and the Atlantic coast of the United States north to Delaware Bay (Abbott 1974, Counts 1980). The species has moderate commercial importance in the southern portions of its range (Wolfe & Petteway 1968), but little is known if its growth and reproductive biology north of Chesapeake Bay. Studies of populations in the Potomac River, MD (Pfitzenmeyer & Drobeck 1964), suggest a late summer or fall spawning period and growth to between 35 and 45 mm SL in approximately 4 y. The latter observation, however, was based on analyses of growth lines on the shell exterior, which can be unreliable guides to individual age (see Lutz & Rhoads 1980). Mathematical determinations of size-at-age from sequential samples in the Neuse River, NC, suggest a similar size/age relationship (Wolfe & Petteway 1968). Fairbanks (1963) suggested that *R. cuneata* spawns twice, once in spring and once in fall, in Louisiana and attains a length of approximately 30 mm in 3 y.

The intertidal sand flats and fringing marsh near the collection site were inundated with oil from a spill on September 29, 1985, when approximately 400,000 gallons of crude were released into the Delaware River south of Philadelphia, PA, from the tanker *Grand Eagle* (see Jacobsen 1987). Because high tides and river flows associated with the passage of hurricane Gloria only several days prior to the spill were still occurring at the time of the accident, it was feared that a significant portion of the Delaware River estuary might be adversely affected by oil. The spill was contained to the area north of Pea Patch Island, with the major damage occurring on the western (Delaware) shore. Approximately one-third of the spilled oil was recovered, whereas the remainder was either unaccounted for (attached to fringing marsh vegetation, particles, etc.) or evaporated.

Sampling of *Rangia cuneata* began approximately 6 wk after the spill occurred. Mortality of clams was observed through the fall and winter of 1985 to 1986, as noted by the presence of gaping clams (clams with the soft tissues intact, the valves not tightly closed and in a moribund, nonresponsive condition) and a large number of empty shells at the collection site. The frequency of collection of "gapers" dropped to zero as temperatures rose in spring 1986 and remained low throughout the remainder of the sampling period. Empty shells, however, were still a common occurrence along the shore and in shallow subtidal areas. Cold temperatures in winter in this northernmost portion of its range have been thought to cause mass mortalities of wedge clams and may limit its distribution north of Delaware Bay (Gallagher & Wells 1969).

The shell of *Rangia cuneata* is composed of three primary layers: (1) an inner CCL layer; (2) a thin pallial myostracum to which the mantle is attached; and (3) an outer crossed-lamellar layer. Both the inner and outer layers were analyzed to determine the periodicity of growth pattern formation, estimate age, calculate age-specific and seasonal growth rates, quantify the magnitude of the effects of the oil spill and hurricane on growth, and make inferences about the spawning periodicity of *R. cuneata* at the northernmost extent of its range. The information presented here on population dynamics and growth of *R. cuneata* in the Delaware River was previously published by Fritz et al. (1990a) and is reprinted here with their permission (including their Fig. 2–8 as Fig. 20–23, a portion of 25, and 26–28 here, and their Tables 1 and 2 as Table 2 here); the information on the effects of the *Grand Eagle* oil spill and hurricane Gloria on wedge clam growth is new.

Seasonal Changes in Inner Layer Microstructure

The inner shell layer of *Rangia cuneata* is composed of a series of interdigitating first-order (1 deg) lamellae, each composed of second-order (2 deg) lamellae, resulting in a CCL microstructure formed by regions of the mantle dorsal to the pallial line. The CCL microstructure of the inner layer is periodically replaced by thin bands of prisms that are formed during periods of slow shell growth.

In March 1986 (Fig. 18A), two prism bands were observed on the fracture shell section; the first was approximately 3 μM thick and located 15 μM from the inner shell surface, whereas the second, located within a zone of CCL microstructure, was only 1 μM thick and located approximately 2–3 μM from the inner shell surface. Based on the appearance of the inner shell surface (Fig. 18B), which was composed of slightly etched 2 deg lamellae

TABLE 2.

(A) Mean and range in shell length (mm) of spring and fall recruits of *Rangia cuneata* at annual growth marks (Fritz et al. 1990a). (B) Calculated parameters of the von Bertalanffy growth equations [see text equation (1)] for spring and fall recruits.

	Annulus	Spring			Fall		
	Number	Mean	N	Range	Mean	N	Range
A.	1	20.4	55	16.0–25.0	10.6	112	6.0–15.7
	2	38.2	41	30.0–47.3	32.6	107	21.9–41.0
	3	51.8	10	46.3–58.5	47.2	88	35.9–54.9
	4	55.8	8	49.6–61.0	52.4	69	41.0–61.9
	5	60.6	2	59.0–62.2	54.7	9	44.7–58.0
	6		–	–	58.6	2	57.7–59.4
B.	L_∞	66.2	–	–	60.6	–	–
	K	0.519	–	–	0.604	–	–
	t_0	0.273	–	–	0.189	–	–

N, number of specimens analyzed.

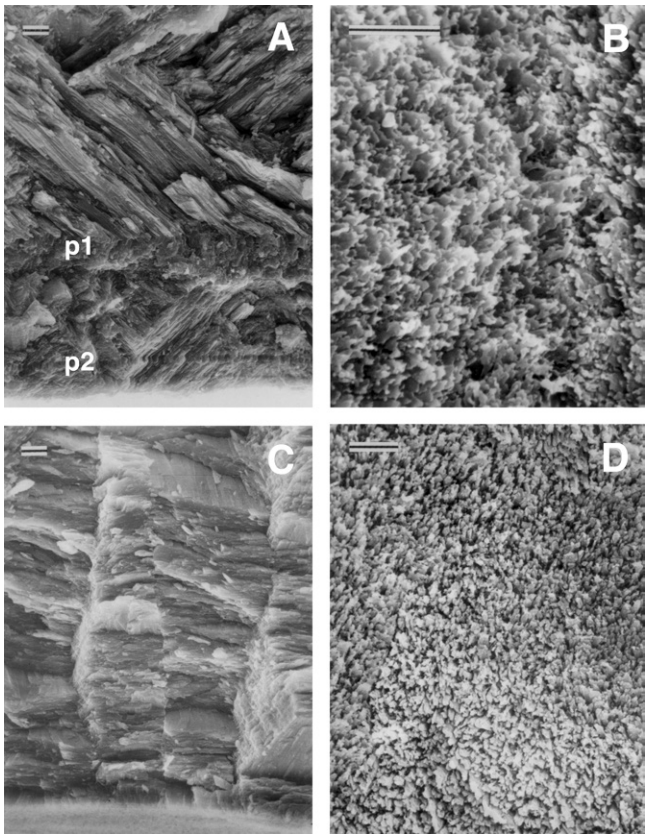

Figure 18. Scanning electron micrographs of radial fracture (A and C; inner surface at the bottom) and inner surfaces (B and D) of the inner complex crossed-lamellar shell layer of *Rangia cuneata* collected in March (A and B) and May 1986 (C and D). In A, p1 and p2 are prismatic bands. Growth is to the right. Scale bars in each micrograph = 3 μM.

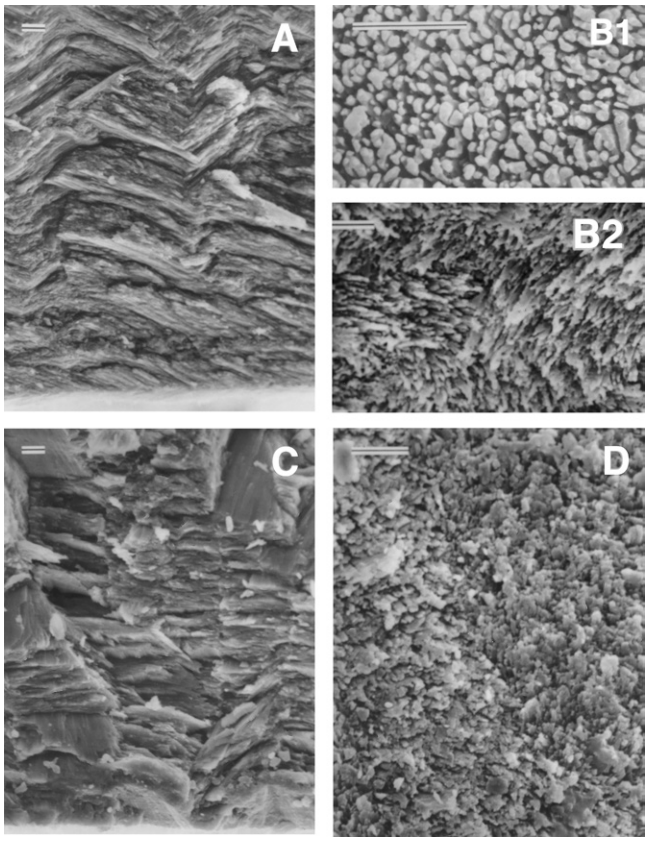

Figure 19. Scanning electron micrographs of radial fracture (A and C; inner surface at the bottom) and inner surfaces (B1, B2, and D) of the inner complex crossed-lamellar shell layer of *Rangia cuneata* collected in July (A, B1, and B2) and September 1986 (C and D). Growth is to the right. Scale bars in each micrograph = 4 μM.

tips, the zone of CCL microstructure was most probably deposited in early spring 1986. Thus, the thicker prismatic band, which also had a granular appearance (evidence of dissolution), was formed during winter, whereas the thinner prismatic band may have resulted from a short period of reduced shell growth rates in early spring. In late spring (May 1986; Fig. 18C, D), shell growth rates increased resulting in a thick zone of CCL microstructure along the fracture radial surface and a characteristic pattern of interwoven tips of 2 deg lamellae along the inner shell surface.

In July 1986, both recent and current deposition of prismatic bands were discernible along the fracture (Fig. 19A) and inner shell surfaces (Fig. 19B1), suggesting that shell growth rates in summer were slower than in spring. Even within a single specimen, the composition and texture of the inner shell surface varied between prismatic columns (Fig. 19B1) and interwoven tips of 2 deg lamellae (Fig. 19B2). The inner layer in September 1986 (Fig. 19C, D) appeared similar to that observed in May, with the exception that the inner shell surface was composed of slightly larger 1 deg and 2 deg lamellae.

Growth of the inner layer was most rapid during the first 2 y after the settlement, with approximately 80% of the total thickness of the inner layer of a 5-y-old specimen being deposited during this period. With increasing age, annual growth rates of the inner layer decreased considerably, such that the two or three most recently deposited annual increments of a 5-y-old were hardly distinguishable from one another. Because of the slow rates of inner layer deposition, the small annual increments after age 2, and the confusing series of prismatic and CCL bands, the inner layer was not considered useful for analyses of shell growth patterns with respect to environmental perturbations or age determination. The number and thickness of prismatic bands, at least two of the largest of which were formed each year, may have some value in impact analyses. Distinguishing annual increments in the inner layer and the time of formation of each prismatic and CCL band was haphazard at best, and inaccurate at worst.

Seasonal Changes in Outer Layer Microstructure

The outer shell layer of *Rangia cuneata* is deposited by regions of the mantle ventral to its attachment to the shell, the pallial myostracum. The outer shell layer is formed incrementally, with increments representing periods of active shell growth and increment boundaries periods of inactivity, or shell dissolution. Microgrowth increment boundaries represent former positions of the inner shell surface and result from periodic short-term (on the order of hours) growth cessations (Lutz & Rhoads 1980, Fritz & Haven 1983, Deith 1985, Fritz & Lutz 1986). The outer shell layer is composed of 1 deg lamellae deposited approximately parallel to the ventral shell

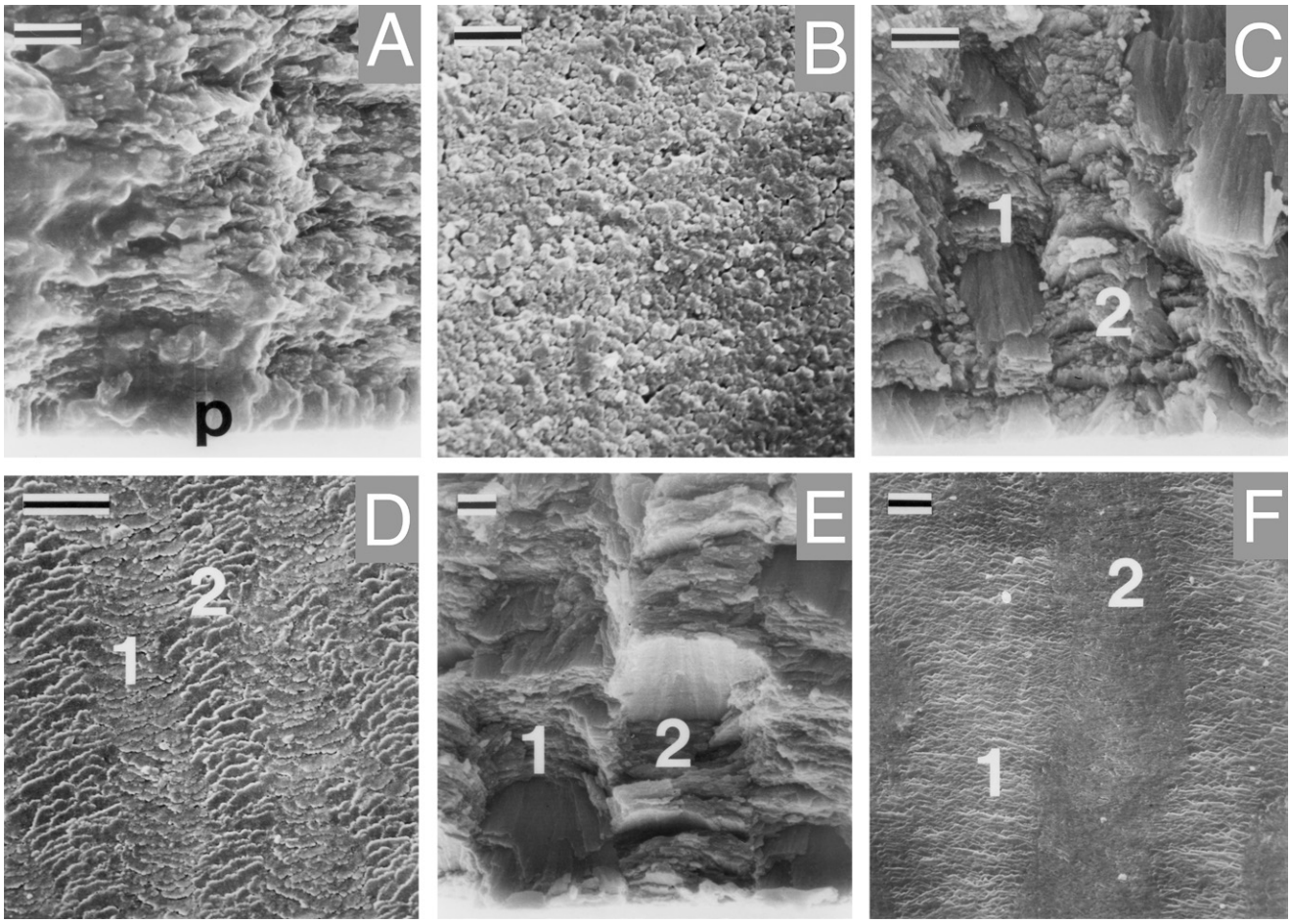

Figure 20. Scanning electron micrographs of radial fracture (A, C, and E; inner surface is at the bottom) and inner surfaces (B, D, and E) of the outer crossed-lamellar shell layer of *Rangia cuneata* collected in March (A and B; p = prismatic band on inner shell surface), May (C and D) and July 1986 (E and F). 1 and 2 denote adjacent 1 deg lamellae. Growth is to the right. Scale bars in each micrograph = 3 μM. Modified from Figure 2 of Fritz et al. (1990a).

margin and perpendicular to microgrowth increment boundaries. First-order lamellae are composed of 2 deg lamellae that are arranged much like shingles on a roof, with their angle of deposition in each 1 deg lamella alternating at approximately 90 deg with respect to those in adjacent 1 deg lamellae (Figs. 20 and 21). Second-order lamellae are themselves composed of 3 deg lamellae, which are generally poorly defined, small, lath or rod-like crystalline units joined at their sides (see Taylor et al. 1969, Carter 1980, Deith 1985).

In March (Fig. 20A, B), the fractured radial surface of the outer layer revealed the presence of a thin band of prisms, approximately 2 μM thick, along the inner surface of the outer layer. This prism band replaced the crossed-lamellae deposited during the remainder of the year and was a result of an extended period of slow shell growth during winter. Along its inner surface, the composition of the outer layer varied between slightly etched prism tips [which are evidence of dissolution of shell carbonates during winter; left portion of Fig. 20B (Lutz & Rhoads 1977)] and prism tips with a thin organic (?) coating (right portion of Fig. 20B). In Figure 20A, immediately above the prism band, the angle of deposition of 2 deg lamellae with respect to the inner surface of the outer layer is small, and 1 deg lamellae are not readily distinguishable. This region of the shell was deposited in late fall/early winter and its poor organization and the small deposition angle of 2 deg lamellae could be a result of declining water temperatures.

By contrast, in spring (May), 2 deg lamellae are angled steeply with respect to the inner shell surface resulting in the exposure of broad faces of some 2 deg lamellae in the fracture radial section (Fig. 20C). Second-order lamellae terminate along the inner shell surface (Fig. 20D) in a characteristic shingled pattern with their angle of deposition alternating in adjacent 1 deg lamellae. This pattern was also observed in specimens collected in fall (September and October) and was characteristic of periods of relatively rapid shell growth.

In summer (July), deposition rates of the outer layer were slower than in spring and fall (this will be discussed further in the following section) resulting in the formation of wider (dorsoventrally) 1 deg lamellae (Fig. 20E). Second-order lamellae within summer-deposited 1 deg lamellae were laid down at smaller angles with respect to the inner shell surface than those formed in spring or fall. The smaller angle of deposition of 2 deg lamellae in summer than in spring or fall yielded a smoother inner shell surface (Fig. 20F). The tips of each 2 deg lamellae were each sharply angled in summer, whereas the ends of those deposited in spring and fall were more lobate (Fig. 20D).

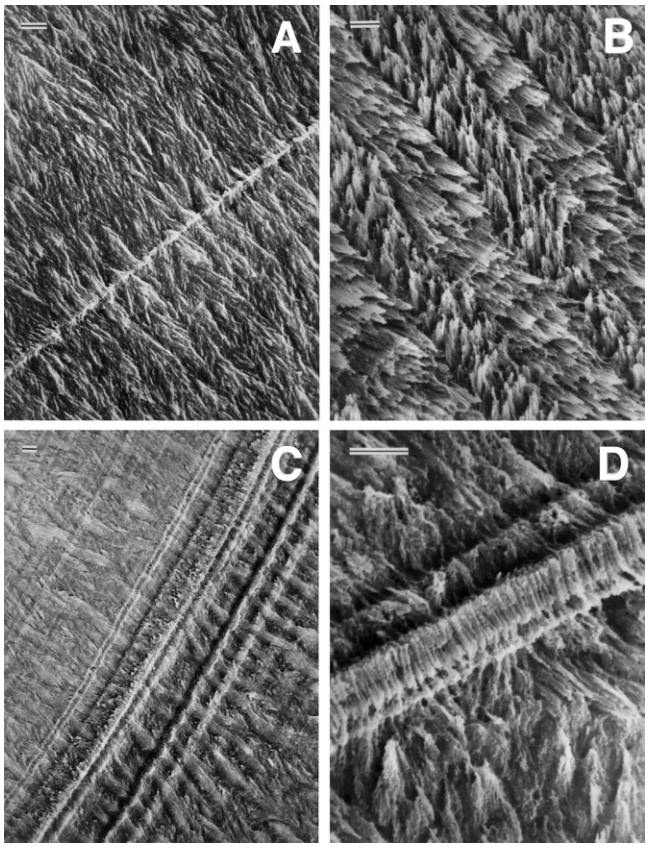

Figure 21. Scanning electron micrographs of polished and etched radial sections of the outer crossed-lamellar shell layer of an *Rangia cuneata* specimen collected in May 1986. Micrographs were taken midway between inner and outer surfaces in regions of the outer layer deposited in spring 1986 (A; fast growth), late summer 1985 (B; slow growth), fall 1984 [C; border between fast (upper left) and slow (lower right) growth], and winter 1985 to 1986 (D; prismatic band in slow growth). The inner shell surface is beyond the bottom of each micrograph and growth is to the right. Microgrowth increment boundaries are diagonal raised lines from lower left to upper right. Scale bars = 5 μM. Modified from Figure 3 of Fritz et al. (1990a).

Differences in the depositional patterns of the outer layer in spring/fall and summer are more clearly evident in polished and etched radial sections. The etching process revealed the broad faces of each spring-deposited, steeply-angled 2 deg lamellae and the boundaries of microgrowth increments, which remain as continuous ridges across the outer layer running perpendicular to each 1 deg lamella (Fig. 21A). The dorsal and ventral edges of 1 deg lamellae deposited in spring are not readily distinguishable (Fig. 21A). This suggests that during periods of relatively rapid growth (e.g., spring), crystalline units within the outer layer tend to be poorly organized relative to the discrete 1 deg and 2 deg lamellae deposited during periods of slower growth (e.g., summer; Fig. 21B). Wada (1961) and Deith (1985) also found that during periods of slow shell growth, crystalline units were larger and deposited in a more orderly fashion, respectively, than during periods of rapid shell growth. Analyses of polished and etched sections also suggest that 2 deg lamellae were deposited at smaller angles with respect to the inner shell surface in summer than in spring. The etchant more clearly revealed the edges of each angled 2 deg lamella in summer-deposited than in spring-deposited outer layer.

Long-term growth cessations (possibly on the order of days) are represented in polished and etched radial sections of the outer layer as thick microgrowth increment boundaries (Fig. 21C) or, in the case of growth cessations in winter, as thin bands of prisms (Fig. 21D). The gcm shown in Figure 21C occurred in the fall of 1985, and could have resulted from one or more of the following events: (1) spawning, (2) the oil spill, or (3) the freshwater and turbulence associated with passage of Gloria (this will be discussed further in the following). The composition of the outer layer changed abruptly at the gcm, from fast-growth crossed-lamellar microstructure preceding it (left portion of Fig. 21C) to one resembling slow-growth microstructure following it (right portion of Fig. 21C). This strongly suggests that the gcm was caused by an event that occurred suddenly (as shown by the lack of slow-growth microstructure immediately preceding it), and that growth slowed following the event. Kennish and Olsson (1975), in their descriptions of growth breaks in the shells of *Mercenaria mercenaria* resulting from spawning events and storms, found similar changes in the outer prismatic layer, with a greater amount of "crossed-lamellar microstructures" present following the gcm.

During winter, a thin band of prisms replaced the crossed-lamellar microstructure of the outer shell layer (Fig. 21D). Prism bands were composed of thin, rod-like columnar subunits (prisms), which often had a granular texture (evidence of dissolution) on their depositional faces. Winter prism bands varied in thickness within an individual for different winters and also between specimens for the same winter, but generally ranged between 3 and 8 μM. The micrograph in Figure 20A, taken on a specimen collected in March 1986, shows the band in the midst of formation, with slow growth crossed-lamellar microstructure immediately preceding it. Similarly, in Figure 21D, slow growth microstructure not only precedes, but also follows the prism band, suggesting that growth in spring did not resume suddenly, but probably increased slowly over an extended period.

A series of annual outer shell layer increments deposited in 1985 by clams of three different ages are shown in Figure 22. Zones of fast and slow-growth crossed-lamellar microstructure appear as light and dark regions, respectively, in acetate peel replicas of polished and etched radial shell sections. Microgrowth increment boundaries, which parallel the inner shell surface, are represented as thin dark lines. Zones of fast growth crossed-lamellar microstructure form a larger percentage of each annual increment in younger (Fig. 22A) than in older (Fig. 22B, C) clams. Furthermore, the zone of fast growth microstructure formed in fall became increasingly smaller with age. Prismatic bands formed in winter appear as thick dark lines surrounded on both sides by fast growth microstructure in younger specimens, suggesting that growth rates were relatively rapid in fall and spring. In older specimens (or annual increments deposited when the clam was over 3 y of age), the winter prismatic band was preceded (dorsal) by slow-growth microstructure formed in fall and followed (ventral) by fast-growth microstructure formed in spring. Growth cessation marks, possibly resulting from spawning in spring and fall (Fig. 19C), appeared as distinct microgrowth increment boundaries in both fast and slow-growth microstructure, and were often accompanied by an indentation in the shell exterior surface.

Microgrowth increment boundaries are clearly visible in both regions of fast and slow-growth crossed-lamellar microstructure.

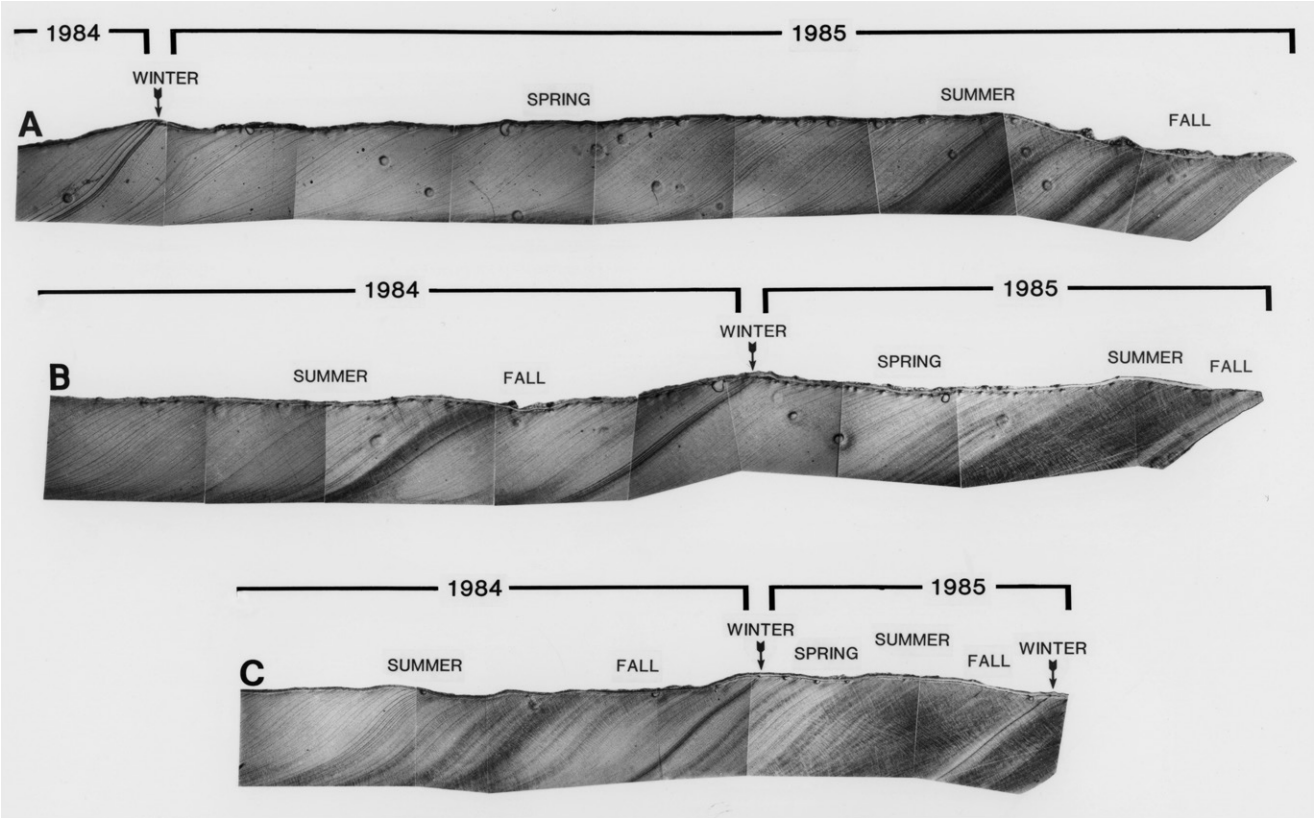

Figure 22. Light micrographs of acetate peel replicas of polished and etched radial sections of the outer crossed-lamellar shell layer of *Rangia cuneata* that recruited in 1983 (A; collected in February 1986), 1982 (B; collected in April 1986), and 1981 (C; collected in March 1987). Complete annual increments deposited in 1985 are marked along with the regions formed each season. Partial annual increments formed in 1984 are also marked along with seasonal deposition. Microgrowth increment boundaries appear as thin dark lines, whereas winter prismatic bands are thicker and more distinct. Growth is to the right, and scale is the same in each series of micrographs. Modified from Figure 4 of Fritz et al. (1990a).

Microgrowth increments represent alternating periods of valve closure (possibly accompanied by anaerobic respiration) and active pumping of water and shell deposition (aerobic respiration), respectively (Lutz & Rhoads 1977). In other species, this cycle has been shown to occur in synchrony with either the solar or lunar day, respectively, in species living subtidally [e.g., *Mercenaria mercenaria* (Pannella & MacClintock 1968, Fritz & Haven 1983) and *Meretrix lusoria* (Roeding, 1798) (Koike 1975)] or intertidally (e.g., *Cerastoderma edule* (Linnaeus, 1758) (Richardson et al. 1979) and *Clinocardium nuttalli* (Conrad, 1837) (Evans 1972)]. In either case, the time of formation of regions of the outer shell layer could be dated through counts of increments from the ventral shell margin (the date of collection) dorsally to the region of interest. This method is accurate only during those periods when the animal is young (ages 0–3) and depositing shell at relatively rapid rates (in spring and fall, and in parts of the summer). As shell growth rates decline in winter and with age, the amount of time represented by gcm increases and the ability to date the time of formation of regions of the shell decreases. In the wedge clam, it is not known whether microgrowth increments are deposited at the rate of one per solar day or two per lunar day (one on each high tide).

Age Determination, Seasonal Growth Rates, and Population Studies

Age of individual specimens was determined by counting the number of winter prismatic bands in the outer shell layer in analyses of acetate peel replicas of polished and etched radial sections. With increasing age (and size), prismatic bands in the inner shell layer became increasingly close together and it became more difficult to distinguish annually produced increments. By contrast, prismatic bands in the outer layer were easily distinguishable even in the oldest specimens analyzed (6 y old). In the first three annual increments, winter prismatic bands in the outer layer (Fig. 21D) appeared as thick dark lines in acetate peels (Fig. 22A, B, C) preceded (dorsal) and followed (ventral) by rapid growth crossed-lamellar microstructure deposited in spring and fall (Fig. 21A). With increasing age, the microstructure of the outer layer deposited in the summer and fall preceding the winter prismatic band became increasingly dark in acetate peel replicas (Fig. 22A, B, C), which is how slow-growth crossed-lamellar microstructure is represented in acetate peels (Fig. 21B). Consequently, in the most recently deposited annual increments of older specimens, the outer layer consisted of alternating regions of rapid-growth microstructure deposited in spring (which appear clear in acetate peels) and slow-growth microstructure deposited in summer and fall, followed by a winter prismatic band.

During the first three annual increments, winter prismatic bands (Fig. 21D) were distinguished from spring or fall spawning (?) marks (Fig. 21C) in acetate peel replicas by (1) the thickness, intensity, and definition of the line; winter prismatic bands

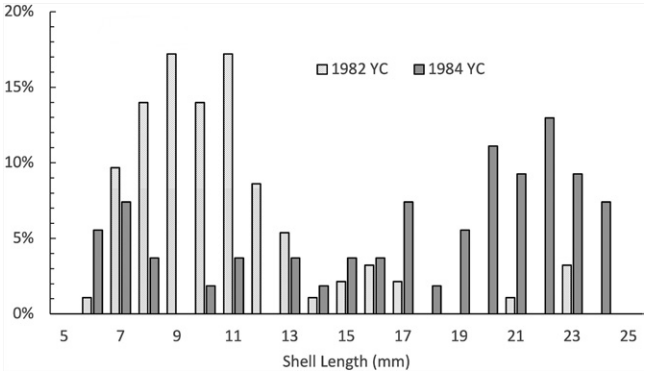

Figure 23. Length frequency at the first annulus (winter prismatic band) for the 182 (*n* = 93) and 1984 (*n* = 54) year-classes of *Rangia cuneata*. Modified from Figure 5 of Fritz et al. (1990a).

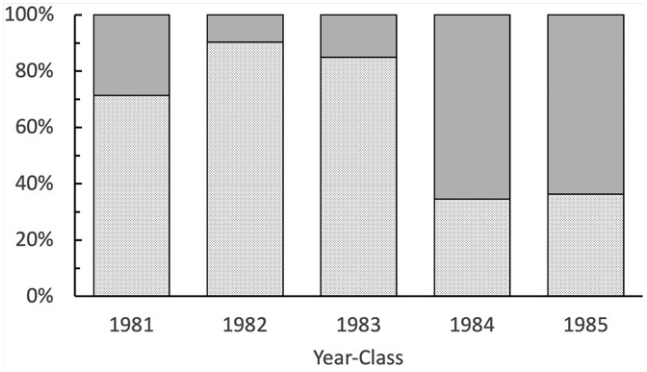

Figure 24. Percent-frequency of spring (solid gray) and fall (dotted) recruits in each year-class (YC) of *Rangia cuneata*. Number of clams analyzed in each YC: 1981 *n* = 7; 1982 *n* = 93; 1983 *n* = 20; 1984 *n* = 54; and 1985 *n* = 11.

were thicker (dorsoventrally), darker, and usually occurred as a single line, rather than as a series of closely spaced, dark micro-growth increment boundaries and (2) the presence of vertical lamellae separating each columnar prism, which were often discernible within the winter prismatic band and were rarely present in spawning marks (Fig. 21C, D). Along the outer shell surface, however, spawning marks and winter prismatic bands were very difficult to distinguish from each other. In most cases, but not all, the darkest rings on the shell exterior were associated with spawning marks and not winter prismatic bands. Furthermore, a distinct ring, located at approximately 20 mm SL, was present on the shell exterior of almost every specimen collected. This ring, which was usually the most prominent on the exterior of the shell, was associated with a spawning mark in shell microstructure and not a winter prismatic band. In the previous studies of the growth of *Rangia cuneata* that used only external rings for age determination (Fairbanks 1963, Pfitzenmeyer & Drobeck 1964), a prominent ring associated with the first spawning, if present in their samples, could have easily been misidentified as an annually formed ring. This in turn would have led them to overestimate individual ages and underestimate growth rate.

Five YC (1981 to 1985) were represented in the collections from November 1985 through March 1987, with the two most numerous being those spawned in 1982 and 1984. The locations of winter prismatic bands identified in shell microstructure were used to identify specific growth rings on the shell exterior surface. Shell length at each winter band, or annulus, was measured directly off the unsectioned valve of each specimen. The size (SL) at the first annulus, ranged from 6 to 25 mm in all specimens analyzed (Table 2). Modal lengths at the first annulus of each YC were either between 8 and 12 mm, or between 20 and 23 mm, as shown for the 1982 and 1984 YC in Figure 23. The bimodal length frequency at the first annulus suggests that the species has two spawning periods each year, one in spring and one in fall. Individual specimens were assigned to either a spring or fall spawning if the SL at the first annulus was greater or less than 16 mm, respectively. Prior to 1984, fall recruits dominated each YC, whereas in both 1984 and 1985, spring recruits were more numerous in our samples (Fig. 24).

Because of the large difference in SL at the first annulus between spring and fall recruits, their growth rates were analyzed separately (Table 2A, Fig. 25). Growth rates of the two groups were almost identical in each YC, but the mean SL of the fall recruits through the fifth annulus was always less than that of the spring recruits; there was considerable overlap in the ranges in SL at all annuli after the first (Table 2A).

Growth equations [von Bertalanffy; modification of the methods of Walford (1946) and Beverton (1954) as described by Ricker (1975)] were developed separately for spring and fall recruits (Table 2B) and had the following form:

$$l_t = L_\infty\ [1 - e^{-K(t-t_0)}]. \quad (1)$$

where l_t is the estimated SL (in mm) at time t (in years), L_∞ is the asymptotic SL, e is the base of the natural logarithm, K is a growth constant, and t_0 is the hypothetical age when SL is equal to zero. Fall recruits were assigned an age of 0.5 y at the first annulus, whereas spring recruits were assigned an age of 1 y. L_∞ was larger and K was smaller for spring than for fall recruits. In the von Bertalanffy growth equation, the lower the value of K, the faster L_∞ is approached, or the faster the growth rate. With the 0.5-y difference in age, however, there was little difference in the size-at-age between the two groups (Fig. 26), suggesting that size- and age-specific growth rates were independent of recruitment time, but at a sampling time, the 0.5-y difference in age between spring and fall recruits of the same YC resulted in a 5–10 mm difference in SL.

The computed SL at each age were greater in our study of Delaware River populations than in studies of southern populations of *Rangia cuneata*. Fairbanks (1963) used external growth lines to determine SL at age of *R. cuneata* populations in Louisiana, whereas Wolfe and Petteway (1968) determined growth rates and size-at-age from changes in modal size-frequency in sequential samples from the Neuse River, NC. Both methods appear to have underestimated growth rate because of the inaccuracies in interpretations of external growth lines (distinguishing spawning from winter lines) and the changes in length frequency distributions over time because of the size differences of fall and spring recruits of the same YC at any point in time. In their studies, 2- and 3-y-old clams ranged in SL from 20 to 29 mm and 24–38 mm, respectively. In our study, 2- and 3-y-old spring recruits ranged in SL from 30.0 to 47.3 mm (mean of 39 mm) and 46.3–58.5 mm (mean of 50 mm),

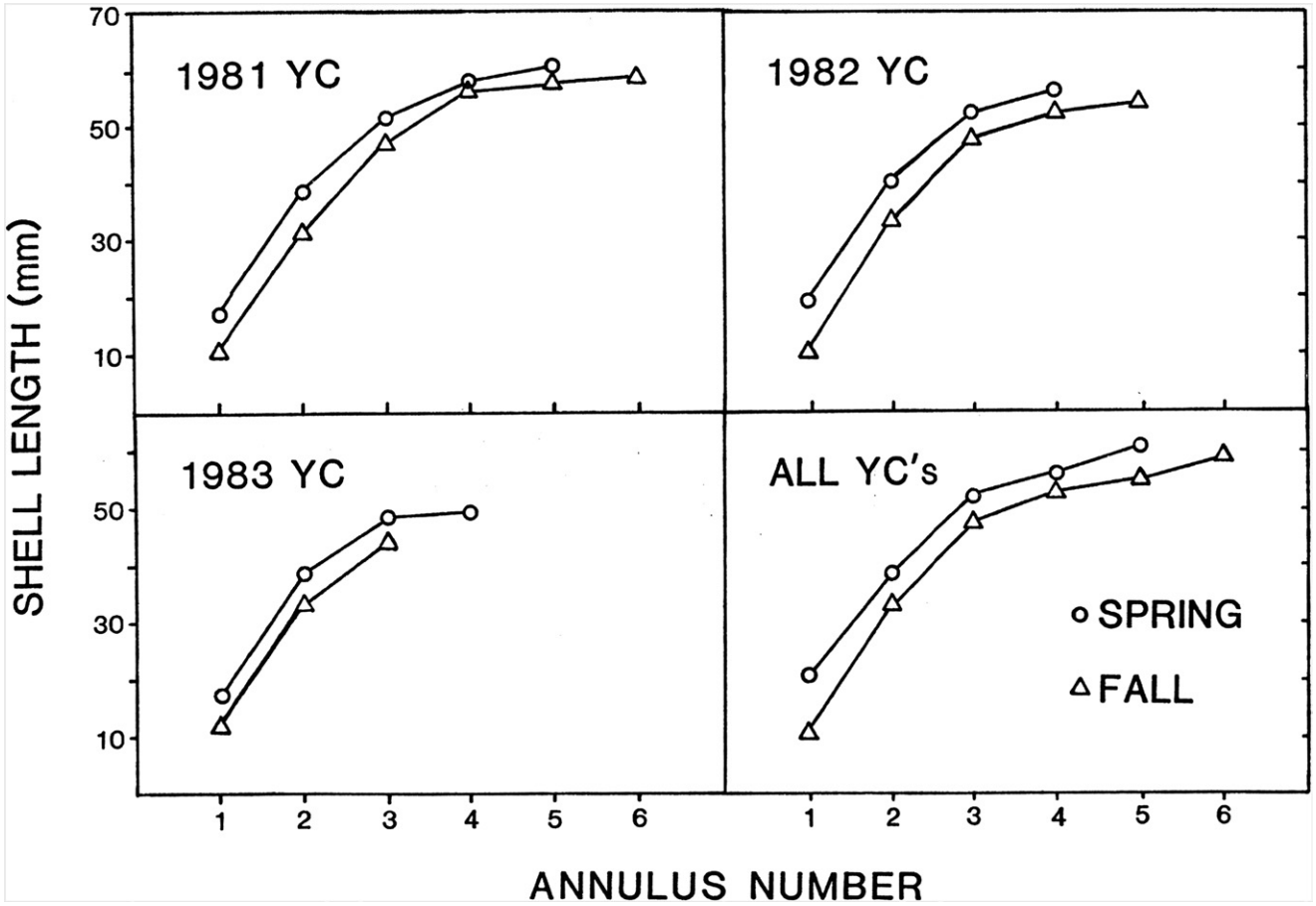

Figure 25. Mean shell length at each annulus (winter prismatic band) of spring and fall recruits of the 1981, 1982, 1983, and all year-classes of *Rangia cuneata*. Modified from Figure 6 of Fritz et al. (1990a).

respectively, or between 10 and 25 mm greater at each age than in the southern studies. Even if the comparison is made with fall recruits only, the shell length-at-age is considerably greater in the Delaware River populations than that reported for southern populations. The possibility also exists, however, that growth rates in the Delaware River are greater than those to the south. Because this is the most northern population of *R. cuneata* on the east coast of North America and shell growth is limited to only the period from May through mid-December each year (see following), this seems unlikely.

In 1986, shell growth resumed in mid-May and continued to mid-December (Fig. 27). Growth rates of the 1984 YC were

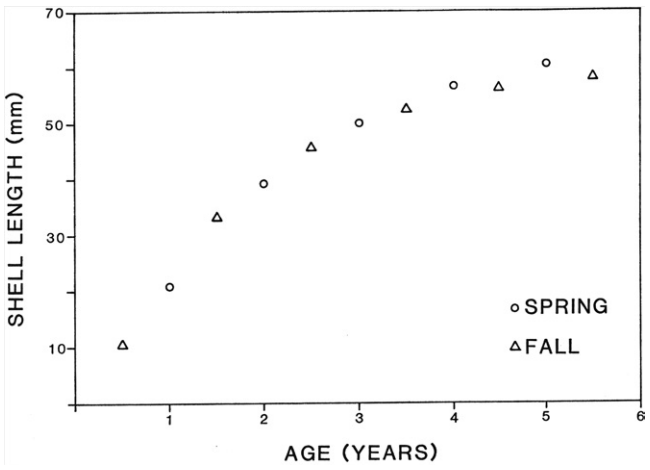

Figure 26. Estimated shell length-at-age of spring and fall recruits of *Rangia cuneata* based on von Bertalanffy growth equations in Table 2B. Modified from Figure 6 of Fritz et al. (1990a).

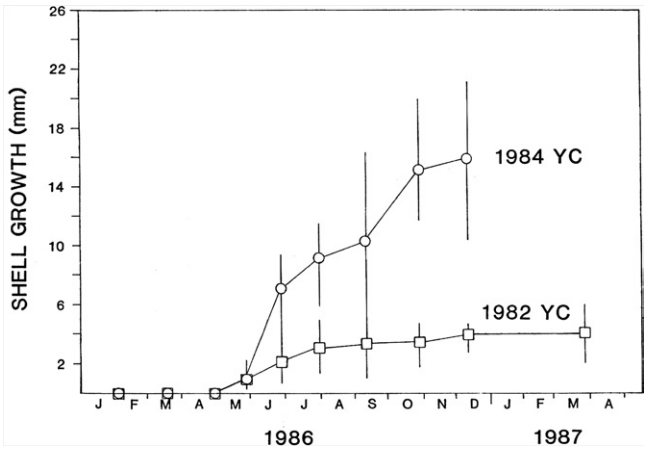

Figure 27. Shell growth (mean and range in mm) from the winter 1985 to 1986 prismatic band in the outer shell layer to the ventral shell margin by the 1982 and 1984 y-classes of *Rangia cuneata*. Modified from Figure 7 of Fritz et al. (1990a).

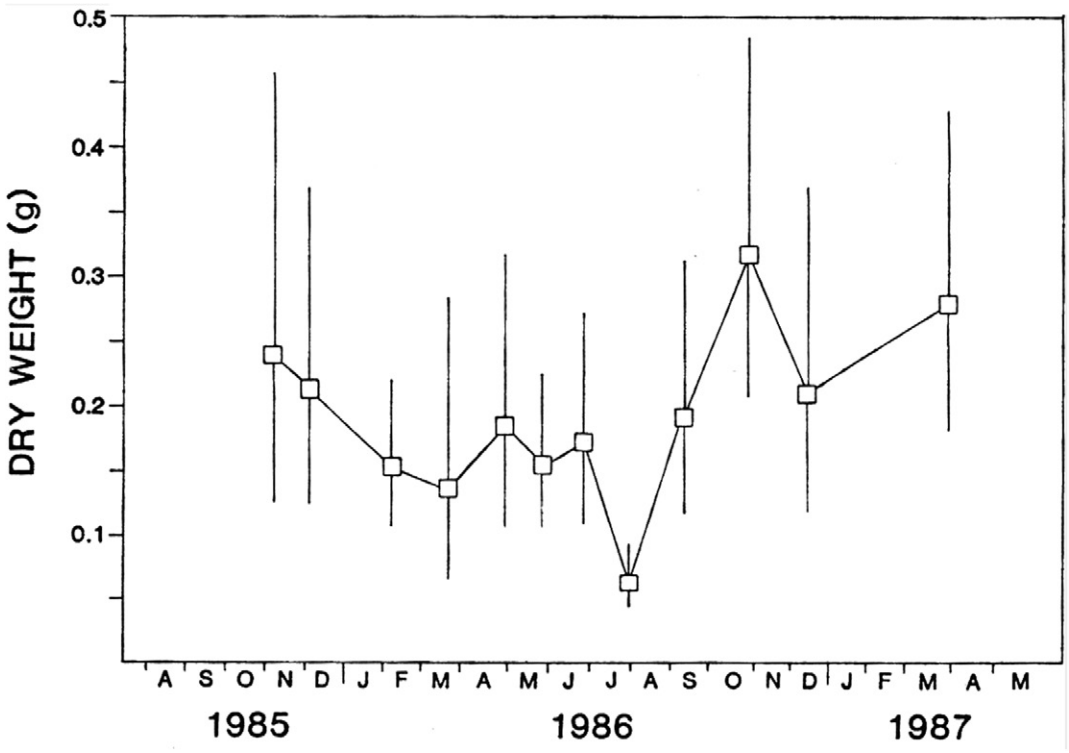

Figure 28. Estimated total dry tissue weight (DTW) of a standard 30 mm specimen of *Rangia cuneata* collected from the Delaware River between November 1985 and March 1987. DTW of a standard specimen were calculated from separate linear regressions of log-transformed tissue weights on log-transformed shell lengths for each collection date. Modified from Figure 8 of Fritz et al. (1990a).

greater in spring (late May through June) and fall (mid-September to through October) than in summer (July through August).

With increasing age, not only did total annual growth rates decline (Figs. 25 and 26), but growth rates tended to remain low from summer through the following winter (Fig. 27; 1982 YC). Spring was the only season when shell growth rates were relatively rapid in specimens older than 3 y. In 1986, members of the 1982 YC had deposited over 75% of their total annual increment by the end of July, while the 1984 YC had deposited only 57%.

Spring and fall were also periods of relatively high DTW compared with winter and summer (Fig. 28). Estimated dry weight declined from late 1985 through March 1986, but increased slightly through April 1986. This increase in dry weight occurred prior to any detectable shell growth (Fig. 27). Spawning most likely occurred in late May and early June, because observations of freshly shucked specimens in late May revealed both ripe and recently spent individuals. Dry weight declined to the lowest calculated value in late July, which coincided with the observed decline in shell growth rates. Through late summer and fall, however, dry weight increased rapidly to its highest calculated value in late October, before dropping in December 1986 and increasing slightly into March 1987. Peaks in dry weight in both spring and fall strongly suggest that *Rangia cuneata* spawns twice each year in the Delaware River, a pattern that Fairbanks (1963) also reported for *R. cuneata* in Louisiana.

Analysis of Shell Growth in 1985

In September 1985, two events occurred that could have adversely affected shell (and tissue) growth of *Rangia cuneata*. Unfortunately, the two events, high river flows and low salinities caused by hurricane Gloria and the spill of 400,000 gallons of oil from the tanker *Grand Eagle*, occurred simultaneously. Thus, distinguishing effects resulting from each event independently in analyses of shell microstructure was not possible. Two factors, however, suggest that what was observed was more likely because of the effects of the hurricane than exposure to the oil: (1) the *R. cuneata* population at the site was exclusively subtidal and (2) the oil was confined to the intertidal area, such as bulkheads and the stalks of intertidal vegetation, and supratidal wetlands. Because of the recent passage of the hurricane, the intertidal zone at this time was approximately 1 m higher in elevation than normal, which further isolated the *R. cuneata* population from exposure to oil.

Three different analyses of shell growth in 1985 were conducted. First, SL of similarly aged individuals in 1984 and 1985 were compared with see whether there were any differences in size-at-age in the 2 y (Table 3). All conditions being similar, each pair of YC should have achieved nearly the same mean SL in 1984 and 1985, assuming there were no significant differences in their initial sizes. For each of the ages tested (1.5, 2.5, and 3.5 y), however, SL was significantly smaller in 1985 than in 1984. Tests of initial size (SL at the first annulus) revealed no significant differences between the 1983 and 1984, and the 1981 and 1982 YC. In the case of the 2.5-y-olds, the 1983 YC was significantly larger at age 0.5 y than was the 1982 YC, but by 1985, the 1983 YC was significantly smaller than the 1982 YC in 1984 despite its larger initial size.

Second, annual increments for 1984 through 1986, as measured along the surface of maximum growth (the height axis, or greatest distance from the umbo to the ventral margin of the

TABLE 3.

Shell lengths of 1.5-, 2.5-, and 3.5—y—old *Rangia cuneata* in the 1981 to 1984 y-classes (YC) at the end of 1984 and 1985.

		Shell length at the end of:							
		1984			1985			*t*-Test	
YC	Age X	Mean	N	STD	Mean	N	STD	Age 0.5	Age X
1983	1.5	33.4	14	3.91	–	–	–	$P > 0.05$	$P < 0.01$
1984	1.5	–	–	–	29.2	16	4.19	–	–
1982	2.5	47.6	73	3.59				$P < 0.01$	$P < 0.02$
1983	2.5	–	–	–	44.1	9	3.82	(83 > 82)	–
1981	3.5	56.2	3	1.15	–	–	–	$P > 0.05$	$P < 0.001$
1982	3.5	–	–	–	52.6	66	3.82	–	–

Only data for fall recruits are reported. Student's *t*-test results are reported from tests of the differences in mean shell length of the two YC at age 0.5 y and at each age X (1.5, 2.5, and 3.5 y). At age 0.5 y, the 1983 YC was significantly larger than the 1982 YC, yet by age 2.5 y, the 1982 YC at the end of 1984 was significantly longer than the 1983 YC was at the end of 1985. N, number of specimens; STD, standard deviation of the sample. Highlighted cells indicate statistically significant differences ($P < 0.05$); YC, year-class.

shell; Pannella & MacClintock 1968) were compared in individuals of the same age (Table 4) in a similar manner to the analysis of shell length-at-age. The mean annual increment deposited by 1.5 and 2.5 y old clams in 1985 was significantly smaller than that deposited by clams of the same age in 1984, but the initial sizes (age 0.5 y) were not significantly different. Furthermore,

TABLE 4.

Annual growth increments formed in 1984 to 1986 by the 1981 to 1985 y-classes (YC; fall recruits only) of *Rangia cuneata*.

		Annual increment formed in									
		1984			1985				1986		
YC	**Age**	**Mean**	**N**	**STD**	**Mean**	**N**	**STD**		**Mean**	**N**	**STD**
1983	0.5	26.38	9	2.63	–	–	–	–	–	–	–
1984	0.5	–	–	–	23.99	10	4.32	–	–	–	–
1985	0.5	–	–	–	–	–	–	–	25.50	1	–
1982	1.5	18.44	57	3.81	–	–	–	–	–	–	–
1983	1.5	–	–	–	13.16	10	2.41	–	–	–	–
1984	1.5	–	–	–	–	–	–	–	19.00	4	4.88
1981	2.5	11.09	4	1.05	–	–	–	–	–	–	–
1982	2.5	–	–	–	5.56	55	1.71	–	–	–	–
1983	2.5	–	–	–	–	–	–	–	8.50	1	–
		***t*-test results comparing growth in:**									
		1984:1985			**1985:1986**				**1984:1986**		
1983	0.5	$P > 0.05$	–	–	–	–	–	–	–	–	–
1984	0.5	–	–	–	na	–	–	–	–	–	–
1985	0.5	–	–	–	–	–	–	–	na	–	–
1982	1.5	$P < 0.001$	–	–	–	–	–	–	–	–	–
1983	1.5	–	–	–	$P < 0.05$	–	–	–	–	–	–
1984	1.5	–	–	–	–	–	–	–	$P > 0.05$	–	–
1981	2.5	$P < 0.001$	–	–	–	–	–	–	–	–	–
1982	2.5	–	–	–	na	–	–	–	–	–	–
1983	2.5	–	–	–	–	–	–	–	na	–	–

Age in years at the beginning of 1984, 1985, and 1986. Student's *t*-tests compared length of annual increments formed each year when each YC was the same age (0.5-, 1.5-, or 2.5-y-old). Within each age, shell lengths at the beginning of each year were not significantly different for all pairs of YCs except for one: the 1984 YC was smaller than the 1982 YC when each was 1.5-y-old (data not shown in table); annual increments formed in 1984 and 1986 by the two YC, however, were not significantly different (data shown in table). N, number of specimens analyzed; STD, standard deviation of the sample. Highlighted cells indicate statistically significant differences; YC, year-class.

1.5-y-olds deposited a significantly larger annual increment in 1986 than in 1985. These data, along with shell length-at-age data in Table 3, strongly suggest that growth rates of *Rangia cuneata* were significantly lower in 1985 than in 1984. Data also suggest that the growth rates returned to pre1985 levels in 1986.

Both quantitative analyzes revealed that size-at-age and growth rates were smaller and lower, respectively, in 1985 than in either 1984 or 1986. The third type of analysis consisted of qualitative comparisons of the microstructure of the outer layer deposited in 1984 and 1985. These analyzes revealed that the slow-growth crossed-lamellar microstructure usually deposited in summer (and longer into fall with increasing age) formed a larger proportion of the total annual increment in 1985 than in the previous year for similarly aged individuals. This can be seen by comparing the micrographs of acetate peels in Figure 22. The 1983 YC specimen (Fig. 22A) was collected at the end of its third growing season in February 1986, whereas the 1982 YC specimen (Fig. 22B) was nearly the same age at the end of 1984. The annual increment deposited in 1985 by the 1983 YC specimen was not only smaller than the 1984 increment of the 1982 YC specimen (Table 4), but also contained more of the slow-growth microstructure and about the same amount of fast-growth microstructure in the spring of each year. This suggests that the reduced growth rates observed in 1985 resulted from an event in late summer that caused the period of slow growth in summer to be continued through the fall. In this manner, the period of increased growth rates that usually occurred in fall (Fig. 27) was restricted to a shorter period in late fall 1985. A similar scenario is also suggested through comparisons of the shell microstructure deposited by the 1982 YC in 1985 (Fig. 22B) and the 1981 YC in 1984 (Fig. 22C).

Analyzes of shell microstructure of *Rangia cuneata* revealed the presence of prismatic bands formed each winter in the outer crossed-lamellar layer that were useful in age determination. During spring and fall (in specimens younger than 3 y old), the 2 deg lamellae in the outer layer were deposited at a greater angle with respect to the inner shell surface than in summer. Spring and fall were also periods of faster shell growth than summer. Thus, the fast-growth crossed-lamellar microstructure (spring and fall) was composed of steeply angled 2 deg lamellae within loosely arranged 1 deg lamellae. Slow-growth crossed-lamellar microstructure(summer) consisted of well-defined 1 deg lamellae in which the 2 deg lamellae were deposited at smaller angles with respect to the inner shell surface than in the fast-growth microstructure. The inner CCL layer also contained prismatic bands formed in winter and summer, but the low deposition rates of this layer (after age 2 y) reduced the value of inner layer analyses.

Bimodal length frequency at the first annulus (prismatic band in the outer layer), as well as peaks in calculated dry weight in spring and fall strongly suggest that *Rangia cuneata* spawns twice each year in the Delaware River, in spring and fall. Age- and size-specific growth rates of recruits from each spawning were nearly identical, but the 0.5-y difference in age between spring and fall recruits resulted in a difference of 5–10 mm in SL at any one time, depending on age.

Quantitative analyses of shell growth (shell length-at-age and length of annual increments) revealed that growth rates were slower in 1985 than in either 1984 or 1986. Furthermore,

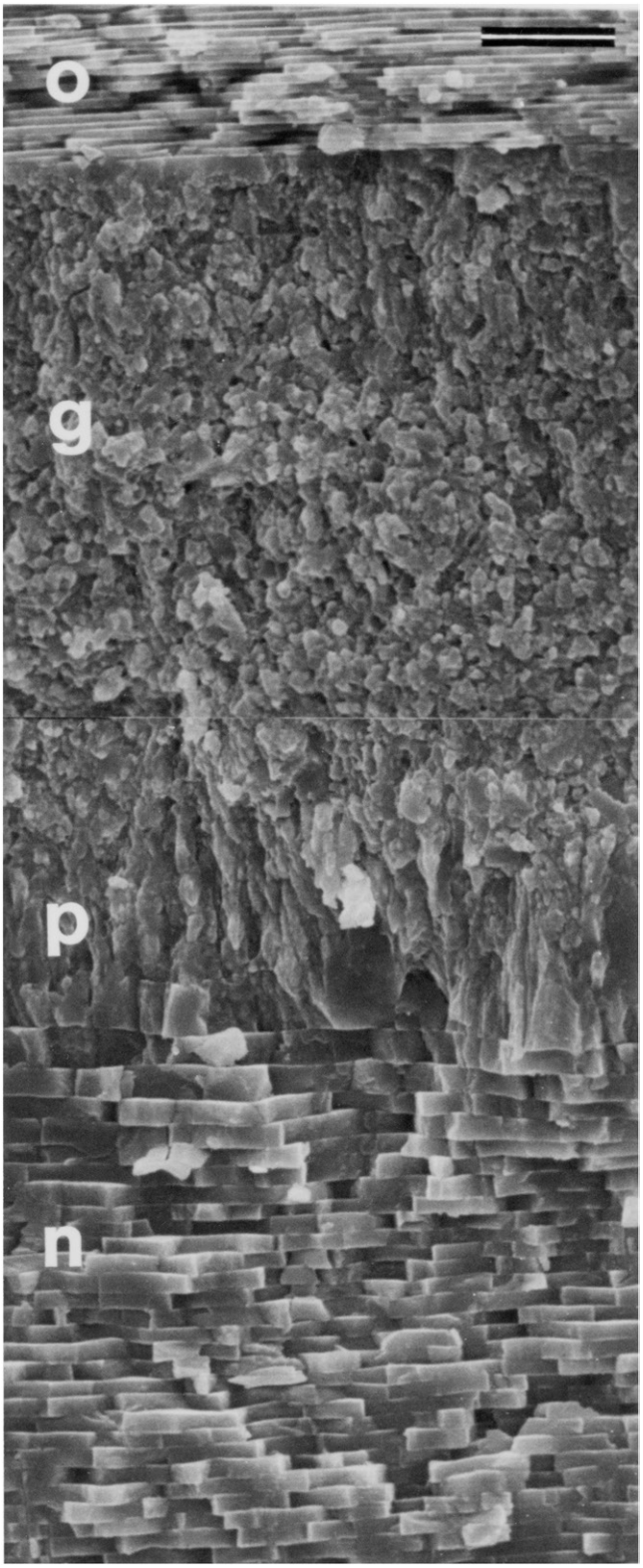

Figure 29. Scanning electron micrograph of a fracture section of *Geukensia demissa* shell showing the outer aragonitic nacreous layer (o), and the three sublayer microstructures of the inner aragonitic layer: granular (g), prismatic (p), and nacreous (n). Growth is to the right and inner surface is beyond the bottom of the micrograph. Scale bar = 4.3 µM.

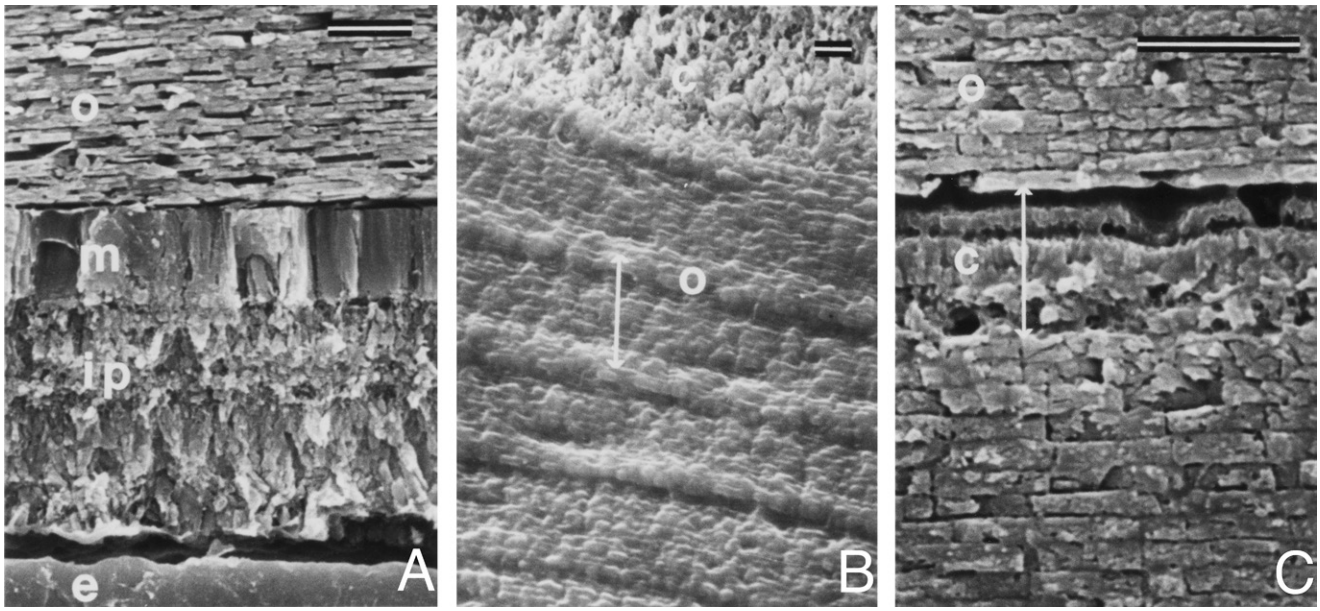

Figure 30. Scanning electron micrographs of polished and etched radial shell sections of *Geukensia demissa*. Growth is to the right in A and C, and to the left in B. Scale bars = 4.3 μM. (A) Micrograph taken just anterior to pallial line showing outer nacreous layer (o), the pallial myostracum (m) an irregular prismatic (ip) sublayer of the inner layer and the epoxy embedding medium (e). (B) Outer blocky calcitic layer (c) and a series of microgrowth increments in o; the double-headed arrow delineates one increment. (C) Growth disturbance (double-headed arrow) formed in fall 1985 (likely because of Hurricane Gloria in late September 1985) in the o of specimen collected from Delaware Bay. An abrupt growth disruption (top of arrow) apparently caused the mantle to completely disengage from the posterior shell margin. Upon growth resumption, thin layers of periostracum and c were formed, and then underlain with o (bottom).

this reduced rate of annual growth was because of slower than expected growth rates in fall 1985, the same time that hurricane Gloria passed near New Jersey and an oil spill occurred at the site. Although it was not possible to link the effects of either event alone with decreased growth, it was suspected that the high turbulence and low salinities associated with the hurricane more likely resulted in the observed effects than the immediate effects of the oil spill, which was restricted to the upper intertidal zone.

Geukensia demissa, the Ribbed Mussel

The Atlantic ribbed mussel, *Geukensia demissa*, is a common epifaunal member of the intertidal community along the east coast of North America. It attaches to hard substrates such as bulkheads, jetties, and the stems of intertidal grasses by means of its byssus. The ribbed mussel deposits a complex series of crystal types in its four-layered shell [from exterior to interior: (1) a thin (usually <10 μM thick) calcitic layer composed of blocks or granules directly beneath the periostracum; (2) an outer nacreous aragonitic layer; (3) a thin (approximately 3 μM thick) pallial myostracum, also composed of aragonite, to which the mantle is attached; and (4) an inner aragonitic layer with sublayers of granular, prismatic, and nacreous units (Figs. 29–31; Blackwell et al. 1977, Lutz & Rhoads 1978, Lutz & Castagna 1980, Lutz & Clark 1984)]. Seasonal changes in shell microstructure were more prominent in the inner layer, but observed growth patterns in the outer layer may also be useful in reconstructing growth histories of individual mussels.

Seasonal high water temperatures were similar at each collection site: approximately 1°C in January, approximately 10°C in April, 22°C–27°C in June to August (with the coolest summer temperatures at Sandy Hook Bay) and approximately 10°C in November each year. Mussel populations at each site, however, were exposed to ambient air temperatures during each low tide. In addition, salinity regimes at each site were quite different from one another. At the Maurice River site off Delaware Bay, the daily range in salinity was greater (10‰–20‰ difference between high and low tides depending on the month) and the monthly means in salinity were approximately 5‰–10‰ lower (11‰–16‰) than at the other three sites (Delaware Bay: 20‰–25‰; Sandy Hook Bay: 21‰–27‰; and Great Bay: 21‰–30‰).

Outer Nacreous Layer

The outer aragonitic layer is deposited by portions of the mantle posterior to the pallial line (or myostracum). It is composed of nacreous tablets deposited parallel to the inner shell surface (Fig. 29) and arranged in a series of microgrowth increments, which reflect alternating periods of shell growth and growth cessation (Figs. 30B and 31A). In polished and etched shell sections, periods of growth cessation, or increment boundaries, appear as ridges because these areas are more resistant to dissolution by etching solutions (Fig. 30B). According to the theory of growth line formation proposed by Lutz and Rhoads (1977), increment boundaries contain a greater proportion of organic material than the increments themselves, which results in less dissolution of these areas of the shell during etching. This theory is based on the results of a series of experiments by Dugal (1939) and Crenshaw and Neff (1969) in which shell carbonates were shown to buffer the acidic end products of glycolysis (anaerobic respiration). Dissolution of carbonates along the inner shell surface would leave an organic-rich layer (relative to the shell beneath it) upon which new shell is deposited during the next period of aerobic metabolism. These processes

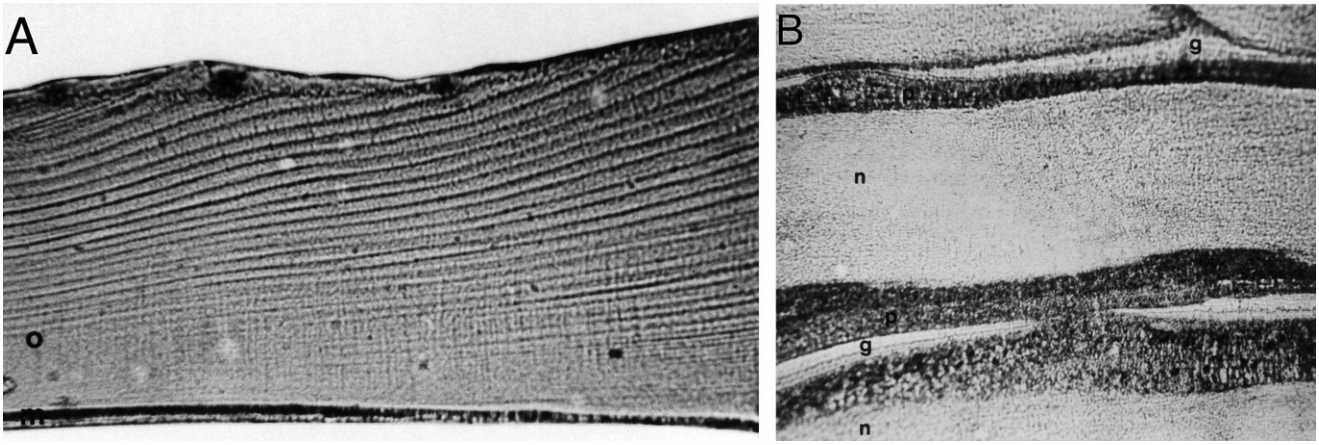

Figure 31. Light micrographs of acetate peels of polished and etched radial sections of *Geukensia demissa* shells. Growth is to the right. (A) Outer layer (o) showing a series of microgrowth increments and the pallial myostracum (m). Horizontal field width (HFW) = 0.7 mm. (B) Inner layer with the three basic sublayers; granular (g), prismatic (p), and nacreous (n). HFW = 0.73 mm.

appear to be operating at the posterior margin of the shell during alternating periods of tidal inundation (aerobic metabolism and increment deposition) and aerial exposure (anaerobic metabolism or air-gaping; Lent 1969), resulting in dissolution and formation of an increment boundary. When an acetate peel replica of the etched surface is made, the increment boundaries (ridges) appear as distinct growth lines in the outer layer separating microgrowth increments (Fig. 31A). Wilbur (1972) suggested that during periods of adverse environmental conditions (e.g., cold temperatures, extreme salinity fluctuations, and extended period of aerial exposure) that would result in metabolic stress, shell decalcification may predominate over shell formation (see also Lutz & Rhoads 1977, 1980, Lutz & Clark 1984). The greater (or more prolonged) the stress, the greater

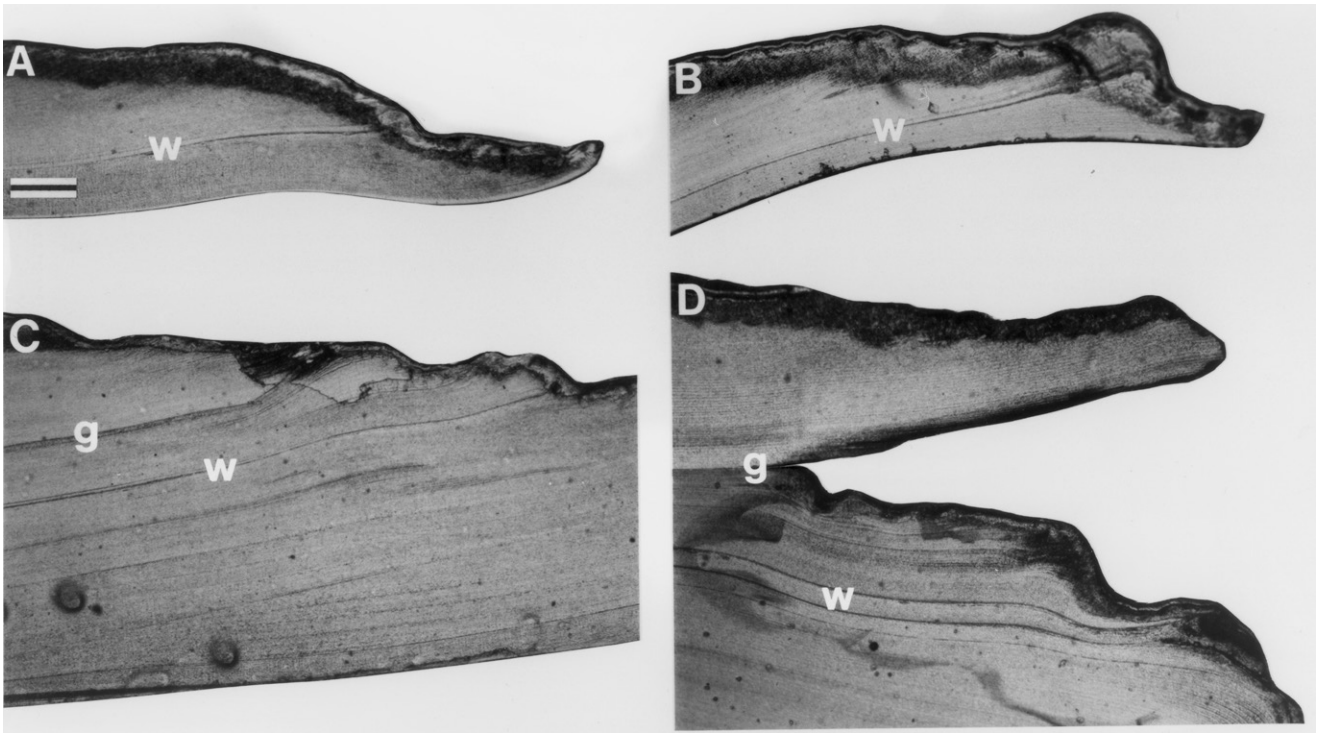

Figure 32. Light micrographs of acetate peel replicas of polished and etched radial sections of outer layers of *Geukensia demissa* shells at the posterior margin tips (A and B) and at portions of the shell deposited in fall 1985 through spring 1986 (C and D). Growth is to the right and the inner shell surface is at the bottom. Scale bar = 0.2 mm (same scale for all micrographs). (A) 7-y-old specimen collected June 1988 from Great Bay. Shell growth in spring 1988 from the winter 1987 to 1988 growth cessation mark (gcm) (w) to the shell margin is 0.615 mm. (B) 9-y-old specimen collected June 1988 from Sandy Hook Bay. Shell growth in spring 1988 from w to the shell margin is 0.615 mm. (C) Same specimen as in A. The disturbance associated with Hurricane Gloria in late September 1985 resulted in a gcm (g), which was followed (posteriorly) by the winter 1985 to 1986 gcm (w). (D) 8-y-old specimen collected July 1988 from Sandy Hook Bay. At g, extensive shell terracing resulted from the disturbance associated with Hurricane Gloria, suggesting that the mantle was disengaged from the posterior shell margin. Growth in fall 1985 resumed at a point anterior to the shell margin, which created the terrace, and the winter 1985 to 1986 gcm (w) was formed subsequently.

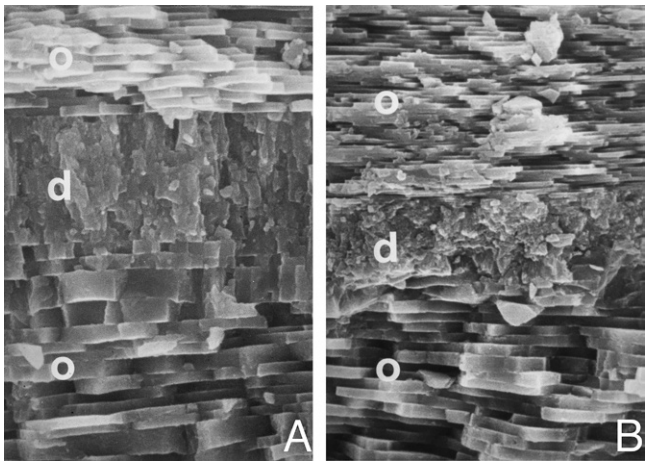

Figure 33. Scanning electron micrographs of fracture sections of the outer nacreous layer (o) of *Geukensia demissa* shells showing the winter 1985 to 1986 growth cessation mark (d). Note the thin tablets formed in fall 1985 (top) and the thicker tablets formed in spring 1986 (bottom). Both specimens collected from Delaware Bay; A in June 1986 and B in November 1986.

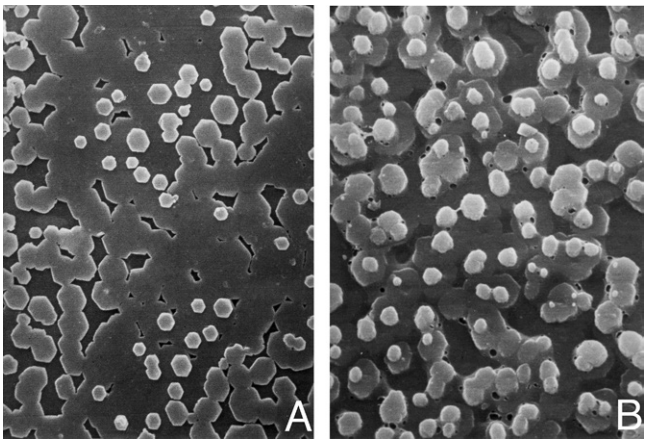

Figure 35. Scanning electron micrographs of inner surfaces of the outer nacreous shell layer of *Geukensia demissa*. Both micrographs taken within the posterior shell margin dentition. (A) Specimen collected in September 1986 from the Maurice River and growth is to the right. (B) Specimen collected in May 1987 from the Delaware River and growth is to the left.

the dissolution of the inner shell surface resulting from it, which would leave a thicker, more prominent increment boundary, or gcm (Figs. 32–34).

The seasonal sequence of outer layer nacre formation described here is very similar to that described by Lutz and Clark (1984) for *Geukensia demissa* and Wada (1972) for *Pinctada martensii* (=*Pinctada martensii fucata* Gould 1850) and *Pinna attenuate* (Reeve 1858). Microgrowth increments in the outer nacreous layer were widest (growth was most rapid) in early summer and early fall. This was accompanied by deposition of crisp, regular, and hexagonal tablets at all sites (Figs. 35 and 36E). Nacre deposition during fast-growth periods appeared as crystal waves across the inner surface of the outer layer, where tablets in one layer were being formed on the nearly completed layer beneath it (Figs. 35A and 36E). During the hottest portions of the summer, it was not uncommon to find dissolved nacre tablets along the inner shell surface (Fig. 36C) much like those observed in winter (Fig. 37). When temperatures were cool (e.g., during early spring and late fall), growth was slower (microgrowth increments were

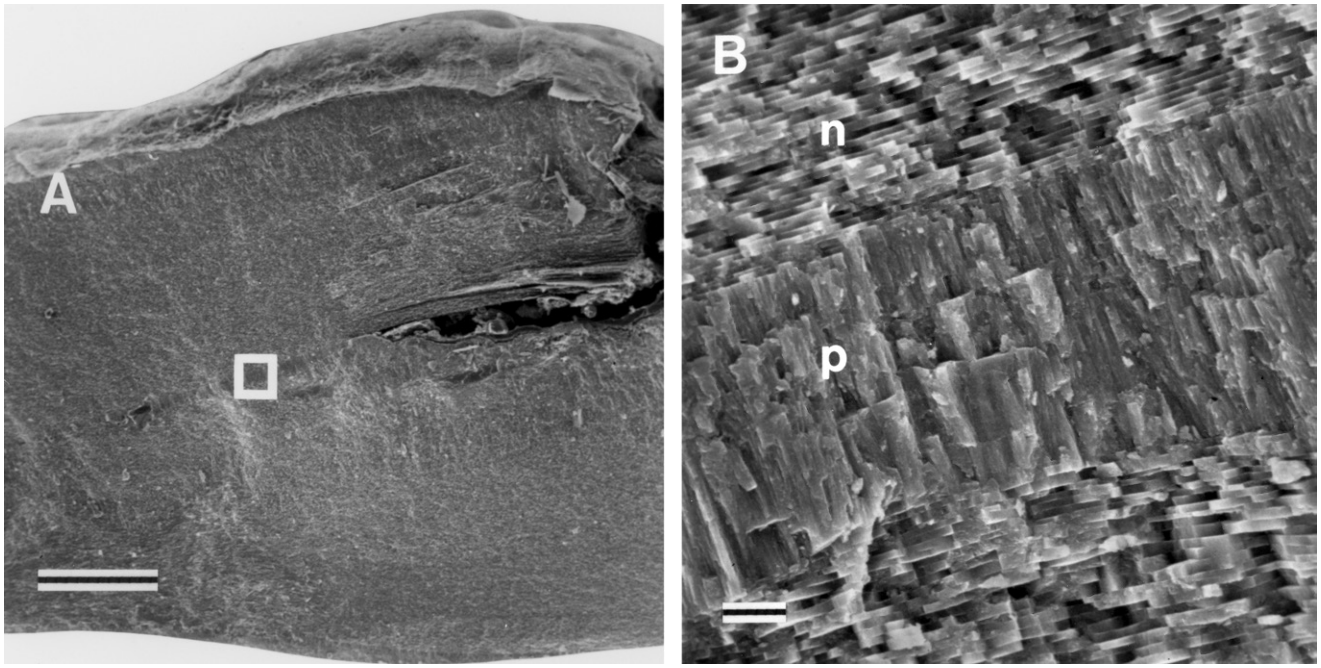

Figure 34. Scanning electron micrographs of fracture sections of the outer shell layer of *Geukensia demissa* collected in July 1988 from Great Bay. Growth is to the right and the inner shell surface is at the bottom (A; scale bar = 0.25 mm) or beyond the bottom (B; scale bar = 5 μM) of each micrograph. Low-magnification micrograph (A) shows the growth cessation mark and shell terracing associated with winter 1987 to 1988, and the square denotes the location of the micrograph in (B). n—layers of nacreous tablets; p—prismatic sublayer within outer layer deposited in winter 1987 to 1988.

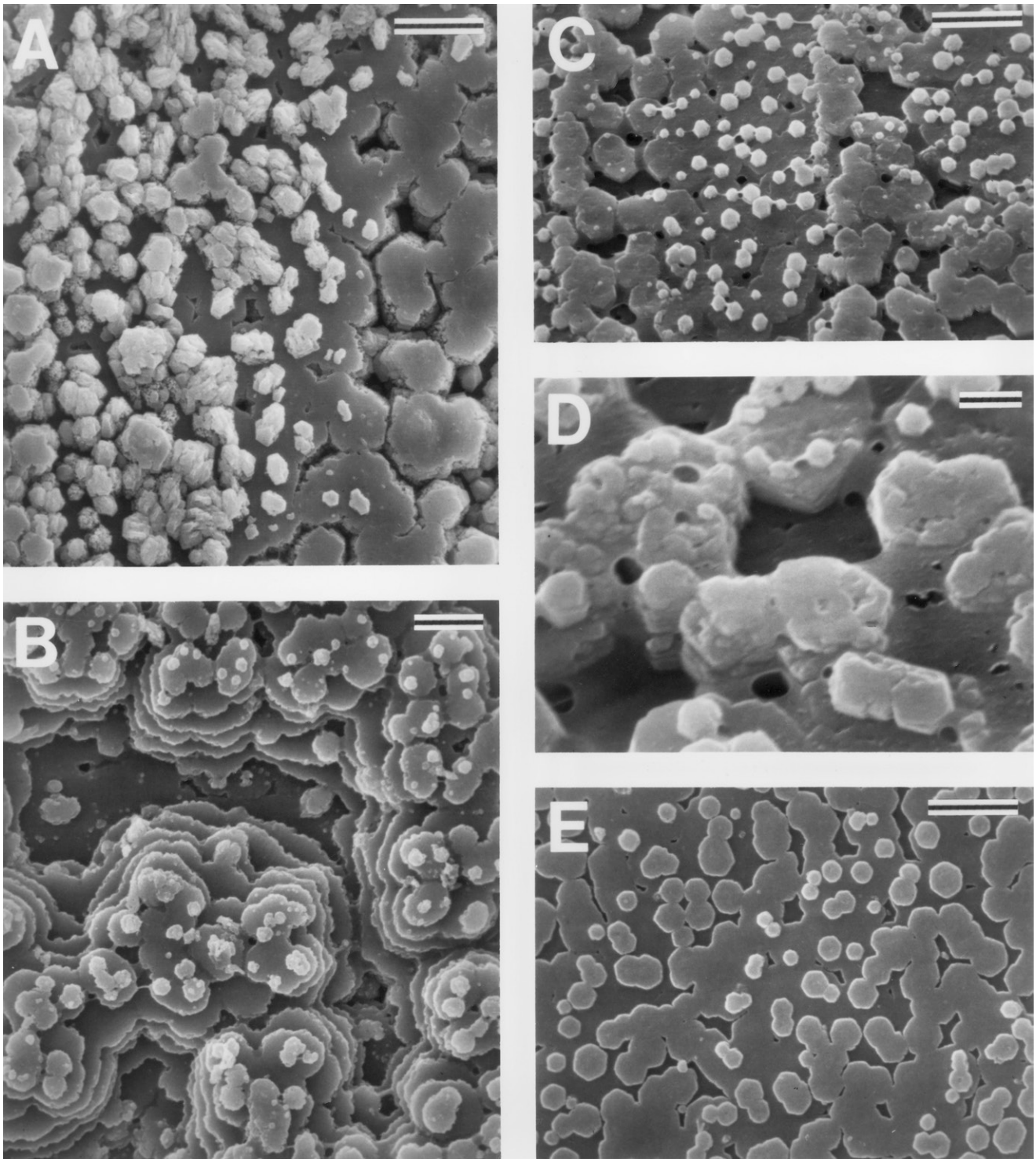

Figure 36. Scanning electron micrographs of inner surfaces of the outer nacreous shell layer of *Geukensia demissa*. Growth is to the right. Scale bars in A, B, C, and E = 5 μM; in D = 1 μM. (A) 2-y-old collected in November 1987 from Great Bay with dissolved, stacked nacre associated with slow growth. (B) 2-y-old collected in May 1988 from Great Bay with extensive conical stacking associated with slow growth. (C and D) 2-y-old collected in July 1988 from Great Bay with wave-form nacre with some evidence of stacking and dissolution. (E) 1-y-old collected in October 1988 from Great Bay with crisp, wave-form nacre associated with fast shell growth.

narrower) and nacreous tablets were thinner (in fracture section; Fig. 33) than in summer. In addition, nacreous tablets were often stacked one on top of another, incompletely formed tablet instead of being distributed in crystal waves as in warmer months (Figs. 35B and 36A, B). In winter, when shell growth ceased, there was evidence of dissolution of nacre tablets along both fracture and inner surfaces, which often left a gcm in outer layer microstructure (Figs. 30C and 32–34). Severe storms, such

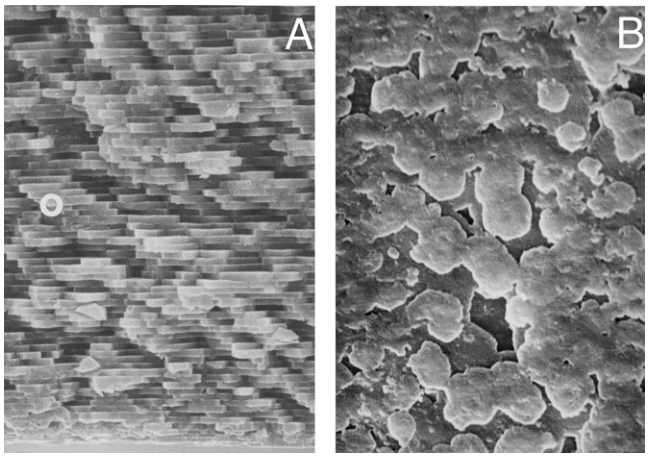

Figure 37. Scanning electron micrographs of a fracture section (A) and the inner surface (B) of the outer nacreous shell layer (o) of *Geukensia demissa* collected March 1987 from the Maurice River. Growth is to the right. (A) Regular nacre tablet deposition in o, with evidence of tablet dissolution near the inner shell surface (bottom). (B) Dissolution in winter of nacreous tablets deposited in fall 1986. Note the remnants of stacked tablet deposition.

as Hurricane Gloria in September 1985, also resulted in a cessation of growth and a mark left in shell microstructure (Figs. 32C, D). Growth cessation marks in the outer layer consisted of prismatic sublayers within the nacreous microstructure (Fig. 34) or granular sublayers consisting of dissolved and reworked prisms or nacreous tablets (Fig. 33).

Inner Aragonitic Layer

The microstructure of the inner aragonitic layer of *Geukensia demissa* seasonally alternates between two different depositional types, nacre and prisms (Lutz 1977, Lutz & Rhoads 1978, Lutz & Castagna 1980, Lutz & Clark 1984), which will hereafter be referred to as sublayers of the inner layer (Figs. 29 and 31B). There is also a third microstructure present, granular, which results from a reworking of the originally deposited microstructure (Lutz & Rhoads 1978, Lutz & Castagna 1980, Lutz & Clark 1984). Granular sublayers in the inner layer are not depositional features *per se*, but a result of dissolution and redeposition of the sublayer present along the inner shell surface by processes similar to those described for outer layer microgrowth increment formation (Lutz and Rhoads 1977, 1978, Lutz & Clark 1984).

Nacreous tablets in the inner layer in both fracture and polished/etched sections appear much like those in the outer layer, except that those in the inner layer are usually thicker and are not arranged as a series of increments. In acetate peel replicas of polished and etched sections of the inner layer, nacre sublayers appear as relatively clear areas with the individual nacre layers represented as small striations parallel to the inner shell surface. Prismatic columns are arranged perpendicular to the inner shell surface and granular microstructure appears as a sublayer of small granules or spheres of carbonate. Prismatic columns appear as relatively dark areas, and often have striations arranged perpendicular to the inner shell surface. Granular microstructure is represented in acetate peels as clear areas, with no or little apparent structure.

The general cycle of sublayer deposition within the inner shell layer of *Geukensia demissa* at each of the four sites was

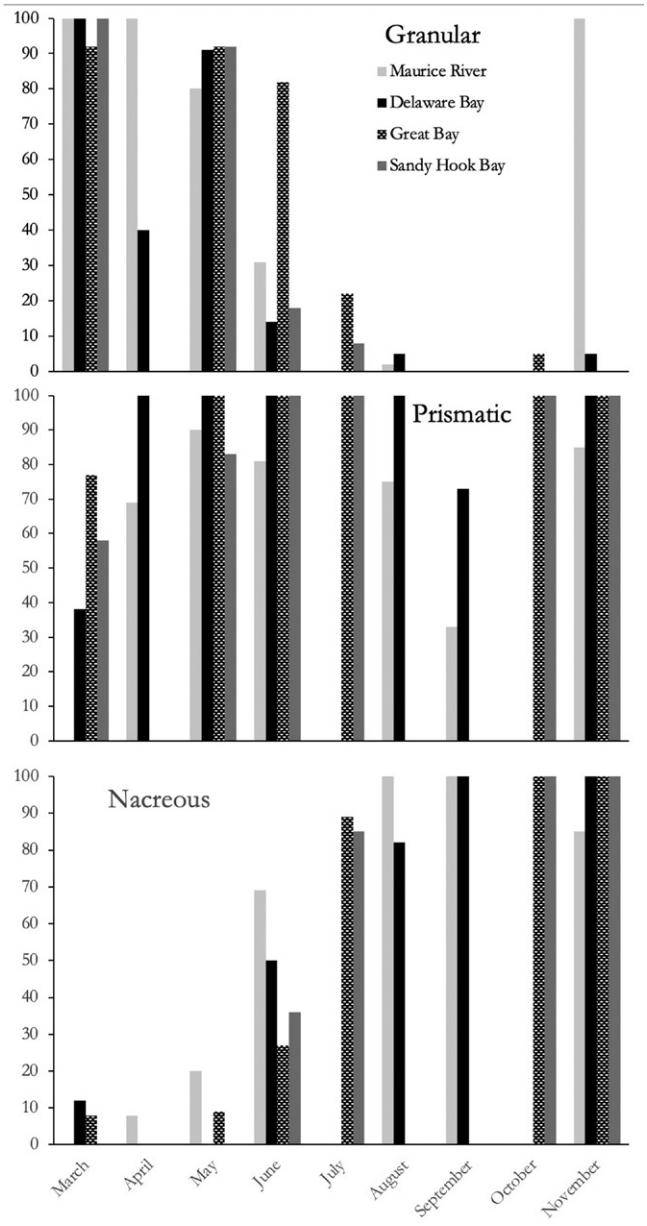

Figure 38. Percent of *Geukensia demissa* specimens sampled each month and site that had granular, prismatic, or nacreous microstructure along some portion of the inner surface of the inner shell layer. More than one microstructure could be present; thus, percentages sum to >100%.

similar to that described by Lutz and Clark (1984) for populations in the mid-Atlantic region (Cape Cod to Cape Hatteras), with formation of (1) prismatic sublayers in late spring and late fall; (2) nacreous sublayers in summer and early fall; and (3) occasional irregular prismatic sublayers in the warmest periods and granular sublayers as remnants of dissolution during the coldest months. As shown in the depositional sequences observed in this study (Figs. 38–51), there was considerable site-specific variation superimposed on this general pattern of microstructural sublayer formation in the inner shell layer.

In March, granular microstructure was the most commonly observed sublayer present along the inner surface of the inner shell layer at all four sites, and in the Maurice River, it was the only microstructure observed. At the other three sites, prisms

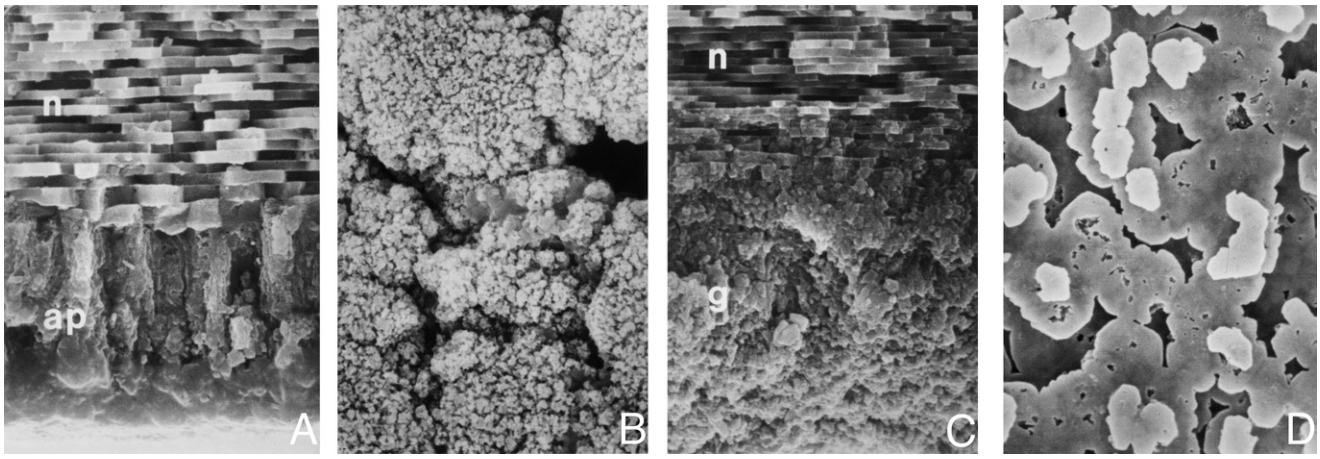

Figure 39. Scanning electron micrographs of fracture sections (A and C; inner surface at the bottom) and inner surfaces (B and D) of the inner shell layer of *Geukensia demissa* collected in March 1987 from the Maurice River. Growth is to the right. (A, B, and D) Same specimen showing altered prismatic (ap) along the inner surface and nacre (n) above deposited in fall 1986 (A), and with coarse granular (B) and reworked nacre along the inner surface. (D) Different specimen with granular (g) along inner surface, n above and no evidence of prismatic microstructure remaining.

were the second most commonly observed sublayer, followed by nacre (Figs. 38–40 and 41A–E). Granular sublayers were generally only several μM's thick across most regions of the inner shell margin, and were the remnants of either dissolved nacre or prisms. If prisms or nacre were present on the inner surface, they almost all showed evidence of dissolution. By April, prismatic sublayers had replaced granular as the most commonly observed microstructure in Delaware Bay, but granular was present in all specimens from the Maurice River (Figs. 38, 42, and 43A, B). Furthermore, when prisms were along the inner shell surface, they were more altered or had been subject to more extensive dissolution in the Maurice River than in Delaware Bay. In May, prismatic sublayers became the most common sublayer present at Maurice River, DE Bay, and Great Bay (though granular sublayers were observed as well in >80% of the mussels analyzed), whereas granular sublayers predominated at Sandy Hook Bay (Figs. 38, 41F, G, 44, and 45A, B).

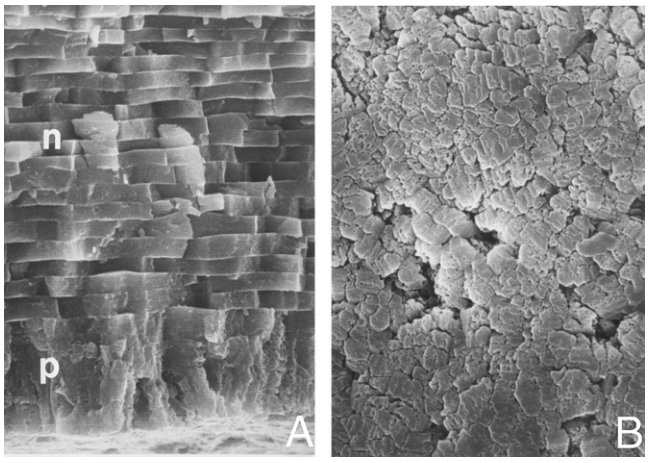

Figure 40. Scanning electron micrographs of fracture section (A; inner surface at the bottom) and inner surface (B) of the inner shell layer of *Geukensia demissa* collected in March 1987 from Delaware Bay. Growth is to the right. There is a thin prismatic sublayer (p) along the inner surface with nacre deposited in fall 1986 above (A) and a lack of granular microstructure (B).

Granular microstructure was usually restricted to regions of the inner shell surface near the pallial line (Figs. 41F, G, and 45A, B), whereas prisms were thickest near the umbo.

Prismatic sublayers in May from Delaware Bay (Fig. 44A, B) were generally less altered with more well-defined edges than those from the Maurice River (Fig. 44C, D). Prismatic sublayers predominated on inner surfaces of the inner shell layer in June and July (Figs. 38, 43C, D, 45C, D, 46, 47A, B, and 48C, D). Nacre was the second most common sublayer observed, particularly in the Maurice River and Delaware Bay where it was generally found in small, isolated patches near the umbo (Figs. 38 and 47C, D). Granular microstructure was relatively uncommon, except at Great Bay where it was observed on approximately 80% of the mussels, and appeared most often as reworked prisms (Fig. 43C, D). In both August and September, nacre was the most commonly observed sublayer (Fig. 49A, B), followed closely by prismatic, whereas granular microstructures (usually altered nacre; Fig. 49C, D) were relatively uncommon (Fig. 38).

All mussels collected in October and November at Delaware, Great, and Sandy Hook Bays had prismatic and nacreous sublayers on the inner surface of the inner shell layer (Figs. 38, 45E, F, 48E, and 50A, B), whereas granular microstructure was relatively uncommon at these three sites (Figs. 48F and 50C, D). In fall, all mussels from the Maurice River had a granular sublayer along some portion of the inner shell surface (Figs. 38 and 51), but both prismatic and nacreous sublayers were also common at this site.

Age Determination

Age in years is determined by counting the number of complete nacreous sublayers present in the inner shell layer (Lutz & Castagna 1980). The inner shell layer is thickest near the umbo and becomes thinner toward the posterior margin. Consequently, inner layer sublayers are most easily distinguished near the umbo (Fig. 52). With increasing distance from the umbo, nacre sublayers become thinner until they disappear leaving a thick band of prisms that was deposited over a series of years. With age, the proportion of each annual increment

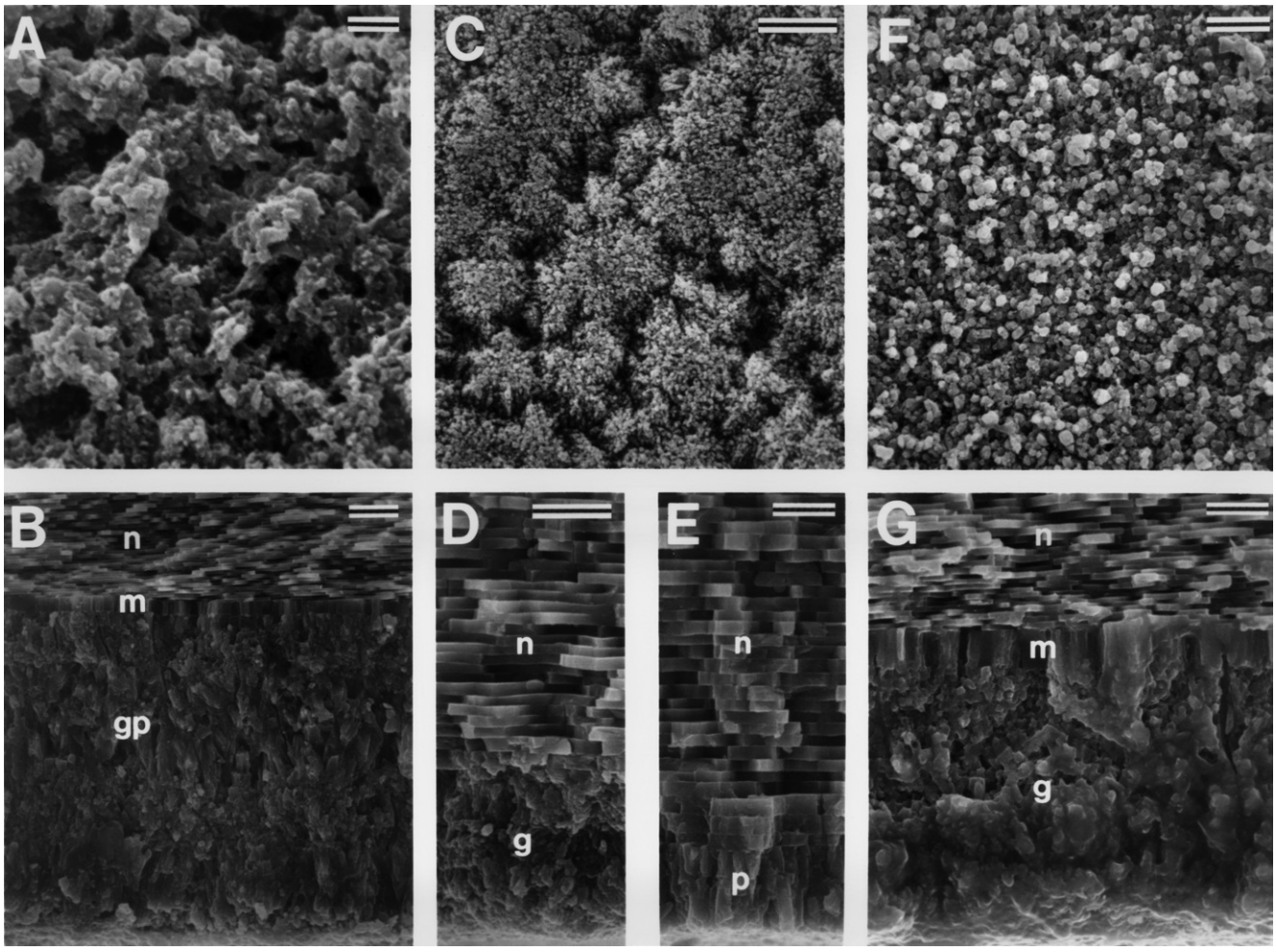

Figure 41. Scanning electron micrographs of inner surfaces (A, C, and F) and fracture sections (B, D, E, and G; inner surface at the bottom) of *Geukensia demissa* shells showing nacreous (n), granular (g), prismatic (p), and granular prismatic (gp) sublayers, and pallial myostracum (m). Growth is to the right. Scale bars: A = 1 μM; B, E, F, and G = 5 μM; in C and D = 4 μM. (A and B) Collected March 1988 from Great Bay, showing outer layer n and m, and inner layer gp just anterior to pallial line. (C and D) Same specimen as A and B. Micrographs taken near the umbo with g inner surface. (E) Collected March 1988. Micrograph taken mid-valve with p on inner surface. (F and G) Collected May 1988. Micrograph taken just anterior to pallial line with g on inner surface, and m and outer layer n.

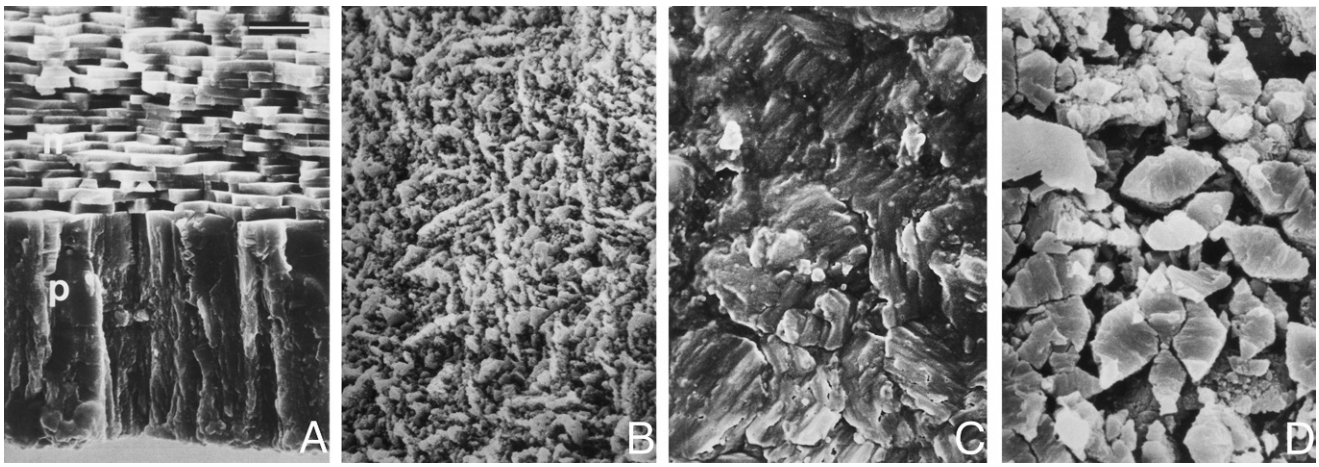

Figure 42. Scanning electron micrographs of a fracture section (A; inner surface at the bottom) and inner surfaces (B–D) of inner shell layers of *Geukensia demissa* collected in April 1986 from Delaware Bay. Growth is to the right. (A and B) 2-y-old with regular prisms (p) and moderate dissolution on the inner surface and nacre (n) above deposited in fall 1985. (C and D. 8-y-old with more and less extensive dissolution, respectively, along inner surface.

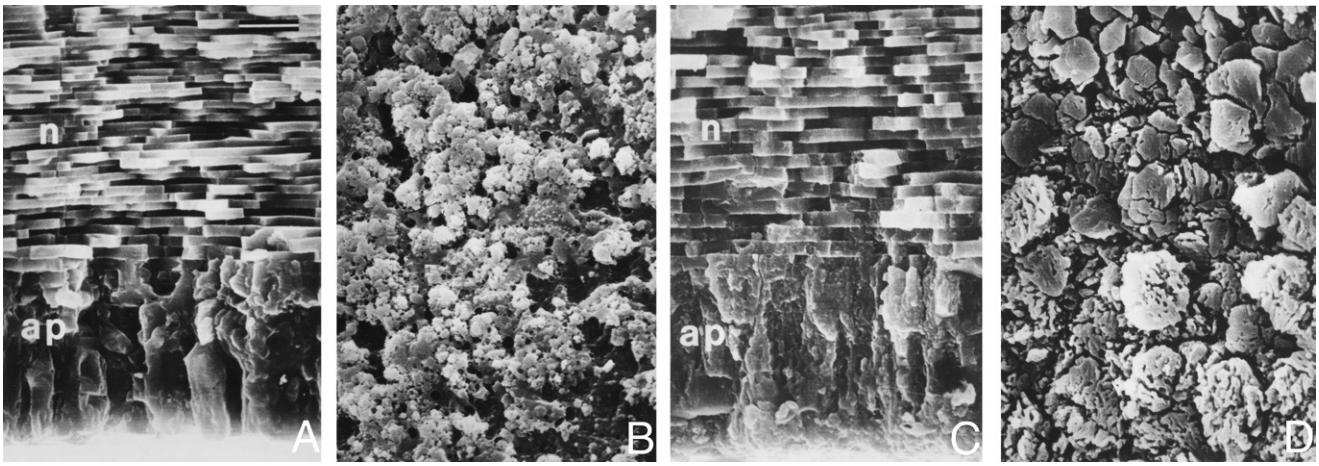

Figure 43. Scanning electron micrographs of fracture sections (A and C) and inner surfaces (B and D) of inner shell layers of *Geukensia demissa* collected in April (A and B) and June 1986 (C and D). Growth is to the right. (A and B) 1-y-old with altered prismatic (ap) sublayer with extensive dissolution along inner surface and nacre (n) above deposited in fall 1985. (C and D) 4-y-old with ap and moderate dissolution along inner surface with n above.

of prismatic, nacreous, prismatic (and granular) sublayers becomes increasingly dominated by prismatic (and granular; Lutz & Clark 1984). Inclusion of additional (irregular?) prismatic sublayers within a single year's nacreous sublayer may cause confusion in assigning age. Additional prismatic sublayers do not usually extend posteriorly as far as the spring or fall prismatic sublayers, where they disappear leaving an uninterrupted, continuous nacre sublayer. Furthermore, additional prismatic sublayers do not connect anteriorly with the thick prismatic and adductor myostracal sublayers present in the umbo area. These two features of additional (irregular) prismatic sublayers are usually sufficient to exclude the "extra" nacreous sublayer in counts to determine age. As with age determinations of most species, however, it is best to analyze large numbers of specimens from each location and be objective as possible in assigning age.

The shell microstructure of the ribbed mussel, *Geukensia demissa*, is sensitive to and reflects changes in the environment, including the short-term acute stress of storms (e.g., Hurricane Gloria), seasonal changes in temperature, food supply, salinity, and so on, and differences in habitat. This suggests that the ribbed mussel is an excellent candidate for use as a bio-monitor of sublethal environmental change. An acute stress in spring, summer, or fall, such as a chemical spill, could be recorded in outer layer microstructure as a gcm. Although more research is required to determine the periodicity of outer layer microgrowth increment formation, the time of formation of a mark could be determined from counts of increments knowing only the date of collection. If the effects of the stressor lingered for some time, this could also be reflected in inner-layer microstructure as a granular sublayer long before significant changes in tissue or shell growth would be discernible. Similarly, if the perturbation caused significant long-lasting changes in the environment, the multiyear growth record in the inner shell layer would enable age determination and growth history reconstruction to discern the magnitude of the impact. Since *G. demissa* is highly resilient to changes in the environment and capable of withstanding abrupt changes, any differences in shell microstructure between control and exposed mussel populations, or between the "expected" and observed microstructure in exposed

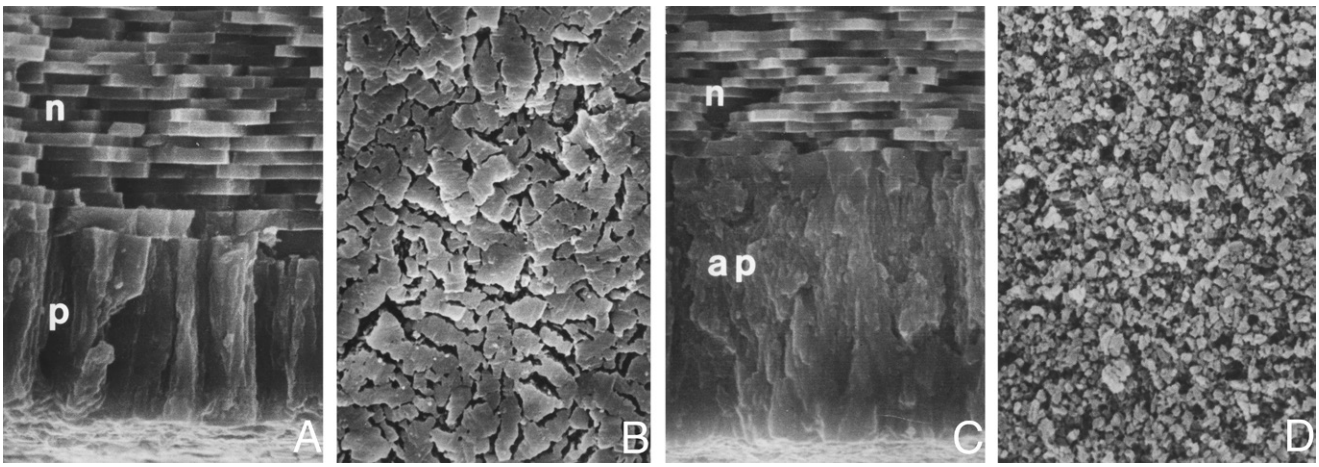

Figure 44. Scanning electron micrographs of fracture sections (A and C) and inner surfaces (B and D) of inner shell layers of *Geukensia demissa* collected in May 1987. Growth is to the right. (A and B) 2-y-old collected from Delaware Bay with crisp prismatic (p) sublayer along inner surface and nacre (n) above deposited in fall 1986. (C and D) 3-y-old with altered prismatic sublayer (ap) along inner surface with evidence of dissolution, and n above.

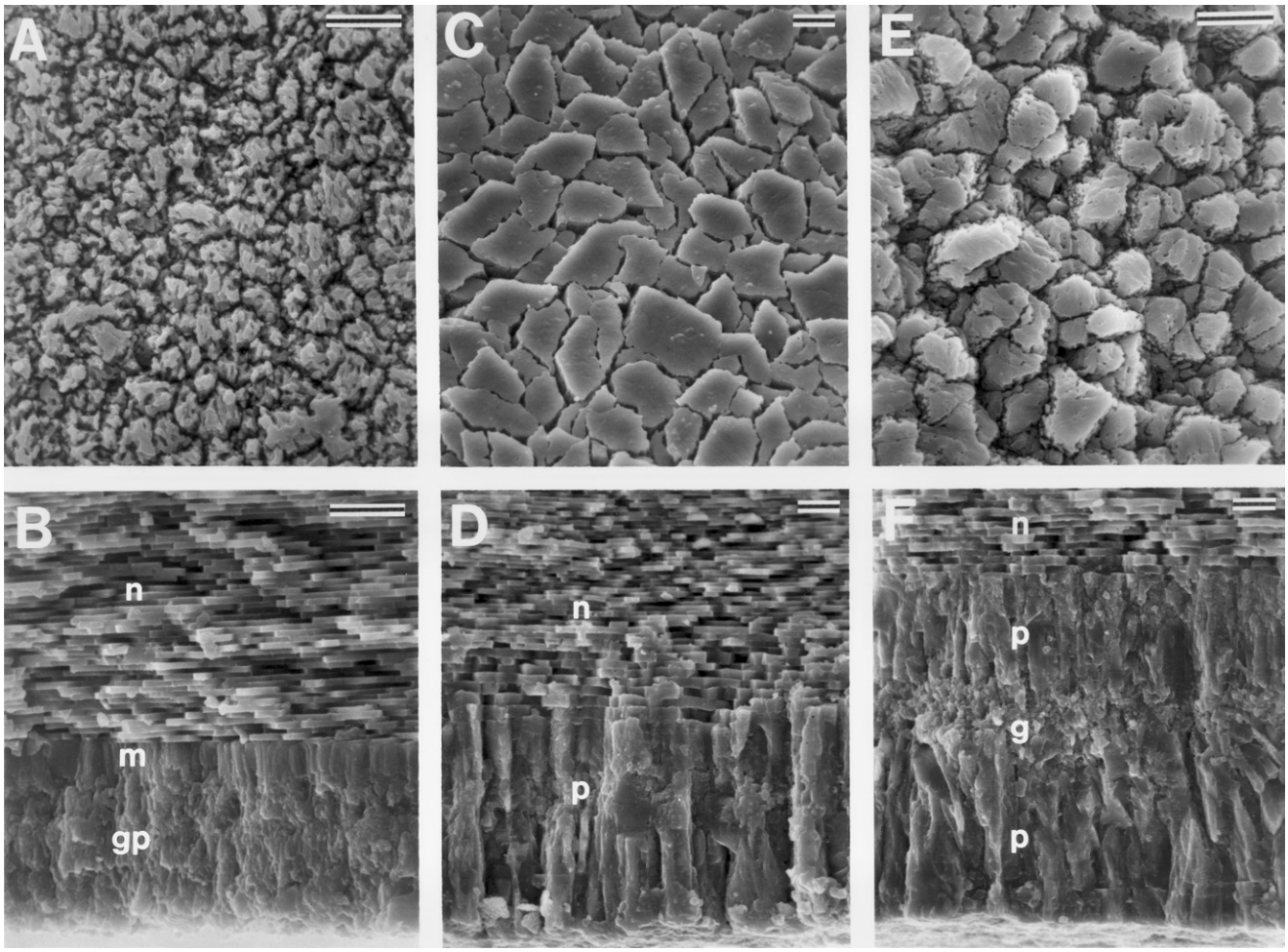

Figure 45. Scanning electron micrographs of inner surfaces (A, C, and E) and fracture radial sections (B, D, and F; inner shell surface at the bottom) of *Geukensia demissa*. Growth is to the right; scale bars = 5 μM. (A and B) 3-y-old collected May 1988 from Great Bay. Micrographs taken just anterior to pallial line showing the granular prismatic (gp) inner surface of the inner shell layer, the pallial myostracum (m) and outer layer nacre (n). (C and D) 8-y-old collected July 1988 from Sandy Hook Bay. Micrographs taken near the umbo showing crisp p along inner surface and inner layer n. (E and F) 4-y-old collected October 1988 from Great Bay. Micrographs taken just anterior to the pallial line and posterior to the most posterior extension of the inner n sublayer formed in summer 1988, showing slightly etched p along inner surface. A period of slow growth in summer 1988 is represented as the granular (g) microstructure within the p sublayer below inner layer n formed in summer-fall 1987.

populations, could, with some certainty, be related to the acute stress of a known perturbation.

Mytilus edulis, the Blue Mussel

The blue mussel, *Mytilus edulis*, is commonly found in both intertidal and subtidal marine habitats attached to almost any structure (e.g., bulkheads, rock jetties, ship wrecks, and artificial reefs). The shell of *M. edulis* has three primary calcareous layers (Fig. 53A): an outer fibrous prismatic layer composed of calcite, a pallial myostracum to which the mantle is attached, and an inner aragonitic nacreous layer (Taylor et al. 1969). Microgrowth increments in the outer prismatic layer are generally nonreflected (Pannella & MacClintock 1968), meaning that increment boundaries are approximately parallel to the inner shell surface (Figs. 52B and 54A) and intersect the outer shell surface at angles <90 deg. As Pannella and MacClintock (1968) describe, the type of microgrowth increment produced, either nonreflected or reflected, depends on the characteristics of the mantle. Nonreflected increments are formed by mantles that are well-extended posteriorly and not recurved around the shell lip back toward the umbo (see Fig. 1 in Panella & MacClintock 1968). This produces a shell with a sharply pointed posterior margin, such as the typically thin-shelled blue mussel (Fig. 54B). Conversely, reflected increments are formed by mantles that wrap around the shell margin, and have their edges pointed back toward the umbo (Fig. 54A). Deposition of reflected increments produces a rounded, less-pointed ventral shell margin when viewed in radial section, such as that of the hard clam, *Mercenaria mercenaria*. A blunt posterior shell margin results when the mantle does not extend beyond the posterior margin, causing a lateral thickening of the shell tip (Fig. 54C).

The inner aragonitic layer is composed of nacreous tablets, which in fracture section, appear as bricks in a wall (Fig. 53A, C), and during periods of rapid shell growth, are hexagonal in shape (Fig. 53D), similar to those deposited by *Geukensia demissa* in both its outer and inner shell layers. Based on examination of a series of specimens collected from Maine subtidal waters, Lutz

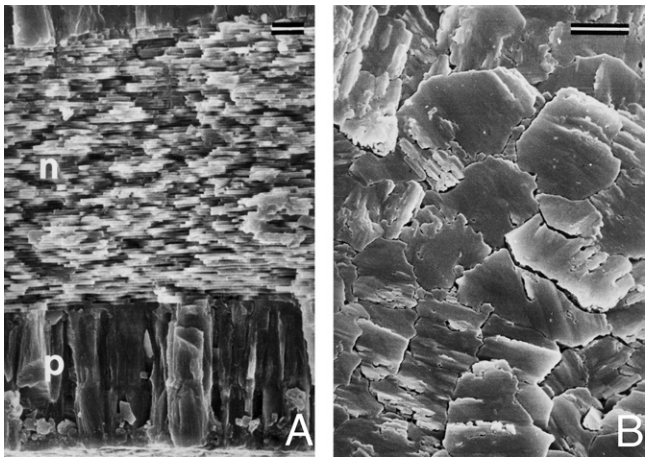

Figure 46. Scanning electron micrographs of fractured radial section (A; inner surface at bottom) and inner surface (B) of the inner shell layer of a 15-y-old *Geukensia demissa* collected June 1986 from Delaware Bay. Growth is to the right; scale bars = 5 μM. Note the crisp prismatic sublayer (p) on the inner surface and lack of granular microstructure. In A, inner layer nacre (n) formed in 1985 is above p formed in summer 1986.

(1976) found that the thickness of nacre tablets varied seasonally; thick tablets were deposited in early spring, thin laminae in late spring, and relatively thick tablets again in summer through fall. Thick tablets were deposited during periods of rapid shell growth, whereas thin tablets were formed during periods of slower shell growth. Lutz (1976) did not find any evidence of dissolution, such as a series of collapsed nacre tablets in fracture section or etched, rounded tablets along the inner shell surface, following periods of adverse weather (i.e., cold or warm water temperatures). Growth cessation marks likely resulting from dissolution were found in all of our specimens in both the inner and outer shell layers, and were useful in determining age and the time of formation of various shell regions (Figs. 53C and 54).

Seasonal changes in the outer shell layer microstructure of *Mytilus edulis* in New Jersey were documented by Fritz et al. (1991) and the information is reprinted here with their permission (including their Figs. 1–4 as Figs. 54B and 55–57 here); information presented here on seasonal changes in inner shell microstructure, age determination, and growth of tissue and shell is new.

Outer Prismatic Layer

The outer shell layer of *Mytilus edulis* is composed of fibrous prisms (Fig. 53A) and divided into a series of microgrowth increments visible only in polished and etched radial sections (Figs. 53B and 54). Two types of fibrous prisms were observed in the outer layer of Delaware Bay mussels: rapid and slow growth. Rapid-growth prisms consisted of long, slender, evenly shaped prisms (Figs. 53A and 55A) with chisel-pointed ends (Fig. 55B) and deposited at angles of approximately 30 deg or less to the inner shell surface. Rapid growth prisms were observed in recently deposited shell regions in mussels collected in spring and fall. Rapid growth prisms were associated with nonreflected microgrowth increments (Figs. 53B and 54).

Slow shell growth prisms consisted of shorter, more unevenly shaped prisms, ranging from spindle or lenticular-shaped (in cross-section) to a shape resembling rapid-growth prisms, but with varying thicknesses along their length (Fig. 55C). The inner surface of the outer layer lost its ordered, sharply pointed texture and had an appearance ranging from slightly etched and variably shaped prism tips (usually seen in winter) to an unordered granular texture (most likely a result of dissolution) in which individual prism tips were almost unrecognizable (usually seen in summer; Fig. 55D). Slow-growth prisms tended to be deposited at angles >30 deg to the inner shell surface, but not all, nor were they all short and spindle-shaped as shown in Figure 55C.

Seasonal changes in the shape of the posterior shell margin were reflected in, and most probably resulted from, seasonal changes in outer layer microstructure. Prismatic needles near the posterior margin in spring- and fall-collected mussels were rapid-growth: long, evenly shaped, and deposited at angles of approximately 30 deg to the inner shell surface (Figs. 55A, B and 56F, G). Summer-collected mussels had slow-growth prisms near the posterior margin (Fig. 55C, D), whereas there was little

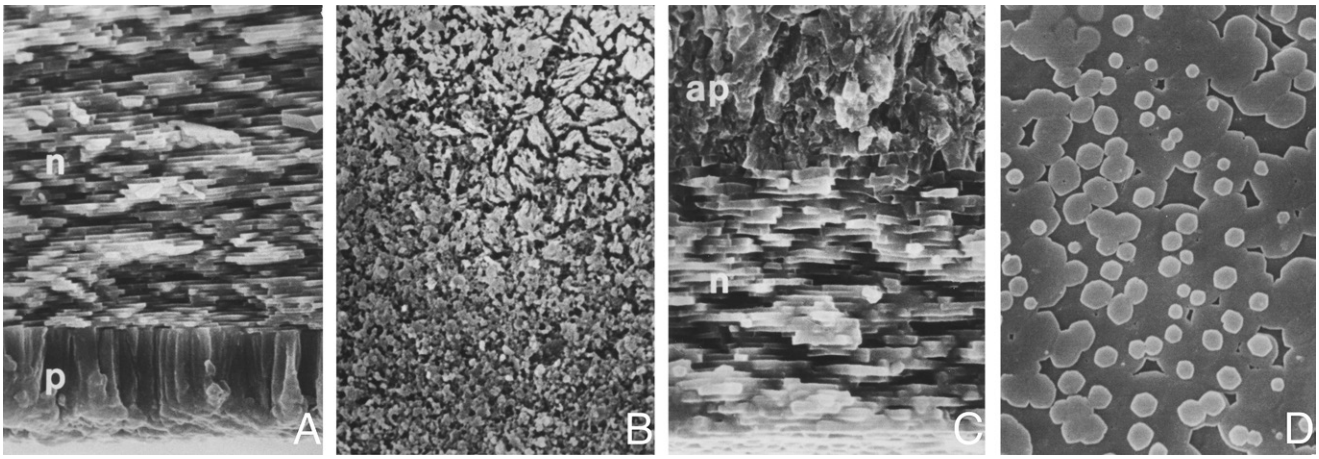

Figure 47. Scanning electron micrographs of fracture sections (A and C) and inner surfaces (B and D) of the inner shell layer of a 1-y-old *Geukensia demissa* collected in June 1986 from Delaware Bay. Growth is to the right. Scale is the same in all micrographs and the same as Fig. 46B. Both a prismatic (p; A and B) and a nacreous (n; C and D) sublayer were being formed at the time of collection on different portions of the inner shell surface. In C, note the altered prismatic sublayer (ap) above the n sublayer.

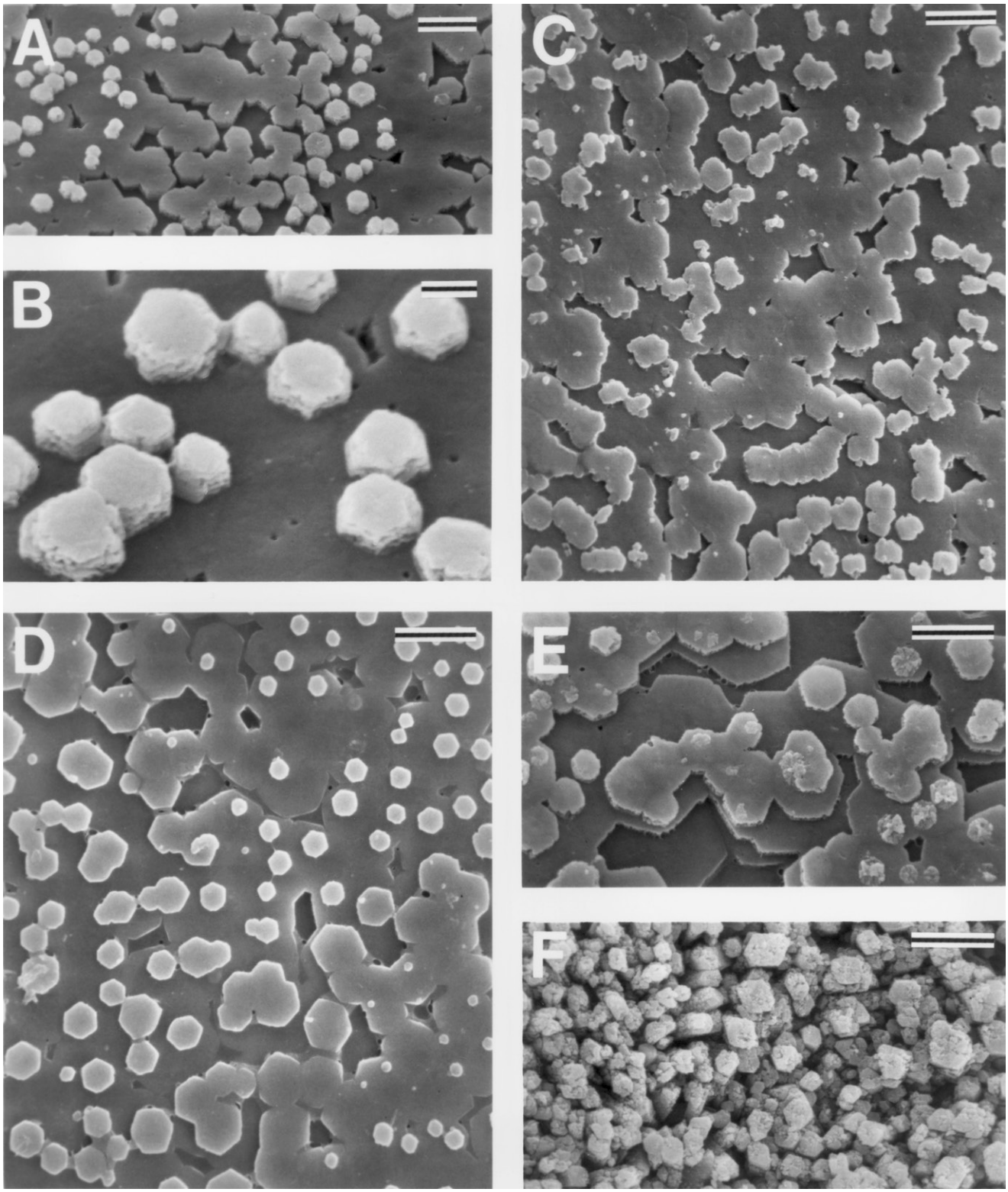

Figure 48. Scanning electron micrographs of inner surfaces of the inner shell layer of *Geukensia demissa* with nacreous and granular sublayers. All micrographs taken near the umbo except F and growth to the right. Scale bars: A, C, D, E, and F = 5 µM; B = 1 µM. (A and B) 2-y-old collected November 1987 from Sandy Hook Bay with slightly etched wave-form nacre. (C) 1-y-old collected July 1988 from Sandy Hook Bay with etched wave-form nacre. (D) 2-y-old collected July 1988 from Great Bay with slightly etched wave-form nacre. (E) 1-y-old collected October 1988 from Sandy Hook Bay with stacked nacre. (F) 4-y-old collected October 1988 from Great Bay (same specimen shown in Figure 3–17E, F). Micrograph taken just anterior to pallial line and shows granular-nacreous microstructure.

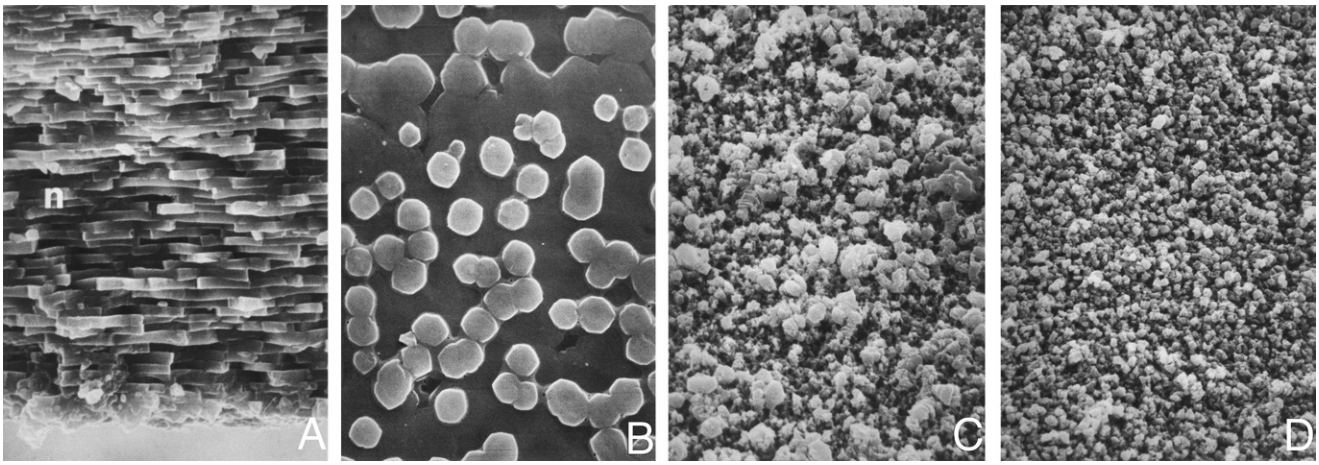

Figure 49. Scanning electron micrographs of fracture section (A) and inner surfaces (B–D) of the inner shell layer of a 1-y-old *Geukensia demissa* collected in August 1986 from Delaware Bay. Growth is to the right. Note the lack of crisp nacre (n) along the inner shell surface and the slight (B), moderate (C), and extreme (D) dissolution (scale is the same in all micrographs and the same as Fig. 46B) of the inner shell surface.

to no shell growth in winter (which resulted in a gcm because of dissolution along the inner shell surface; Fig. 54B, C). Upon resumption of shell growth in late winter, a cone-shaped region of prisms was formed at the posterior shell margin in which prisms were oriented at angles ranging from 51 deg to 140 deg (Figs. 54C and 57).

All micrographs in Figure 56 were taken at or near the inner depositional surface of the outer shell layer in different portions of a single microgrowth increment. Thus, prisms in each of the regions, A, C, and P, in Figure 57 were formed at the same time by different portions of the mantle. Prism orientation appears to be initiated at the shell and mantle margins, and once initiated, individual prisms continue to grow at the original orientation until the outer layer is overlain by the pallial myostracum and inner shell layer (Fig. 53A). Undulations in the shell's exterior surface in summer and winter (Fig. 54B) are related to changes in the orientation of outer layer prisms. Prism growth can be described by considering the ratio of their posterior (P) and inward (I) vectors, which is equivalent to the inverse of the tangent of the angle of deposition. Prisms deposited at an angle of 30 deg have a P/I = 1.73, indicating that outer layer shell growth is 1.73 times greater in the posterior than the inward direction, resulting in a sharply pointed posterior shell margin typically observed in spring and fall. At prism deposition angles >45 deg, P/I < 1, resulting in more blunt posterior margins observed in summer (Fig. 54B) or after a growth disruption (Fig. 54A). As prism deposition angles approach 90 deg, like those in the center of region C (Fig. 57), P/Is approach zero, yielding the steeply terraced shell exterior surfaces found posterior to winter gcm (Fig. 54B, C).

Additional research is necessary to determine the periodicity of microgrowth increment formation by *Mytilus edulis* under various conditions to accurately date the time of formation of gcm of unknown origin. For instance, without the strong stimulus of tidal inundation and exposure, transplanted mussels in the Ciba-Geigy study deposited less distinct microgrowth increments under subtidal conditions than prior to collection from their intertidal location on Cape Cod. Mussels collected from the intertidal location in Delaware Bay deposited relatively distinct microgrowth increments only in spring and a short period

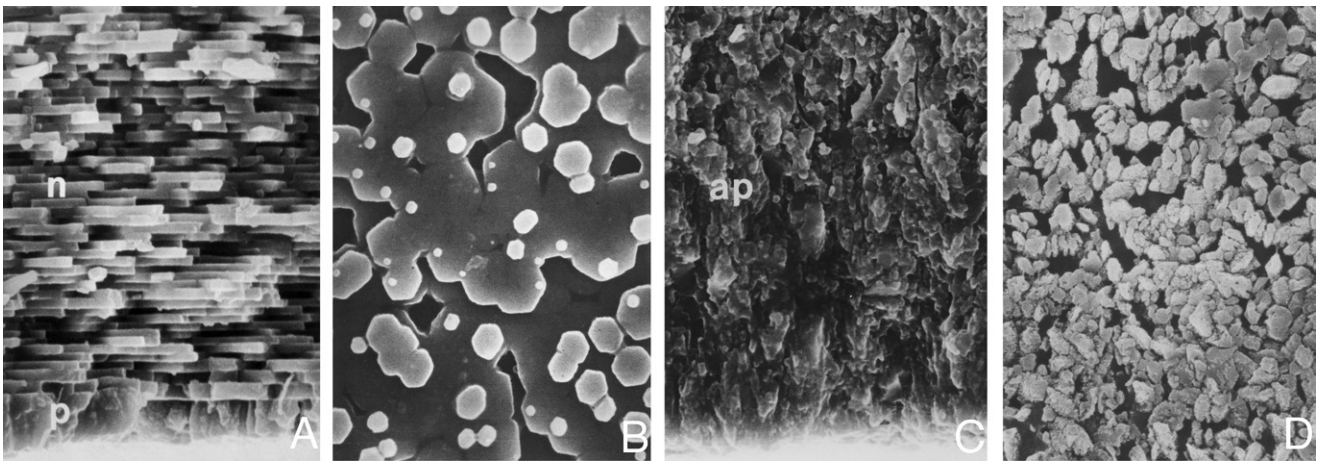

Figure 50. Scanning electron micrographs of fracture sections (A and C) and inner surfaces (B and D) of the inner shell layer of a 0+-y-old *Geukensia demissa* collected in November 1986 from Delaware Bay. Growth is to the right. Note the variety of microstructures on the inner surface, including thin prisms (p; A), nacre (n; B) and irregular/altered prisms (ap; C and D); scale is the same in all micrographs and the same as Fig. 46B.

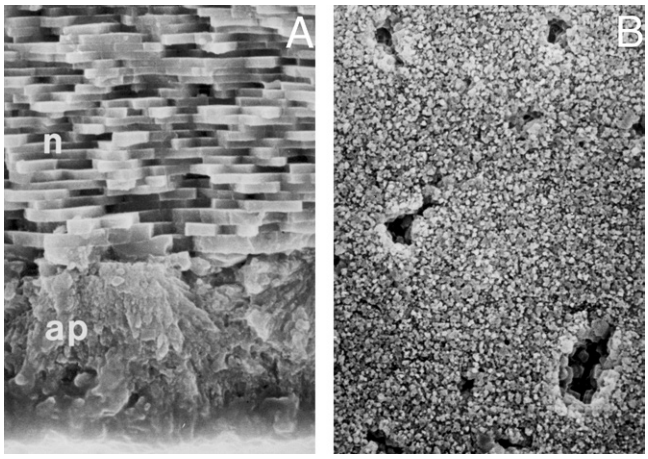

Figure 51. Scanning electron micrographs of a fracture section (A) and inner surface (B) of the inner shell layer of a 1-y-old *Geukensia demissa* collected in November 1986 from the Maurice River. Growth is to the right. Scale is the same in all micrographs and the same as Fig. 46B. Note the altered prismatic microstructure (ap; A) and granular microstructure (B) along the inner shell surface. Pits in inner surface (B) reveal either incomplete deposition of prisms or dissolution to previously deposited nacreous (n) sublayer; scale is the same in both micrographs.

in fall when growth rates were rapid. Nonreflected increments tended to be more distinct than reflected increments, but this may only reflect differences in growth rate or separation of increment boundaries. Increment formation by *M. edulis* may also not conform to theories proposed by Lutz and Rhoads (1977) or Deith (1985). Both theories require that, in polished and etched radial shell sections, increment boundaries appear as ridges because these portions of the shell are more resistant to dissolution either because of a greater proportion of organic material (Lutz & Rhoads 1977) or because of differences in crystal structure (Deith 1985). In blue mussels, however, increment boundaries appear to be depressions in polished and etched sections (Fig. 53B), suggesting that boundaries are less resistant to dissolution than increments. Prism formation appears to be discontinuous across the increment boundary, possibly leaving a thin zone of loosely bound carbonates and matrix.

Inner Nacreous Layer

The inner shell layer of *Mytilus edulis* is composed of aragonitic nacreous tablets, the appearance of which changes seasonally depending on the rates of growth and dissolution. In March, all specimens analyzed had extensive dissolution along the inner shell surface and a lack of recent nacre deposition, such as the remnants of stacked nacre tablets deposited in late fall (Fig. 58A, B). Thus, mussels were in the process of forming a winter gcm (Fig. 53C) at this time. In April, there was evidence of a short period of recent deposition of thin nacre tablets in early spring in some specimens (Fig. 58C), but also dissolution along the inner shell surface [Fig. 58C (bottom) and Fig. 58D]. Above this zone (or in older portions of the shell), relatively thick nacre tablets deposited in fall were present (top of Fig. 58A) that ended abruptly at a thin granular layer (winter gcm) followed by thin spring nacre tablets (see also Fig. 53C). Thin nacre tablets and slight dissolution likely reflect slow growth processes in late winter-early spring because of cold temperatures and the shift of energy resources to gonad development (Lutz 1976, Hilbish 1986).

The most rapid period of shell growth occurred in spring. In May (Fig. 59A, B), mussels were depositing thin crisp, hexagonal nacre tablets in "waves" along the entire inner shell surface. The thickness of the zone of thin nacre tablets (from the winter gcm to the inner shell surface) ranged between 15 and 90 μM. Along the inner shell surfaces of June-collected mussels, there was either a multilayer zone of thick, uniform nacre tablets (Fig. 59C) or a thin zone with thinner and less organized tablets formed after thick uniform tablets. Between the winter gcm (Fig. 53C) and the inner shell surface, however, all specimens analyzed had a wide zone (between 100 and 250 μM thick) of uniformly thick nacre tablets deposited in spring. On the inner shell surface, tablets ranged in shape between slightly pitted hexagons (Fig. 59D) to hourglasses (Fig. 60D). Dissolution and reduced shell growth rates by June could be because of warm water temperatures, spawning or exposure on each low tide (when all animals were collected). If the animals had been collected at high tide, when they would presumably be respiring aerobically, the inner shell surface may not have been as pitted. Pitting and gcm were less commonly observed in subtidal mussels by Lutz (1976). The use of anaerobic respiratory pathways, however, does not explain the deposition of crisp, hourglass-shaped nacre tablets at the Delaware Bay site in September when temperatures were similar (Fig. 60D).

In August and September (Fig. 60), inner shell layers in fracture sections revealed evidence of slow or no growth, and looked similar to June (Figs. 59C, D). August- and September-collected mussels had a zone ranging between 130 and 250 μM, and 150–350 μM thick, respectively, between the winter growth cessation and the inner shell surface, compared with a 100–250 μM range in June.

Between September and November, there was a period of shell growth evidenced by the thick, uniform nacre tablets observed near the inner shell surface in fracture sections (Fig. 61A) and the relatively crisp hexagonal nacre along the inner shell surface (Figs. 53D and 61B). This period of shell growth did not last because it did not result in a significant increase in SL from the September collections, but it was accompanied by deposition of rapid growth prisms in the outer layer. The zone from the winter gcm to the inner shell surface ranged in thickness from 170 to 350 μM in November, which is slightly greater than that observed in September. In November, deposition of stacked (instead of waveform) nacre tablets may have just begun prior to the date of collection in Delaware Bay (Fig. 61B) suggested that growth rates had recently begun to decline. Deposition of stacked nacreous tablets during periods of relatively slow growth was also observed in *Geukensia demissa*.

In summary, nacre tablet thickness in the inner shell layer of *Mytilus edulis* changed seasonally, with thin tablets deposited in early spring, and thick tablets in late spring, early summer, and fall. Growth cessations occurred twice each year, in mid to late summer (when temperatures were at their highest) and winter (when temperatures were at their lowest). The seasonal sequence of nacre deposition in New Jersey is slightly different from that described by Lutz (1976) for subtidal mussels collected in Maine. Lutz observed that the deposition of thin nacre tablets in late spring was both preceded and followed by periods of thick tablet deposition in early spring and summer.

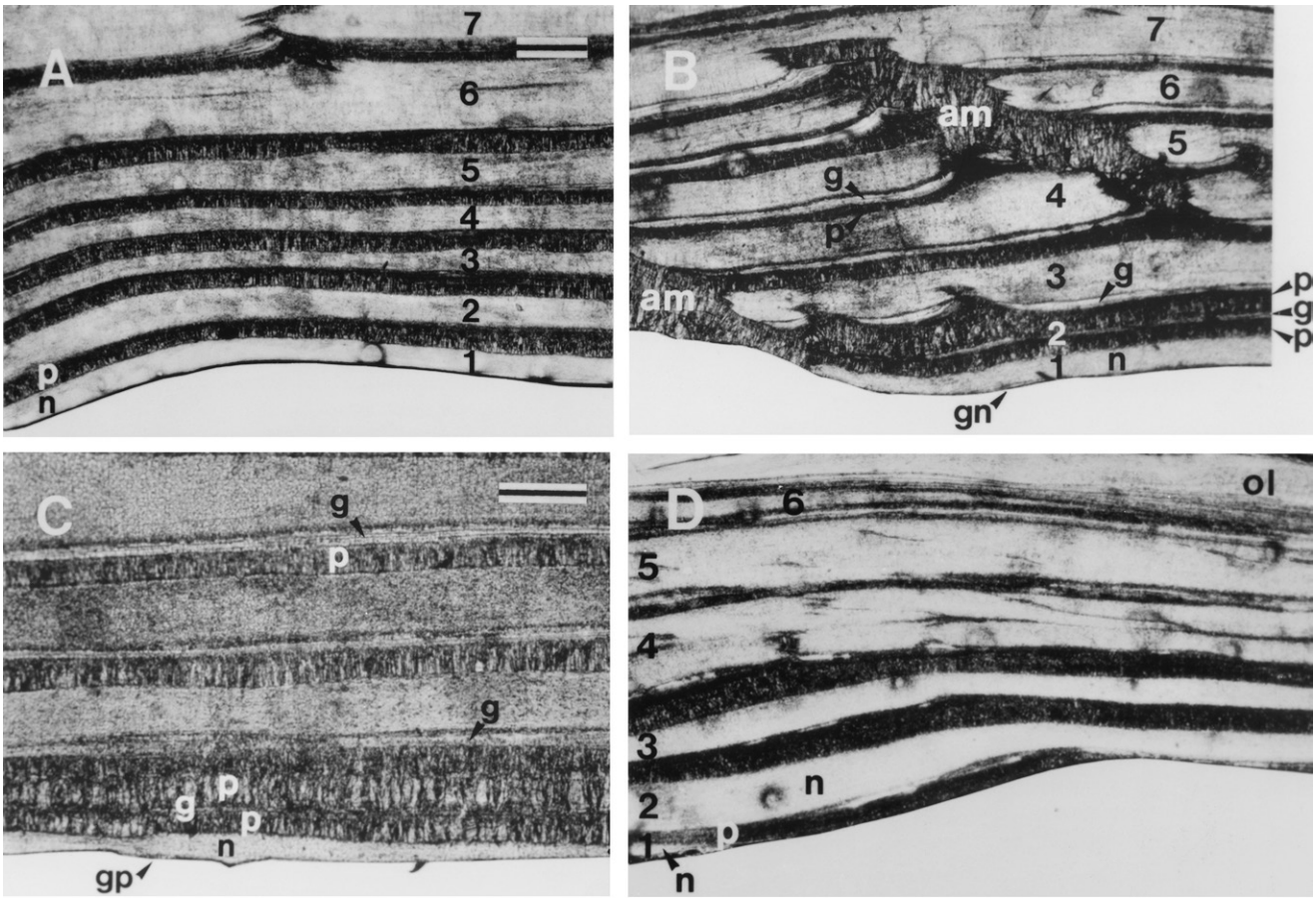

Figure 52. Light micrographs of acetate peel replicas of polished and etched radial sections of the inner shell layers of *Geukensia demissa*. Growth is to the right and the inner shell surface is at the bottom of each micrograph. Numbers refer to nacreous sublayers (n) deposited annually in summer and fall. Prismatic (p), granular (g) and combination (gp and gn) sublayers are also labeled, as is the adductor myostracum (am). Scale bars: in A (B and D are the same scale as A) = 0.2 mm; in C = 0.1 mm. (A) 9-y-old collected November 1987 from Sandy Hook Bay. n labeled 7 through 1 were formed in 1981 to 1987, respectively, with 1 on the inner shell surface. (B & C) 9+-y-old collected March 1988 from Sandy Hook Bay. n labeled as in A, except for 2, which in this region of the shell was not present but instead consisted of p and g sublayers; n2 was present in regions of the shell anterior and posterior to that shown. g consistently formed at bottom of each n resulting from dissolution in winter in B but not in A. (C) posterior to B showing gp along inner surface and thick p-g-p sublayers above n formed in 1987. (D) 5-y-old collected July 1988 from Great Bay. Specimen has 6 n formed in 1983, 1984, 1985, 1986, 1987, and 1988, with the last being formed at time of collection.

In New Jersey, thin tablets were deposited in early spring, followed by thick tablets in late spring, early summer, and fall. Furthermore, Lutz did not describe any winter or summer gcm. The lack of gcm in his samples could be because of both their subtidal growing location (with constant inundation) and a cooler, more suitable temperature regime for the species.

Age Determination

Winter gcm divided the inner nacreous layer into annual bands (Fig. 62), which consisted of (1) a "light" (or translucent) zone formed in spring; (2) a "dark" (or relatively opaque) zone formed in early summer; (3) a horizon of etched nacre tablets (the summer gcm), which often appeared as a dashed, wavy line on acetate peel replicas; and (4) a distinct winter gcm resulting. In younger specimens, there was another band of nacre tablets ("dark" zone) deposited in fall that separated the summer and winter gcm.

Growth cessation marks in the outer layer were also present (Fig. 54), but the pattern of nacre deposition in the inner layer provided a more condensed and clearer record of growth that made age determination less ambiguous. Most of the mussels analyzed in this study were members of the 1985 or 1986 YC (l+ and 0+ y old, respectively, at the time of collection), with the oldest mussel being 5 y old (1981 YC) with a SL of 39.1 mm.

Seasonal Growth in Tissue and Shell

Dry tissue weight (*DTW*) was highly correlated with *SL* when all seasonal collections were pooled (Fig. 63):

$$\ln DW = 2.46 \ln SL - 10.37 \quad r^2 = 0.81; \mathrm{N} = 48 \qquad (2)$$

To enable analysis of seasonal changes in tissue weight, the dry weight of a 25 mm mussel was calculated for each collection based on the sample regressions of dry weight to SL. Sample sizes ranged from six to nine mussels, and correlation coefficients (r^2) from 0.77 (in March 1987) to 0.99 (in November 1986).

Shell length of the 1984 and 1985 YC increased most rapidly between the April and June collections from Delaware Bay

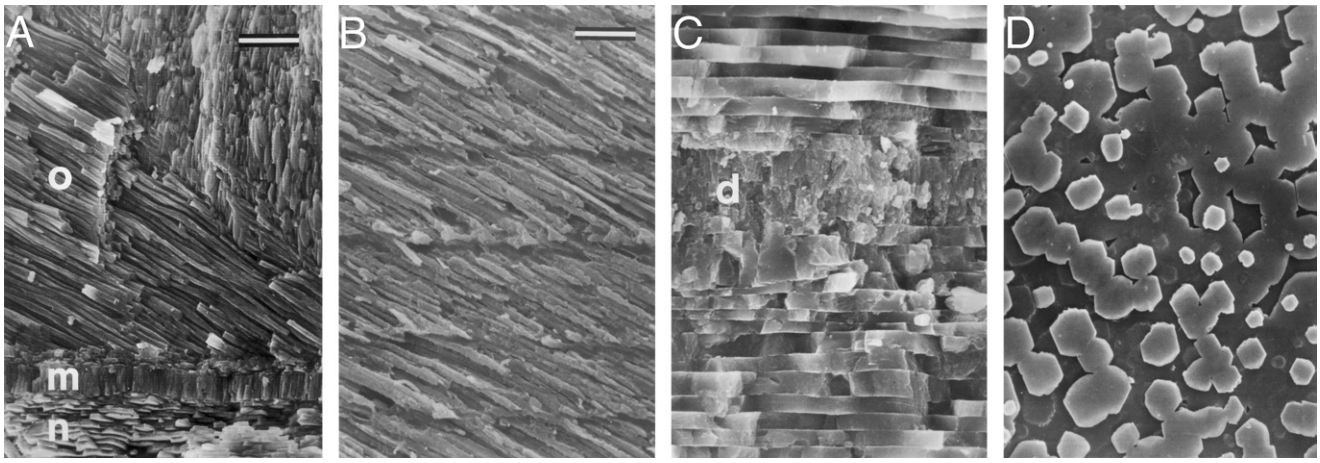

Figure 53. Scanning electron micrographs of *Mytilus edulis* shells. Scale bars: A = 68 µM; B = 4.3 µM; scale in C, and D is the same as B. Growth is to the right and inner shell surface is at or beyond the bottom of A–C. (A) Fracture radial section of 1-y-old collected in June 1986 from Delaware Bay showing three shell layers: outer calcitic prismatic (o), pallial myostracum (m), and inner aragonitic nacreous (n). Micrograph taken just anterior to pallial line. Rapid growth prisms formed in fall 1985 are in the lower left portion of the o, whereas slow-growth prisms formed after the winter 1985 to 1986 growth cessation are in upper right. (B) Polished and etched radial section of 2-y-old collected in August 1986 from Delaware Bay showing four microgrowth increments in the o. (C) Fracture radial section of 3-y-old collected in June 1986 from Delaware Bay showing n with uniformly thick tablets deposited in fall 1985 at top, a growth cessation mark (d) resulting from nacre dissolution in winter 1985–86, thin disorganized nacre and uniformly thick nacre formed in spring 1986 at bottom. (D) Inner n surface of transplanted mussel collected in November 1986 off Ortley Beach showing crisp hexagonal tablets deposited in "waves"; growth is to the upper right.

in 1986 (Fig. 64A). This corresponds with the formation of rapid growth prisms and nonreflected microgrowth increments in the outer layer and waveform, relatively thick nacre tablets along the inner layer surface. From June 1986 through March 1987, little if any increase in SL was evident from our relatively small samples. Between March and May 1987, however, there

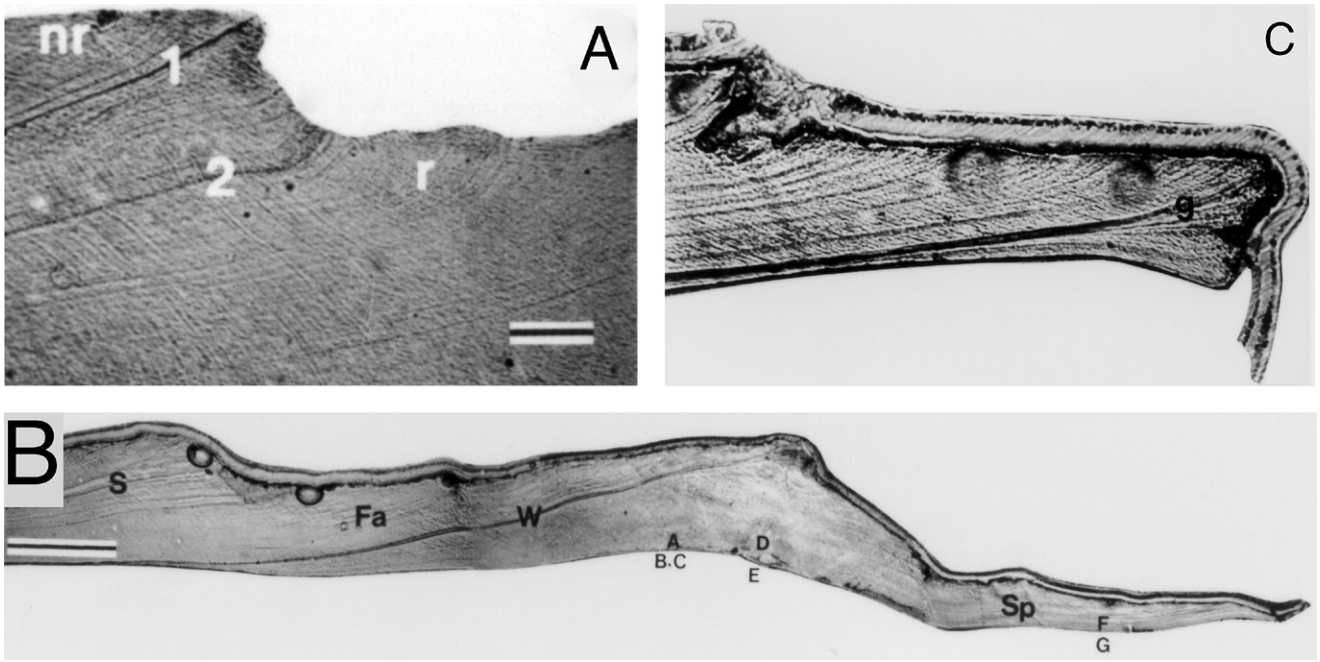

Figure 54. Light micrographs of acetate peel replicas of polished and etched radial sections of *Mytilus edulis* shells showing the outer prismatic layer; growth is to the right and the inner shell surface is at or beyond the bottom of each micrograph. (A) Transplanted mussel collected in November 1986 off Ortley Beach showing deposition of nonreflected microgrowth increments (nr) prior to initial collection on Cape Cod on 10 September 1986, growth cessation marks (gcm) resulting from initial collection (1) and transplantation to New Jersey (2), and reflected microgrowth increments (r) deposited after transplantation in early October 1986. Shell deposited between 1 and 2 was deposited in the holding tank between September 10 and 30, 1986; scale bar = 70 µM. (B) 2-y-old collected May 1988 from the Manasquan River with posterior margin at right showing regions of the outer layer deposited in summer (S) and fall (Fa) 1987, the winter 1987 to 1988 gcm (W), and outer layer deposited in spring 1988 (Sp). A–G represent locations where micrographs in Figure 56 were taken; scale bar = 500 µM. Modified Figure 1 of Fritz et al. (1991). (C) 2+-y -old collected in March 1987 from Delaware Bay showing posterior margin and a gcm (g) formed in winter 1986 to 1987. Horizontal field width is 625 µM.

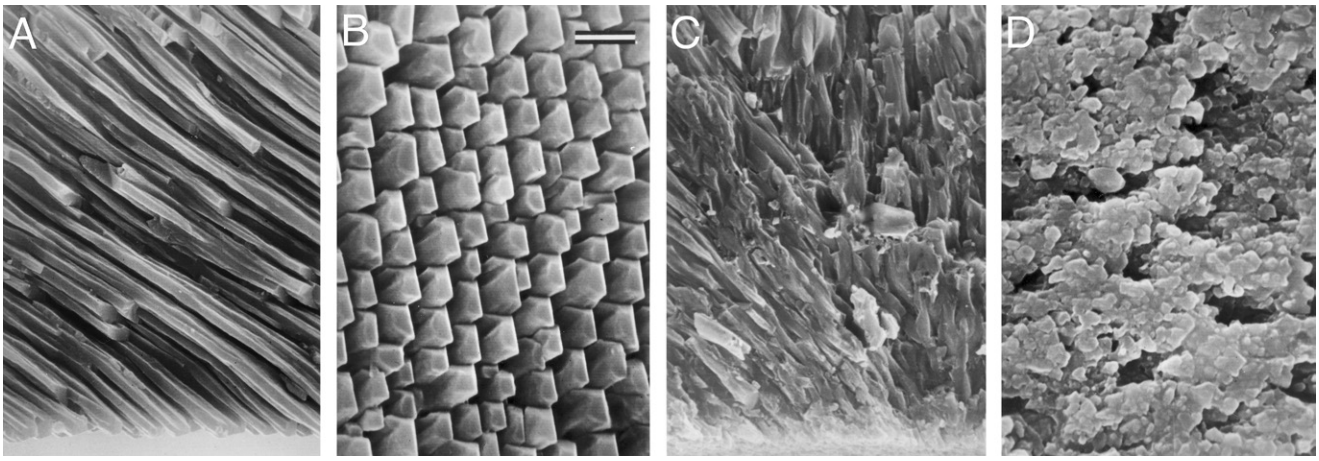

Figure 55. Scanning electron micrographs of fracture radial sections (A and C; inner shell surface at the bottom) and inner surfaces (B and D) of the outer prismatic shell layer of *Mytilus edulis* collected from Delaware Bay; growth is to the right. Scale bar in B = 2 μM; scale is the same in all micrographs. (A) 0+-y-old collected in November 1986 with rapid growth prisms. (B) 3-y-old collected June 1986 with chisel-pointed tips of rapid growth prisms. (C) 2-y-old collected in August 1986 with short, spindle-shaped slow-growth prisms oriented normally (lower left) and vertically (upper right, following a growth cessation in summer). (D) 2-y-old collected in August 1986 with dissolved ends of slow growth prisms. Modified Figure 2 of Fritz et al. (1991).

was no increase in SL by either YC, suggesting that most of the increase in SL observed in 1986 occurred in late spring (between May and June).

Between April and June 1986, there was a slight, nonsignificant increase in DTW of a standard 25 mm mussel, followed by a consistent decline through the summer and fall, with essentially no change through winter (March 1987; Fig. 64B). However, between March and May 1987, the weight of a standard mussel almost doubled in weight and most of the annual increase in dry weight occurred in early spring, likely because of an increase in gonad weight. The increase in tissue weight appears to be at the expense of shell growth because there was little if any increase in SL between March and May 1987 (Fig. 64A). This corresponded with the deposition of thin nacre tablets in the inner shell layer (Fig. 59A). By June, however, most of the increase in tissue (gonad) weight had occurred. By late spring, energy was directed to shell growth.

In summary, gcm in the outer prismatic layer of *Mytilus edulis* were accompanied by formation of slow growth prisms that had a different shape and orientation (with respect to the inner shell surface) than rapid growth prisms. Growth cessations occurred in both summer and winter. Growth cessations resulting from disturbances because of storms and transplantations were also reflected as marks in the outer prismatic shell layer. Slow-growth prisms were associated with reflected microgrowth increments in the outer prismatic layer indicating that the mantle was not well-extended posteriorly and shell growth was directed more inward (laterally). Conversely, rapid growth prisms were associated with nonreflected microgrowth increments suggesting that the mantle was well extended posteriorly. Growth cessation marks (granular sublayers) formed in summer and winter were identified in the inner nacreous layer of *M. edulis* shells. Winter gcm were used to determine age. Thick inner layer nacreous tablets were deposited in late spring, early summer, and sometimes in fall when shell growth rates were the most rapid. Thin tablets were formed in early spring. Deposition of thin tablets may be linked to the shifting of energy reserves to gonad development in preparation for spawning in late spring. Significant shell growth of *M. edulis* in New Jersey was restricted to late spring and early summer (as well as a short period in fall in 1 y old). Consequently, use of shell growth patterns of this species as part of an environmental monitoring program would be limited by the brief duration of rapid shell growth, and its lack of shell growth for much of the year.

Mya arenaria, the Softshell Clam

The softshell clam, *Mya arenaria*, inhabits intertidal mud and sandflats from Labrador to North Carolina along the Atlantic coast of North America (Morris 1975, Brousseau & Baglivo 1987). Softshell clams are commercially harvested over most of this range, and as a result, there is a considerable body of literature on the growth rate of this species throughout its geographic range, with the notable exception of New Jersey (see review in Brousseau & Baglivo 1987).

Water temperatures and salinities ranged between 9.2°C and 31.5°C and 14.6‰ and 21.5‰, respectively, in Newark Bay, and between 3°C and 27°C and 16.0‰ and 24.5‰, respectively, in the Shrewsbury River (Barber 1990) over the course of the study. The shoreline surrounding Newark Bay is highly industrialized. On each collection date during this study, a thin oily residue was pressed out on the sediments with each of the sampler's steps across the intertidal mudflat to the sampling site. By contrast, the Shrewsbury River watershed is composed of residences and farms. Clams from this water body, however, have been found to be affected by a neoplasia evidenced by multinucleated cells within the hemolymph (Barber 1990). Growth rates were determined separately for neoplastic and nonneoplastic individuals collected from the Shrewsbury River.

The aragonitic shells of softshell clams are composed of two layers: an outer crossed-lamellar layer and an inner CCL layer (Kennedy et al. 1969). The left valve of this species is characterized by the presence of a chondrophore, a spoonlike tooth growing from the inside of the umbo. Growth patterns within the inner layer and chondrophore of specimens from

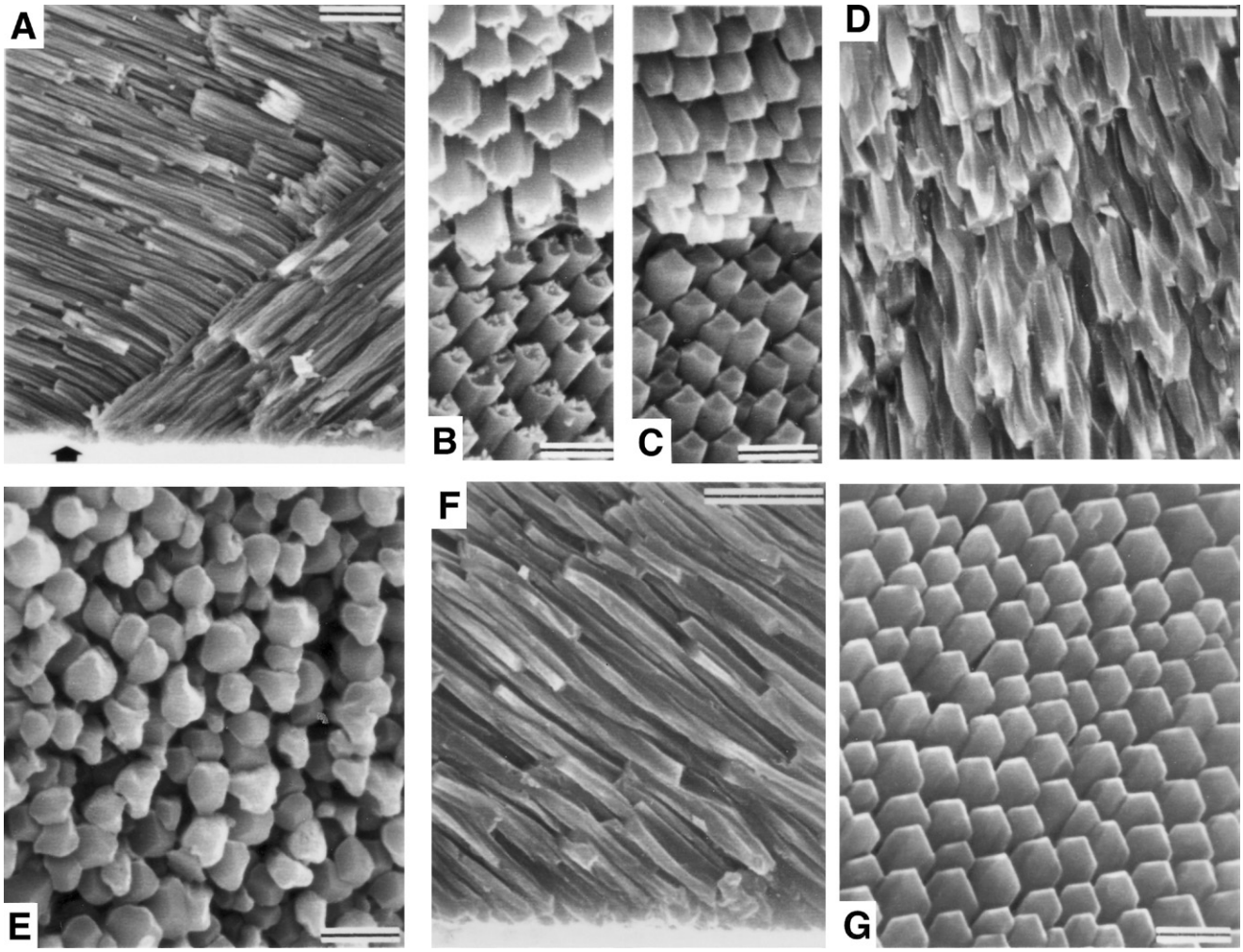

Figure 56. Scanning electron micrographs of fracture radial sections (A, D, and F; inner shell surface at or beyond the bottom) and inner surfaces (B, C, E, and G) of the outer prismatic shell layer of *Mytilus edulis* (same specimen as in Fig. 54B; locations of micrographs match small capital letters in Figs. 54B and 57). Growth is to the right in A and D–G; growth is up in B and C. Arrow in A shows the location along the inner shell surface were B and C were taken. Scale bars: in A = 10 μM; in B, C, E, and G = 2 μM; in D and F = 5 μM. Modified Figure 3 of Fritz et al. (1991).

New Brunswick, Canada, and Long Island Sound, have been described from thin shell sections by MacDonald and Thomas (1982) and Brousseau and Baglivo (1987). Clams from both locations formed inner layer opaque zones (*a.k.a.* growth lines) in spring each year that corresponds with the time of gonad development prior to spawning (Brousseau & Baglivo 1987). MacDonald and Thomas (1980) also noted that the beginning of each translucent zone in the chondrophore and inner layer was associated with a gcm in the outer layer, which they concluded was formed in winter. Neither MacDonald and Thomas

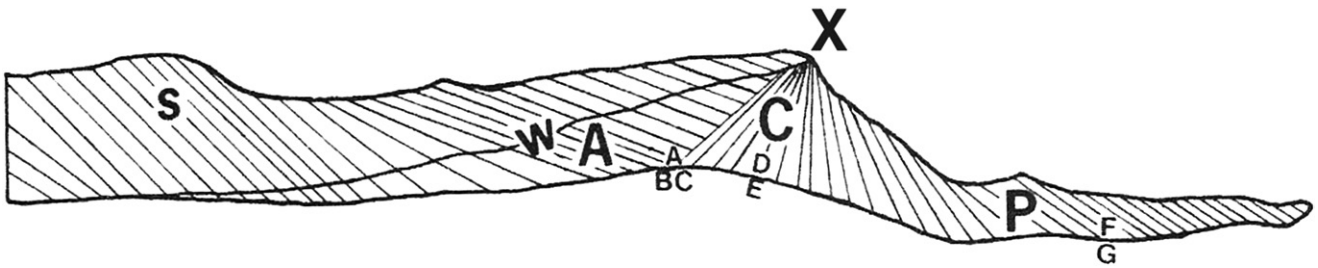

Figure 57. Line drawing showing outer layer prism orientation of the specimen in Figures 54B and 56. Prisms in the cone-shaped region C were initiated at the apex (X) in late winter 1987 to 1988 after the formation of the winter growth cessation mark (w). Prisms anterior to C (A) were initiated in fall 1987 but deposited in late winter and spring, and retained their original orientation. Prisms posterior to C (P) were initiated and deposited in spring 1988. Scale and other notations are the same as in Figure 54B. Modified Figure 4 of Fritz et al. (1991).

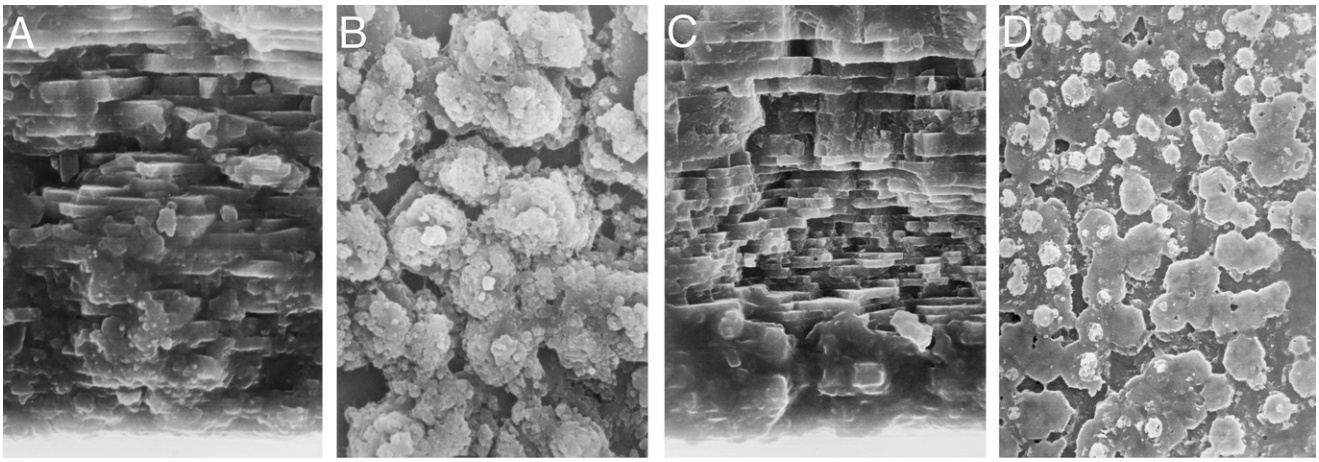

Figure 58. Scanning electron micrographs of fracture radial sections (A and C; inner shell surface at the bottom) and inner surfaces (B and D) of the inner nacreous shell layer of *Mytilus edulis* from Delaware Bay; growth is to the right. Scale is the same as in Figure 53B. (A) 2+-y-old collected in March 1987. (B) 1+-y-old collected in March 1987. Note the dissolved nacre tablets up to 15 μM from the inner shell surface (in A) and the dissolution of stacked nacre deposited in fall 1986 (in B). (C & D) 2+-y-old collected in April 1986 with thick nacre tablets formed in fall 1985 (top of C) and the slight dissolution near and along the inner shell surface (D).

(1980) nor Brousseau and Baglivo (1987) discuss seasonality or the microstructure of bands in the outer shell layer.

Outer Crossed-Lamellar Layer

In the outer shell layer, *Mya arenaria* at both locations tended to form two translucent bands each year, one in summer and one in late fall/winter (Fig. 65[1]), and two opaque bands, one in spring and one in early fall. Clams collected in October and December had translucent bands along the inner growth surface of the outer layer (Fig. 65A, B). The intensity of the translucent bands, that is the degree to which they permitted light to pass, tended to increase with age (Fig. 66A, B). This increase in band definition with age is most probably because of decreasing shell growth rates and hence, more clear representation of seasonal effects in shell microstructure. The ventral-most boundary of outer layer translucent zones consisted of a gcm and was often associated with a terraced exterior shell surface (Fig. 65B, D). Growth cessation mark in the outer layer consisted of lines in thin shell section, and in shell microstructure, were composed of prismatic sublayers (Fig. 67C). Clams collected in May had opaque outer layer bands along the inner growth surface deposited subsequent to the translucent zone of late fall/winter of the previous year (Fig. 65C).

Translucent zones in thin sections of bivalve shells are almost exclusively formed during periods of slow shell growth. This also holds true for *Mya arenaria* collected in New Jersey, with periods of slow shell growth occurring in winter and summer. Reduced shell growth rates in winter are well documented for this species (MacDonald & Thomas 1980, Brousseau & Baglivo 1987). Current year outer layer deposition was observed in three of 10 clams collected in March 1987 from Shrewsbury River, and in eight of 12 clams collected in April 1989 from Newark Bay. Clams that had not resumed growth by these dates tended to be older than those that had. By May at both sites, all clams had resumed growth following the winter growth cessation.

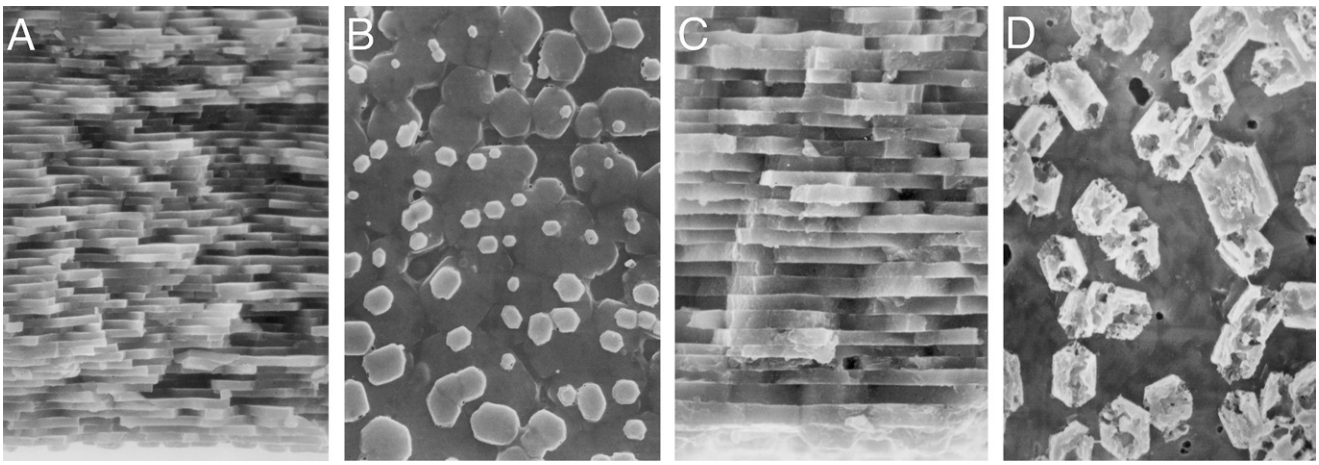

Figure 59. Scanning electron micrographs of fracture radial sections (A and C; inner shell surface at the bottom) and inner surfaces (B and D) of the inner nacreous shell layer of *Mytilus edulis* from Delaware Bay; growth is to the right. Scale is the same as in Figure 53B. (A and B) 2+-y-old collected in May 1987 with thin crisp hexagonal nacre tablets. (C and D) 3-y-old collected in June 1986 with thick, slightly dissolved nacre tablets.

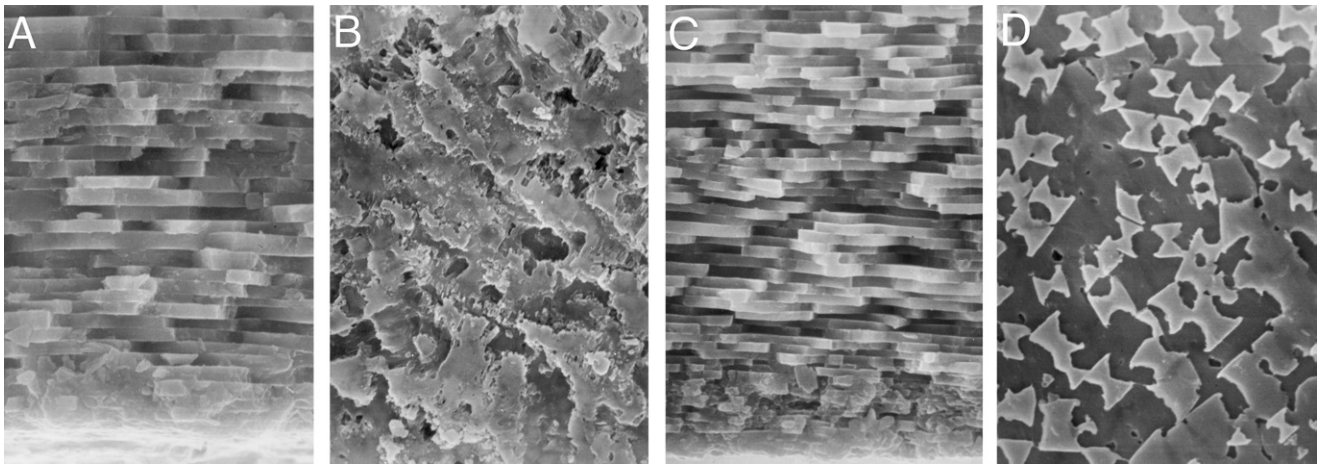

Figure 60. Scanning electron micrographs of fracture radial sections (A and C; inner shell surface at the bottom) and inner surfaces (B and D) of the inner nacreous shell layer of *Mytilus edulis* from Delaware Bay; growth is to the right. Scale is the same as in Figure 53B. (A and B) 2 y old collected in August 1986 with dissolved nacre. (C and D) 2 y old collected in September 1986 with summer growth cessation mark (granular sublayer) near the inner shell surface (C; micrograph taken near umbo) and hourglass nacre (D; also observed in June; micrograph taken near pallial line).

Shell growth from the most recently formed winter gcm in the outer layer to the ventral margin was measured in each specimen to observe seasonality in outer layer deposition. In clams collected from Newark Bay, the most recently formed winter growth cessation was that of the winter of 1988 to 1989, whereas in clams collected from the Shrewsbury River, it was the one formed in the winter of 1986 to 1987. The total mean annual outer layer increment deposited by 2-y-olds in 1988 was compared with partial 1989 increments formed by 2-y-olds collected from Newark Bay on each date. Similarly, the total mean annual outer layer increment deposited by 3-y-olds in 1986 was compared with partial 1987 increments formed by 3-y-olds collected from the Shrewsbury River on each date. Over half (between 58% and 64%) of the total annual outer layer increment was deposited by late May in clams from both systems, suggesting that growth rates in June through December are much slower than in spring (March–May). Growth rate reductions in summer were not observed in specimens of *Mya arenaria* collected in New Brunswick, Canada, by MacDonald and Thomas (1980), which is not surprising considering their more northerly location. Summer growth rate reductions were less pronounced in younger (0+- and 1+ y-old; Fig. 65D) than older individuals, which could have contributed to the more poorly defined bands in younger individuals, as discussed previously.

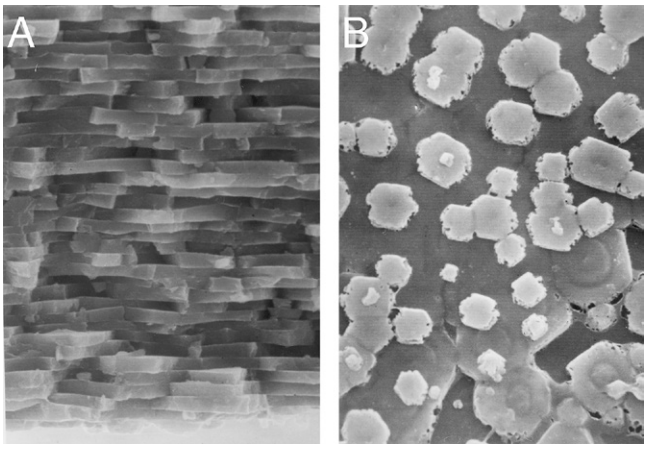

Figure 61. Scanning electron micrographs of fracture radial section (A; inner shell surface at the bottom) and inner surface (B) of the inner nacreous shell layer of a 0+-y-old *Mytilus edulis* collected in November 1986 from Delaware Bay; growth is to the right. Scale is the same as in Figure 53B. Micrographs were taken near the umbo and show relatively crisp, thick nacre that is just beginning to be stacked.

Chondrophore, Inner Complex Crossed-Lamellar Layer, and Age Determination

Softshell clams at both sampled locations formed opaque growth bands in the chondrophore (as viewed in thin shell sections) in early spring associated with gonad development prior to spawning (MacDonald & Thomas 1980, Brousseau & Baglivo 1987) and translucent zones during the remainder of the growing season from late spring through fall (Fig. 66). Translucent bands were observed at the chondrophore margin in specimens collected in summer (Fig. 66A) and fall (Fig. 66B), whereas thin opaque bands were observed at the chondrophore margin in spring (Fig. 66C, D). Age of *Mya arenaria* (in years) is determined by counting either the number of translucent or opaque bands in the chondrophore.

The pattern of seasonal growth band formation in the inner CCL shell layer was similar to that observed in the chondrophore: alternating translucent (disorganized crossed-lamellae; Figs. 67A and 68A, C) and opaque bands (well-organized crossed-lamellae; Figs. 67B and 68A, B) with the occasional inclusion of prismatic sublayers (Fig. 67A, D–E). Growth bands in the chondrophore, however, were more widely separated, and hence easier to count in thin shell sections (Fig. 66) than inner layer growth bands.

Early spring crossed-lamellar sublayers in the inner layer (Fig. 68A, B, D, E, and G), which were opaque in thin section, were interrupted by growth cessations more often (in general) than those formed in late spring through fall (Figs. 67B and 68A, C). Growth cessations in the inner layer were horizons paralleling the inner shell surface resulting from a discontinuity in shell deposition (Fig. 68B, F), which were often followed by a sublayer of prisms (Fig. 67A) or near-perpendicular lamellar elements (Fig. 68E, G). With

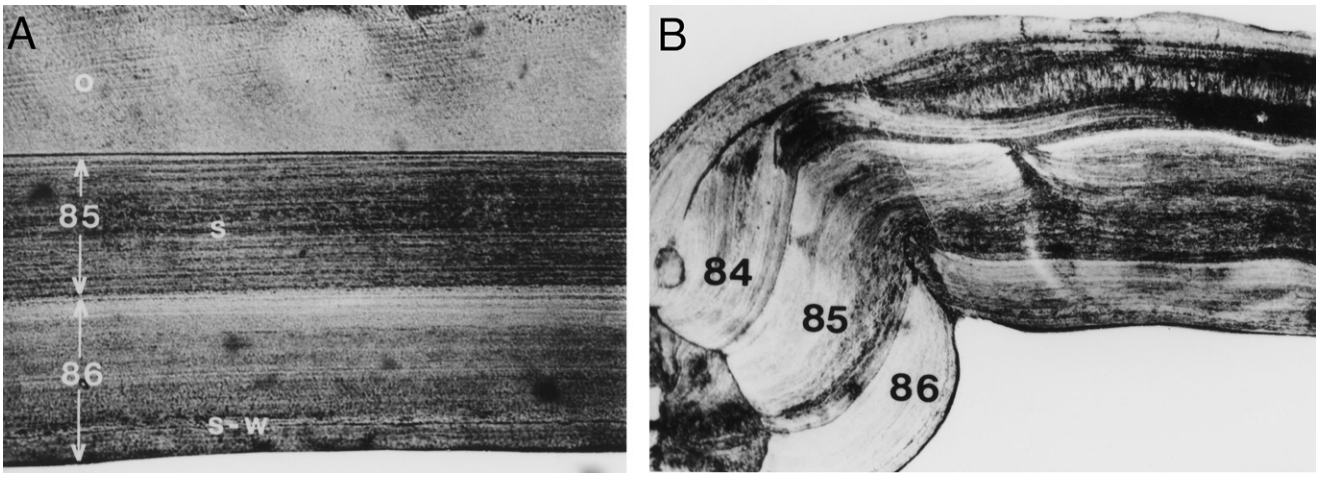

Figure 62. Light micrographs of acetate peel replicas of polished and etched radial shell sections of *Mytilus edulis* from Delaware Bay. Growth is to the right and inner shell surface is at the bottom of each micrograph. (A) Micrograph taken halfway between the umbo and pallial line showing two annual sequences (85 and 86) in the inner nacreous layer of a 3-y-old collected in May 1987; o-outer prismatic layer. The 1984 annual sequence did not extend far enough posteriorly to be seen in this micrograph. There was a thin (30 μM) band of nacreous tablets deposited in spring 1987 along the inner surface. Periods of slow growth in summer 1985 (s) and summer through winter 1986 (s-w) are marked. Horizontal field width (HFW) = 0.72 mm. B. Micrograph taken near the umbo showing three annual sequences (84, 85, and 86) in the inner nacreous layer of a 3-y-old collected in November 1986. Note the sharp discontinuities at the inner margin of each annual increment resulting from no growth during winter. HFW = 1.75 mm.

increasing age, growth cessations in summer became more common in inner layer microstructure. Summer inner layer growth cessations tended to be composed of a single discontinuity and followed by the deposition of prismatic or a nearly perpendicular lamellar microstructure. With increasing age and proximity to the umbo, prismatic, or perpendicular elements were increasingly observed on the inner surface from summer through fall (Fig. 67A).

Growth Rate and Longevity

Age was determined in 63 specimens collected from Newark Bay and 68 specimens collected from the Shrewsbury River. Of the Shrewsbury River group, 36 showed no sign of neoplastic disease whereas 32 had neoplastic cells (Barber 1990). Winter gcm in the outer shell layer were used to locate annuli on the shell exterior surface of the unimbedded valve

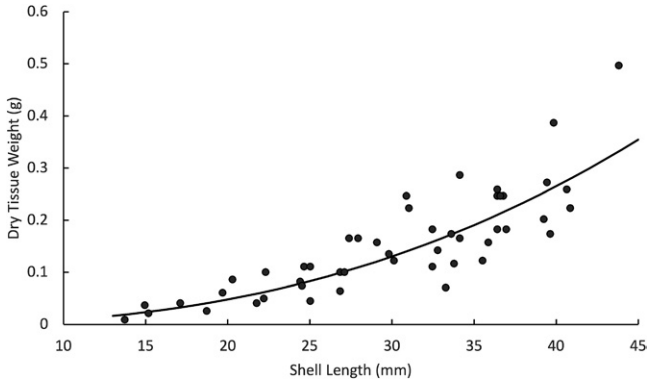

Figure 63. Total dry tissue weight plotted as a function of shell length for *Mytilus edulis* collected from Delaware Bay (N = 48). Line is back-transformed regression from text equation (2).

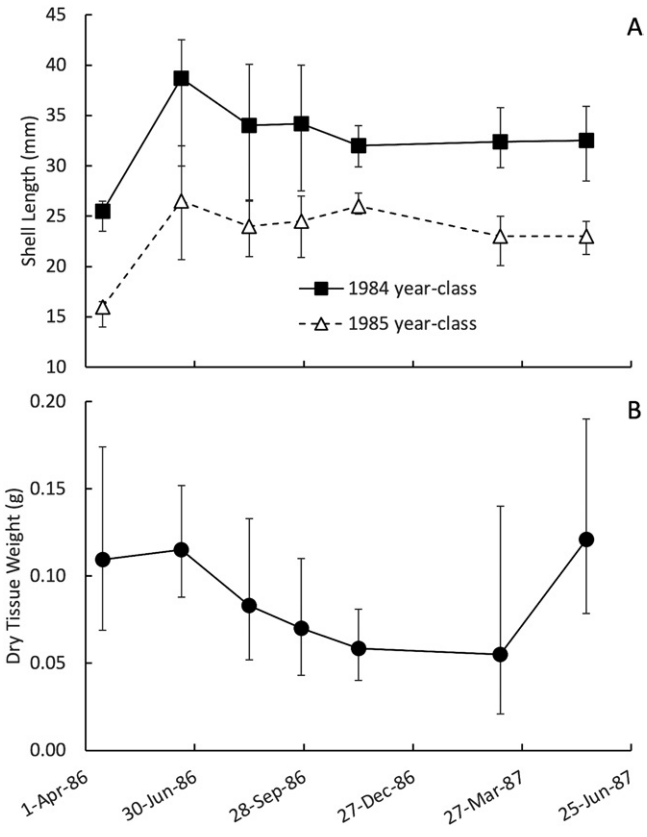

Figure 64. (A) Shell length (mean and range) of the 1984 and 1985 y-classes of *Mytilus edulis* collected from Delaware Bay between April 1986 and May 1987. (B) Estimated total dry tissue weight (mean ± 95% confidence interval) of a 25 mm mussel (approximately 2-y-old) between April 1986 and May 1987.

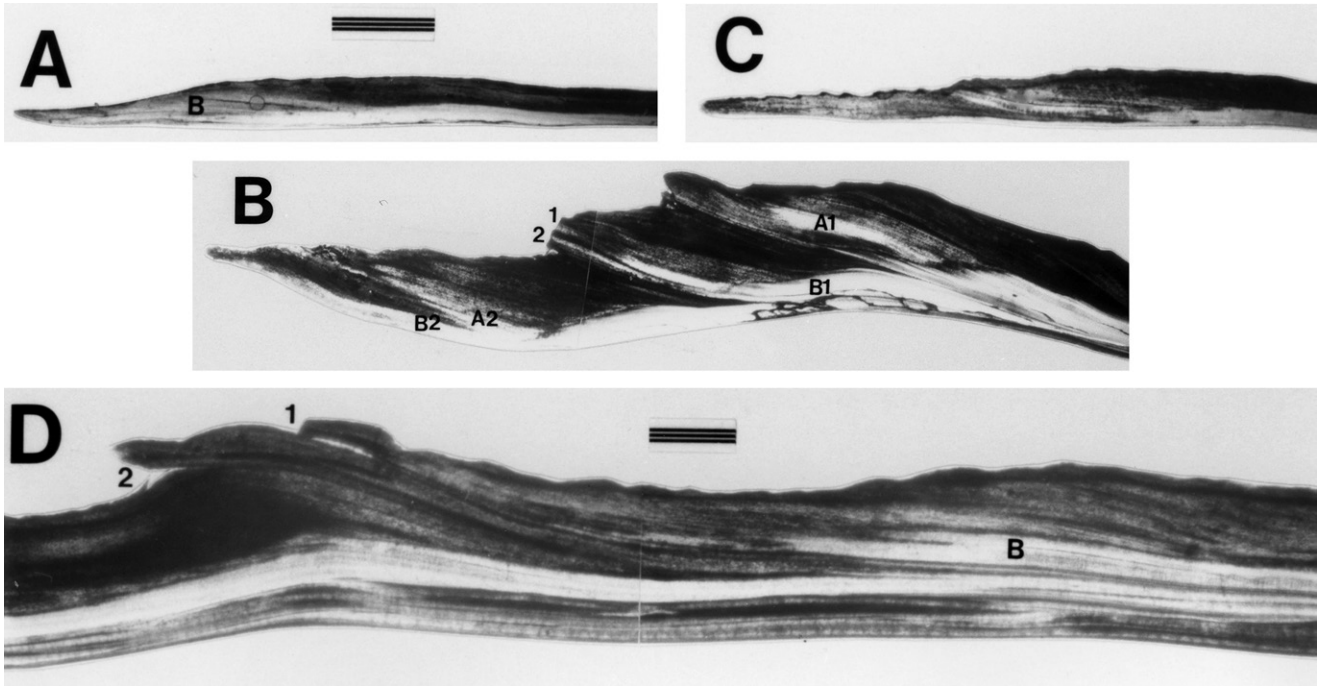

Figure 65. Light micrographs of thin sections of outer layers of *Mya arenaria* shells. Growth is to the left (the ventral shell margin is at the left in A–C) and the shell exterior surface is at the top. Scale bar in A = 1 mm (scale in B & C is the same as A); scale bar in D = 0.25 mm. (A) 2+- y-old collected in October 1988 from Newark Bay with a diffuse translucent band formed in fall along the inner shell surface (B). (B) 4+-y-old collected in December 1986 from Shrewsbury River. A1 and B1 are summer and fall/winter 1985 translucent bands, respectively. B1 is divided into two growth cessation marks (1 and 2) near the shell exterior. A2 and B2 are summer and fall/winter 1986 translucent bands, respectively. The 1986 annual increment in the outer layer consists of the region from 2 in B1 to the ventral shell margin. (C) 3-y-old collected in May 1989 from Newark Bay showing the fall/winter 1988 translucent band (B). Partial 1989 increment was measured from ventral-most extension of B to ventral shell margin. (D) 3+-y-old collected in October 1988 from Newark Bay showing the fall/winter 1986 translucent band (B) and two growth cessation marks (1 and 2) along the shell exterior.

of each pair. Shell length at each annulus was measured, yielding length at age.

There were no significant differences in the SL at each age (1–4 y) between uninfected and neoplastic clams collected from the Shrewsbury River (Fig. 69A; Student's t ranged from 0.028 to 1.54 by age, with all $P > 0.1$ (Sokal & Rohlf 1969). This strongly suggests that the neoplastic individuals were relatively recently infected with the disease, because most heavily infected individuals die relatively quickly (93% within a 3-mo period; Barber 1990).

Because there were no differences in size-at-age between neoplastic and uninfected individuals from the Shrewsbury River, the two groups were pooled and compared with the SL at age of specimens from Newark Bay (Fig. 69B). Shell lengths in Newark Bay were significantly smaller than in the Shrewsbury River at age 1 ($t = 3.066$, $P < 0.01$) and 2 y ($t = 4.094$, $P < 0.001$), but by 3 y of age, clams from the two systems were not significantly different in size ($t = 1.364$, $P > 0.1$). There were too few clams that had reached 4 y of age from Newark Bay to statistically compare their size to those from the Shrewsbury River, but the mean sizes were nearly identical (Fig. 69B).

Softshell clams inhabiting the Shrewsbury River may live at least 1 y longer than their conspecifics inhabiting Newark Bay. Of the 68 specimens from the Shrewsbury River whose age was determined, 20 were 4 y old (the largest had a SL of 73.1 mm) and three were 5 y old (the oldest clams aged with SL ranging from 58.6 to 62.0 mm). Clams of unknown age with lengths as large as 83.3 mm were collected from the Shrewsbury River, and these were likely older than 5 y. By contrast, the oldest aged specimens collected from Newark Bay were three 4-y-olds ranging in length from 57.5 to 58.7 mm, whereas the largest was a 3-y-old with a length of 64.6 mm. The greater range in SL of softshell clams from the Shrewsbury River (22.8–83.3 mm, $N = 107$) than Newark Bay (22.4–64.6 mm, $n = 135$) most likely resulted from greater longevity of Shrewsbury River clams, especially because there was no difference in size at age 3 y between the two sites. At both sites, it would take approximately 3 y to reach the 51 mm harvestable size suggested by Brousseau and Baglivo (1987), which is comparable to the slowest growth rate observed at one of three Long Island Sound sites they studied. They attributed slow growth rates of *Mya arenaria* at this site to the coarse intertidal sediments found there. Similar comparisons are not possible here, because little is known of the particle size distribution of Shrewsbury River sediments. In Newark Bay, however, sediments were very fine, suggesting that particle size alone may not be responsible for the relatively slow growth rates observed here.

Shell Weight

Softshell clams from Newark Bay had unusually thin shells for their size compared with those from the Shrewsbury River. To explore this observation, shell weight (SW; both valves) was regressed against SL (double natural log transformation) separately for clams collected from the two systems. Plotted together (Fig. 70A), there is considerable overlap between clams from the two systems, which, by eye, suggested little difference in

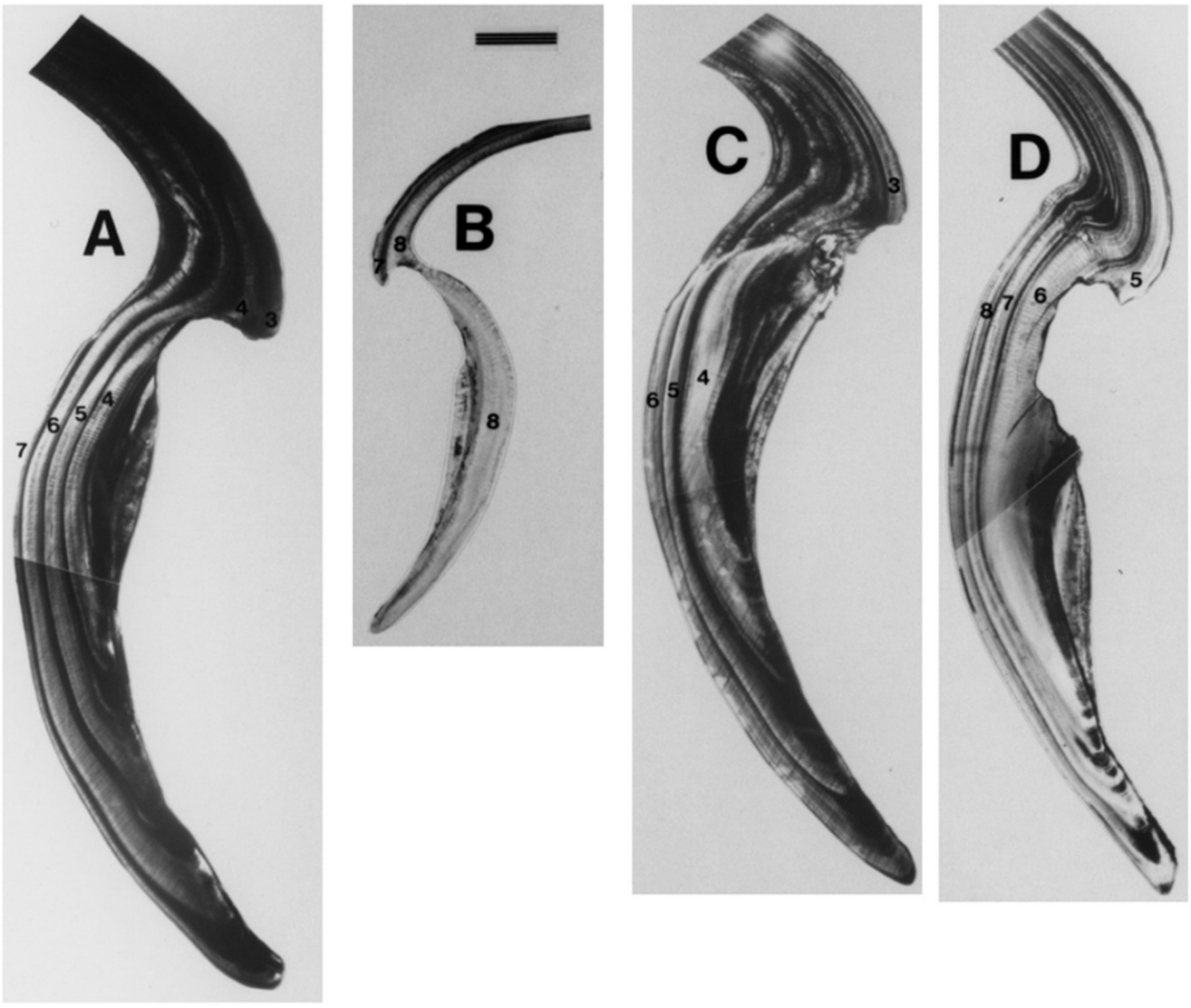

Figure 66. Light micrographs of thin sections of chondrophores of *Mya arenaria* shells. Growth of the chondrophore in each micrograph is down; ventral shell margins are to the left in A, C, and D and to the right in B. the shell exterior surface is at the top. Numbers 3–8 refer to the translucent bands formed in 1983 through 1988, respectively. Scale bar in B = 1 mm (scale is the same for all micrographs). (A) 4+-y-old collected in July 1987 from the Shrewsbury River with a translucent band along the inner (left) surface. (B) 1+-y-old collected in October 1988 from Newark Bay with a translucent band along the inner (right) surface. (C) 3+-y-old collected in March 1987 from the Shrewsbury River with no growth in 1987 (1986 translucent band along inner surface) (D) 4-y-old collected in April 1989 from Newark Bay with no growth in 1989 (1988 translucent band along inner surface).

shell weight at length, and comparison of the slopes of the two regression equations:

$$\text{Newark Bay}: \quad \ln SW = 3.208 \ln SL - 11.11 \quad r^2 = 0.94; \text{N} = 135 \tag{3}$$

$$\text{Shrewsbury River}: \quad \ln SW = 3.363 \ln SL - 11.60 \quad r^2 = 0.95; \text{N} = 107 \tag{4}$$

revealed no significant difference ($F = 2.125$, $P > 0.1$; Sokal & Rohlf 1969) suggesting that the regression lines parallel one another (Fig. 70B). Analysis of covariance, however, to test for a difference in computed values of SW for given values of SL revealed a highly significant difference ($F = 18.856$, $P < 0.001$), with Newark Bay clams having significantly lighter shells than Shrewsbury River clams of the same length. Using text equations (3) and (4), for example, a 60-mm clam from Newark Bay with a SW of 7.59 g would weigh 1.29 g less than a similarly sized clam from Shrewsbury River (SW = 8.88 g), a difference of approximately 15%.

It is not known why softshell clams from Newark Bay are lighter at length than those from the Shrewsbury River, but it may be related to their relatively high exposure to industrial pollutants, such as polychlorinated biphenyls and other hydrocarbons. Greater dissolution of carbonates along the shell exterior of softshell clams from Newark Bay does not appear to be responsible for this difference in shell weight, because the appearance of clams from both sites were similar and the slopes of text equations (3) and (4) were not significantly different. The latter might be expected if shell dissolution were a factor in shell weight differences between the two sites because older, larger clams with greater surface areas

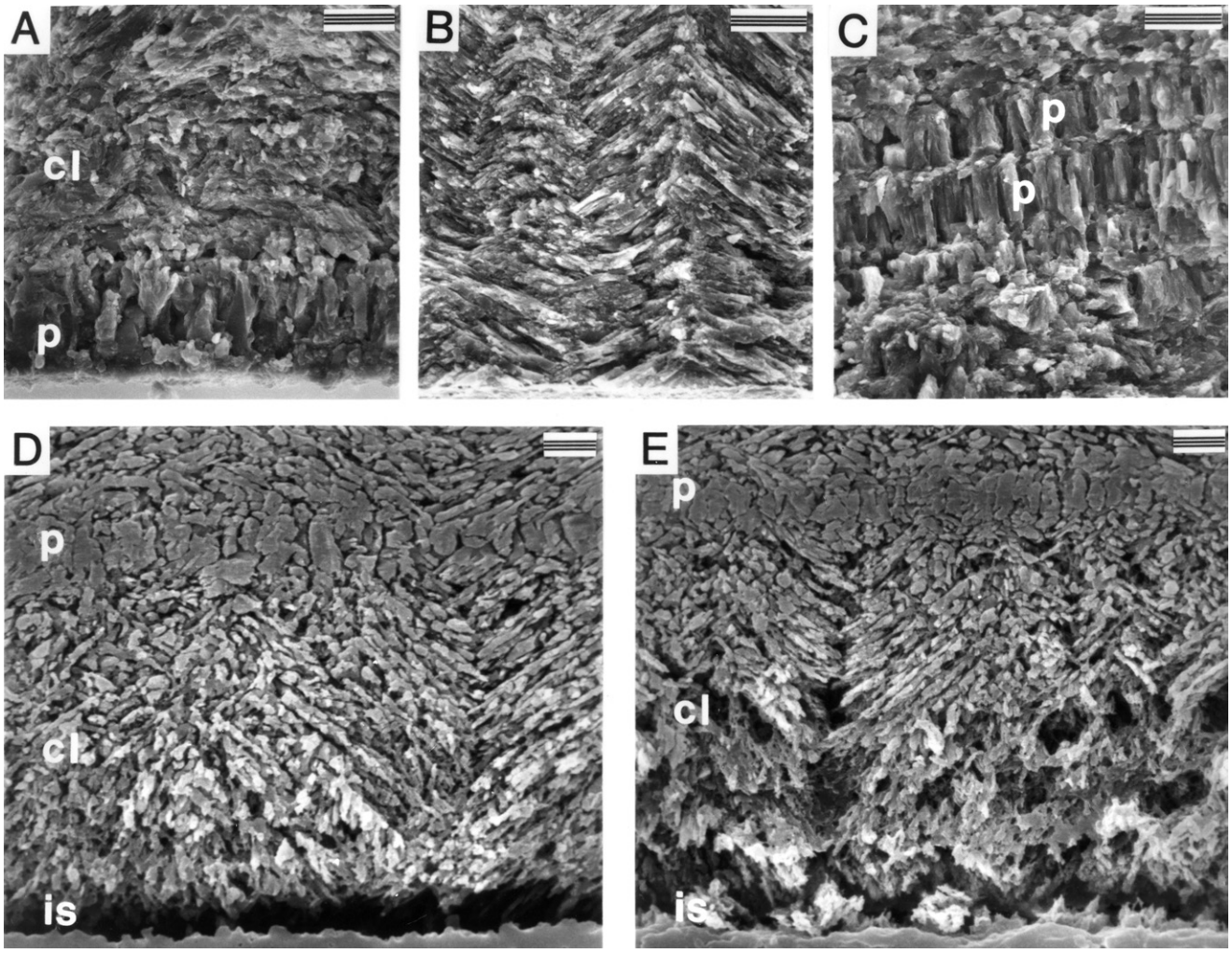

Figure 67. Scanning electron micrographs of fracture (A–C) and polished and etched (D and E) radial sections of *Mya arenaria* shells. The inner surface (is) is at the bottom of A, B, D, and E, and beyond the bottom of C. Prismatic (p) and complex crossed-lamellar (CCL) sublayers are labeled. Growth is to the right. Scale bars in A–C = 10 μM and in D and E = 2 μM. (A) 3+-y-old collected in October 1988 from Newark Bay; p along inner surface of the inner shell layer with disorganized CCL deposited in summer 1988 above. Micrograph was taken midway between umbo and pallial line. (B) 2-y-old collected in May 1989 from Newark Bay. Compare the well-organized cl along the inner surface of the inner layer from spring 1989 with that from summer 1988 in A. (C) 3+-y-old collected in May 1989 from Newark Bay. Micrograph was taken along the fractured radial surface of the outer crossed-lamellar midway between the shell exterior surface and the border with the inner shell layer. Two p's formed in summer 1988 are labeled. (D & E) 4-y-old collected in March 1987 from the Shrewsbury River. Note the strong similarity in the sequence of sublayer formation in the inner shell layer (D) and chondrophore (E); p formed in winter 1986 to 1987 and CCL formed in early spring 1987.

would have been exposed for a longer time than younger, smaller clams. Brousseau and Baglivo (1987) found that the slowest-growing softshell clams had heavier shells than those from sites where growth rates were greater. Using that relationship, our results are contrary to theirs, because growth rates, at least during the first 2 y were slower at Newark Bay than in the Shrewsbury River, yet the shells of clams from Newark Bay were lighter.

Dry Tissue Weight, Gonad Development, and Shell Growth in Newark Bay

Dry tissue weights were measured only for softshell clams collected from Newark Bay. Natural log of individual DTW was regressed against *SL* for each of the five collections and the DTW of a 40 mm *SL* softshell clam was estimated for each collection date (Fig. 71). Computed DTW was greater in April and May 1989 than in June, July, and October 1988. When the summer-fall 1988 data were pooled and compared with pooled spring 1989 data, DTW in spring 1989 (0.719 g) was 55% greater than in summer/fall 1988 (0.464 g). This fits well with what is known of softshell clam reproductive cycles at this latitude. Brousseau (1987) found highest percentages of spent (recently spawned) softshell clams at sites in Long Island Sound in June and July. Thus, the greater DTW in spring 1989 represented the development of gonad prior to spawning, whereas lower DTW in summer/fall 1988 reflects postspawning conditions.

Spring is the season of both gonad development and deposition of an opaque shell growth band in the inner CCL layer and chondrophore in *Mya arenaria* in New Jersey. MacDonald and Thomas (1980) and Brousseau and Baglivo (1987) also found a strong coupling between the reproductive cycle and opaque band formation in *M. arenaria*, but this period is not necessarily a period of slow shell growth. Both the microstructure

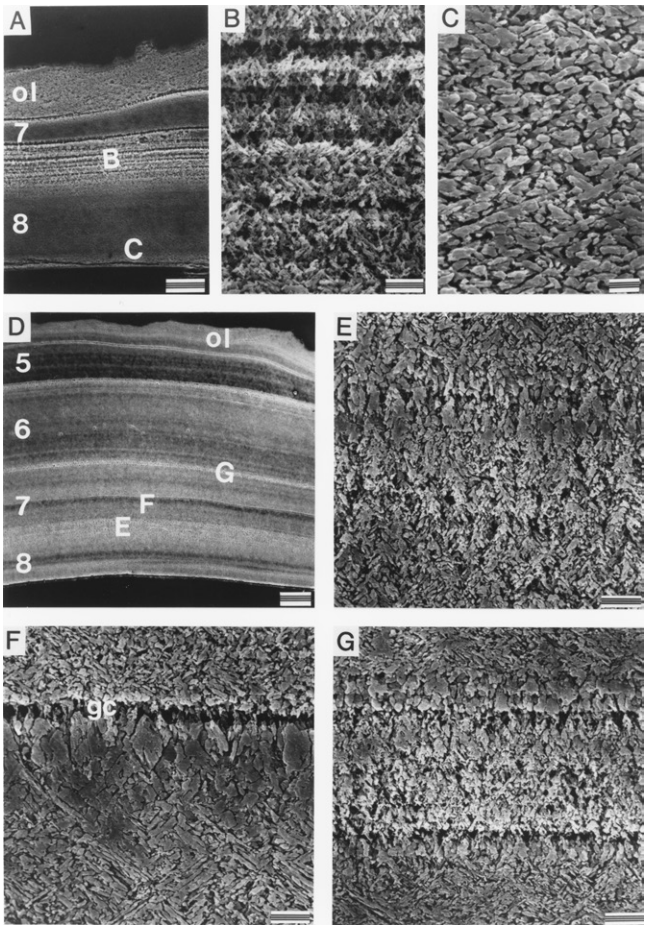

Figure 68. Scanning electron micrographs of polished and etched radial shell sections of *Mya arenaria* collected in July 1988. (A–C) 1+-y-old. (D–G) 3+-y-old. Low-magnification micrographs A and D were taken near the umbo and show the entire cross-section of the shell from outer layer (ol) to inner surface at the bottom; growth is to the right. Capital letters refer to locations in A and D where micrographs in B, C, and E–G were taken, respectively; numbers 5–8 refer to the years 1985 to 1988 when inner layer translucent bands were formed; gc = growth cessation mark. Scale bars: A = 50 μM; B and E–G = 5 μM; C = 2 μM; D = 100 μM.

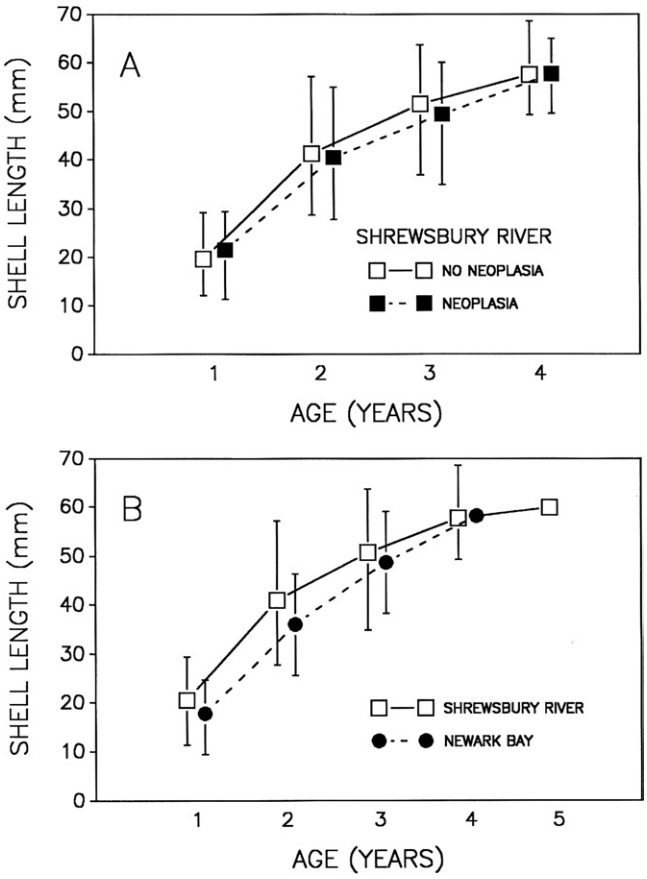

Figure 69. Shell length (mean and range) at ages 1–5 y of *Mya arenaria* collected from Shrewsbury River and Newark Bay. (A) Shell length-at-age of neoplastic and nonneoplastic softshell clams from the Shrewsbury River. (B) Shell-length-at-age of Shrewsbury River and Newark Bay softshell clams.

of opaque bands and seasonal growth data suggest that shell growth rates during spring are faster than during summer and fall. Opaque and translucent bands in other species such as *Spisula solidissima* and *Mercenaria mercenaria* are associated with periods of relatively fast and slow growth, respectively. Based on these data and analogy with other species, shell growth in *M. arenaria* does not appear to be slower in spring because of the simultaneous development of gonad in preparation for early summer spawning. Inhibition of shell growth in *M. arenaria* in New Jersey may occur in late winter and early spring (February and March) when gonad is beginning to be developed, followed in late spring (April and May) by a period of more rapid shell growth. Because of the dates of sampling in this study, however, our data cannot be used to adequately address this question.

In summary, opaque and translucent bands in the inner CCL shell layer of *Mya arenaria* (as viewed in thin radial shell sections) collected from two sites in New Jersey were formed in spring and summer/fall, respectively. Analysis of these bands permitted the determination and reconstruction of growth rates during the lifespan of individual specimens. Microstructural differences between the two types of growth bands in the inner layer and chondrophore corresponded with differences in their optical properties; opaque bands were composed of frequently interrupted, poorly organized crossed-lamellar microstructure, whereas translucent bands were composed of well-organized and relatively continuous crossed-lamellar microstructure. Seasonality of band formation was correlated with the reproductive cycle of softshell clams, such that opaque bands were generally formed during periods of gonad development, whereas translucent bands were formed in postspawning periods. Prismatic sublayers, which are representations of little or no shell growth, were formed in both winter and summer within both the outer crossed-lamellar and inner shell layers. Translucent zones (in thin shell section) accompanied outer layer prismatic sublayer formation. Translucent zone definition and frequency of occurrence of prismatic sublayers increased with age.

Analysis of shells of softshell clams collected from Newark Bay and the Shrewsbury River revealed that (1) clams from Newark Bay were significantly smaller at age 1 and 2 y than clams from Shrewsbury River; (2) clams from Shrewsbury River may live at least 1 y longer than those from Newark Bay; and (3)

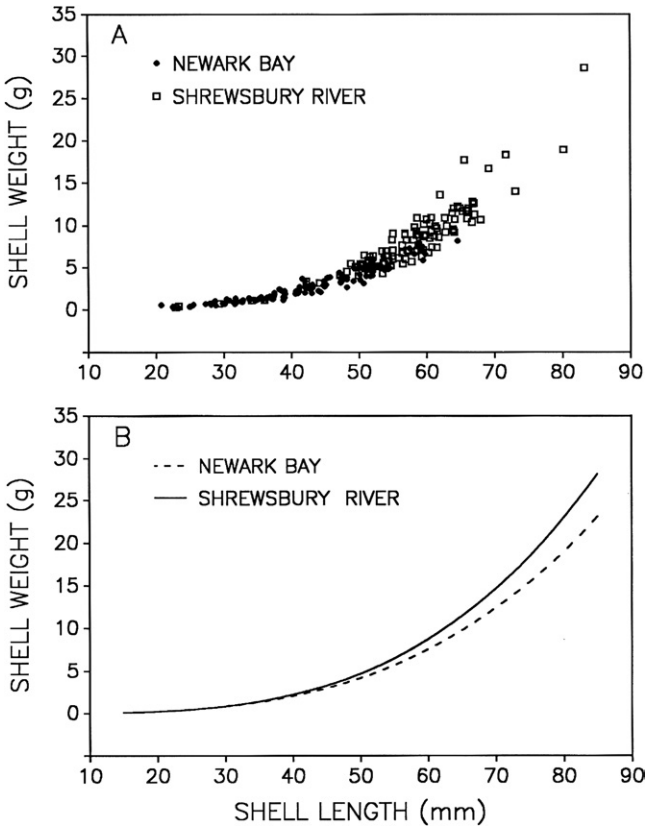

Figure 70. (A) Shell weight plotted against shell length for individual *Mya arenaria* collected from Newark Bay and the Shrewsbury River. (B) Regressions of shell weight on shell length based on text equations (3) and (4), showing similar slopes but significantly lighter shells-at-length in Newark Bay than in the Shrewsbury River.

shells of clams from Newark Bay were significantly lighter than similarly sized clams from the Shrewsbury River. All three of these effects may result from the higher levels of contaminants in Newark Bay compared with Shrewsbury River.

The size-at-age of softshell clams from the Shrewsbury River that were infected with the neoplastic disease was not different from uninfected individuals. Historical analyses of growth rates did not reveal any differences between the two groups of clams,

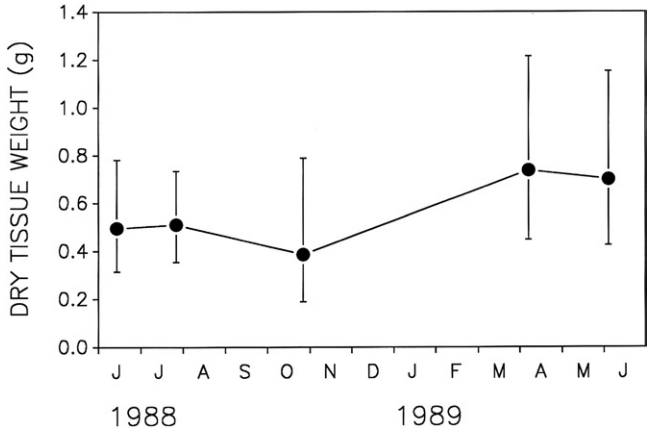

Figure 71. Estimated mean (±95% confidence limits) dry tissue weight (g) of 40 mm shell length *Mya arenaria* in Newark Bay on five collections dates between June 1988 and May 1989.

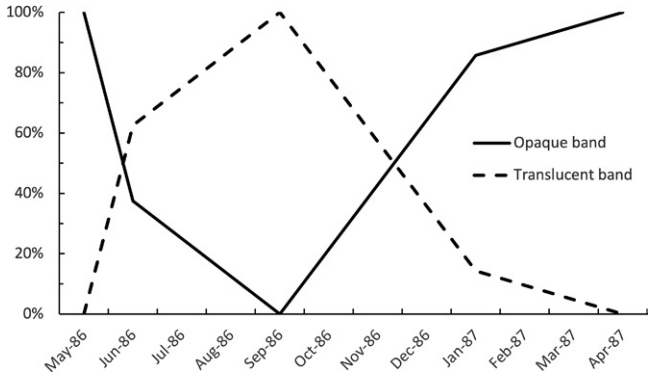

Figure 72. Percent of each sample of *Spisula solidissima* with an opaque or translucent band along the chondrophore margin. Sample sizes: May 1986—12; June 1986—8; September 1986—8; January 1987—14; April 1987—12.

suggesting (and supporting the conclusions of Barber 1990) that disease progression leading to death in heavily infected individuals is relatively rapid and would not be detectable by analysis of annual growth rates.

Spisula solidissima, the Surf Clam

The surf clam, *Spisula solidissima*, has an entirely aragonitic shell with inner and outer layers (separated by a pallial myostracum) composed of a crossed-lamellar microstructure (Taylor et al. 1969, 1973). Barker (1964) first described the growth lines and zones present in radial sections of the outer shell layer and the chondrophore, the extension of the shell from the umbo into the shell's interior to which the hinge ligament is attached. Growth lines and zones reflect seasonal changes in shell growth rates. An annual increment consists of one pair of translucent and opaque zones (Jones 1980a,b, 1981, Jones et al. 1978, 1983, Wagner 1984), which refer to their appearance in thin sections of the chondrophore or the entire shell under transmitted light. Jones (1980a,b) described the microstructure of the translucent band as having a denser, more organized crossed-lamellar microstructure than the opaque zone, which is more porous and has more light-reflecting surfaces than the translucent zone.

The type of growth zone (translucent or opaque in thin section) that was present at the chondrophore margin was recorded to determine the seasonality of zone formation. In addition, the distance from the umbo to the ventral margin of each translucent zone was measured to determine size-at-age, construct a growth curve, and estimate age. Annual increments were measured as the distance from the ventral edge of each translucent zone to the ventral edge of the subsequent one.

Chondrophore Margin Growth Patterns

Translucent zones were observed at the chondrophore margin most often in summer and early fall (June and September), whereas opaque zones were present at the margin most often during the remainder of the year (May, January, and April; Figs. 72 and 73[2]). A single annual increment consisted of one opaque zone (formed in late fall and spring) and one translucent zone (formed in summer and early fall). Translucent zones are formed during periods of reduced shell growth rates, whereas opaque zones are formed during rapid growth periods (Jones et al. 1978, 1983, Jones 1980a,b, Wagner 1984).

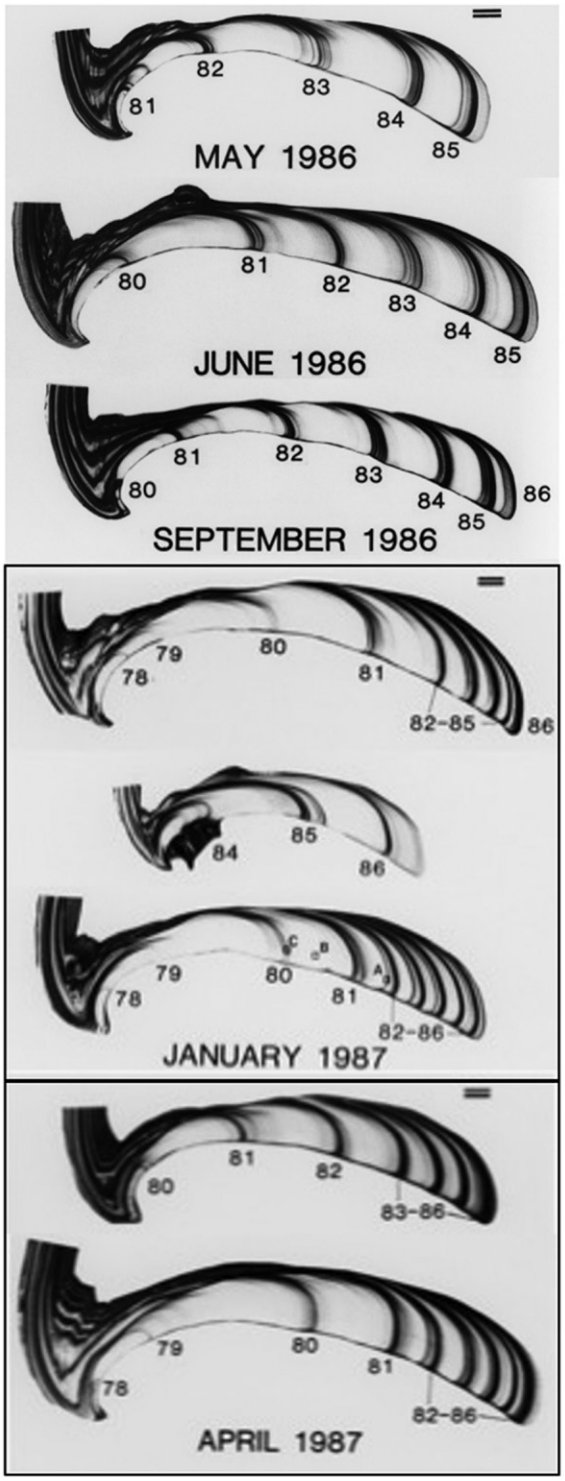

Figure 73. Enlargements of thin sections (using transmitted light) of chondrophores of *Spisula solidissima* shells. Growth is to the right and umbo is at lower left. Scale is the same for: (1) May, June, and September 1986 (bar = 1 mm); (2) January 1987 (3 images; bar = 1 mm); and (3) April 1987 (2 images; bar = 1 mm). Translucent zones appear dark and opaque zones appear light in these "negative" enlargements. Numbers indicate the year (summer and early fall) of translucent zone formation. Clams collected in May and June had opaque zones at the margin; in September—translucent zone; in January—top and bottom: translucent, middle: opaque; in April—both opaque. Squares labeled A, B, and C in January 1987 bottom denote where micrographs in Figure 74 were taken, respectively.

Fourteen percent of the January sample (two of 14) had a translucent zone, rather than an opaque zone at the chondrophore margin. Both of these clams were over 5 y of age, but not all older clams had translucent zones at their margins in late fall and winter. This suggests that a certain percentage of the population older than 5 y do not have a period of fast growth in the late fall after slower growth in summer and early fall. This was also found in *Mercenaria mercenaria* older than 8 y in lower Chesapeake Bay, VA (Fritz 1982, Fritz & Haven 1983).

Deposition of translucent zones by *Spisula solidissima* in summer and early fall off New Jersey coincides with both the period of highest water temperature during the year, and of gonadal development and spawning (Jones et al. 1978, Wagner 1984). Shallow populations of surf clams (living in <10 m of water) tend to begin translucent zone formation earlier in summer and have slower shell growth rates than populations living in deeper waters at comparable population densities, which may be the result of exposure for longer periods of time to higher water temperatures in summer and early fall (Wagner 1984). It is unclear, however, which of the two factors, gonadal development or high temperature, is more important in inducing translucent zone formation in *S. solidissima*. In shallower subtidal waters, *Mya arenaria* formed opaque bands in early spring associated with gonad development, and translucent zones during the remainder of the growing season (late spring through fall).

The translucent zone is composed of a dense and orderly arrangement of crossed lamellae and often has narrow microgrowth increments (Fig. 74A, C). The opaque zone has larger crossed lamellae than the translucent zone, appears less organized, and if microgrowth increments are identifiable, they are wider than those in translucent zones (Fig. 74A, B). Microgrowth increment boundaries appear as ridges in etched radial sections because they are more resistant to acid etchant than the surrounding carbonate. This is most likely the result of a higher concentration of organic matrix in the boundaries. Accumulation of the acidic end products of glycolysis is buffered by shell carbonates during extended periods of valve closure, leaving a residue (increment boundary) along the inner shell surface that has a greater concentration of organic matrix (Lutz & Rhoads 1977). Upon resumption of aerobic metabolism, inorganic shell is deposited. Translucent zones are often composed of a series of tightly spaced microgrowth increments (Fig. 74A), suggesting slow and interrupted growth. By contrast, increments, if present, are wider in opaque zones, suggesting faster and less-interrupted growth (Fig. 74B).

Age Distribution and Shell Length-at-Age

One-third (18/54) of the surf clam specimens collected were members of the 1978 YC, whereas at least one specimen from each of eight other YC (1976, 1977, and 1979–1984) was collected (Fig. 75). Age-distribution data is important for fisheries management and for evaluation of seasonal growth patterns. Shell length-at-age for each surf clam was back-calculated (Fig. 76) using the series of measurements from the umbo to the ventral edge of each translucent zone in chondrophore thin section enlargements (e.g., Fig. 73) and the linear regression of *SL* (in mm) on total chondrophore height (*CH*, in mm) at capture:

$$SL = 5.14(CH) + 51.74 \quad r^2 = 0.68; \mathrm{N} = 54. \tag{5}$$

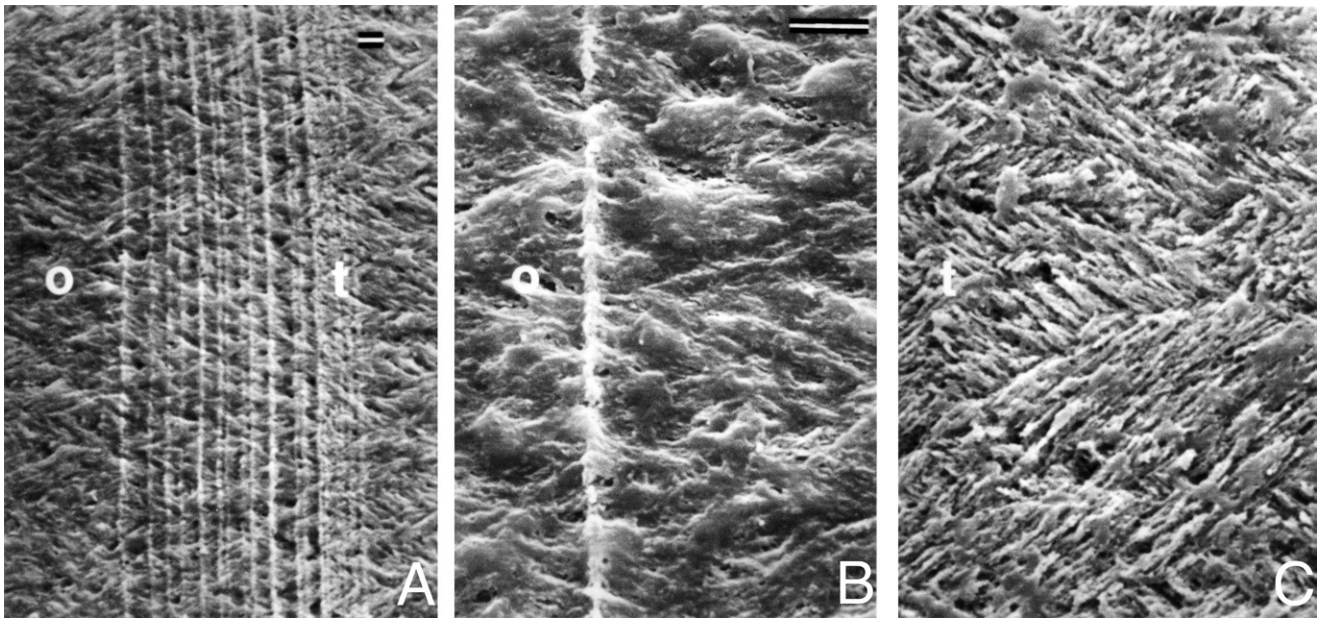

Figure 74. Scanning electron micrographs of polished and etched radial sections of the chondrophore of an *Spisula solidissima* collected in January 1987 [same specimen as in Fig. 73 (January 1987 bottom) with labeled boxes corresponding to locations where micrographs A–C were taken]. Growth is to the right and both scale bars = 4.3 µM (scale in B and C is the same). (A) Boundary of opaque (o) and translucent zones (t), with a series of microgrowth increment boundaries in t. (B) o microstructure with a single microgrowth increment boundary (vertical bright line). (C) t microstructure.

Annual Increments

Each YC of surf clams will be exposed to a unique set of growing conditions and environmental stressors during the course of their lives, and as a consequence, will have their own growth curve. For instance, in Figure 73, the chondrophores of three 1978 YC clams are shown (top and bottom January 1987, and bottom April 1987): note the strong similarity in the spacing of small translucent bands formed in the summers of 1978, 1979, 1980, and 1981. Similarly, the chondrophores of three 1980 YC clams (June and September 1986, and top April 1987 in Fig. 73) reveal strong similarities in the spacing of the translucent zones formed in 1981, 1982, and 1983. The back-calculated growth curve in Figure 76 is based on the mean length-at-age of all clams analyzed, but growth of individual YC can be reconstructed by measuring each annual increment (one pair of translucent and opaque zones) and comparing patterns across ages and years (Fig. 77).

Each of the four largest YC of *Spisula solidissima* sampled grew at different rates at the same age, likely because of the differences in environmental conditions (e.g., temperature and food availability) during those years. For instance, growth by the 1978 YC during y 2 (1979) was between 16% and 40% less than the 1977, 1979, and 1980 YC during their second year. Thus, growth during 1979 may have been slower for all YC, which appears to be the case: growth by the 1977 YC during y 3 and by the 1978 YC during y 2 was less than other YC during those growth years (Fig. 77). Similarly, 1982 was another poor growth year: growth by the 1977 YC in year 6, by the 1978 YC in y 5, by the 1979 YC in y 4, and by the 1980 YC in y 3 was less than other YC during those growth years. Bottom water temperatures off New Jersey in fall 1982 were higher than normal, and

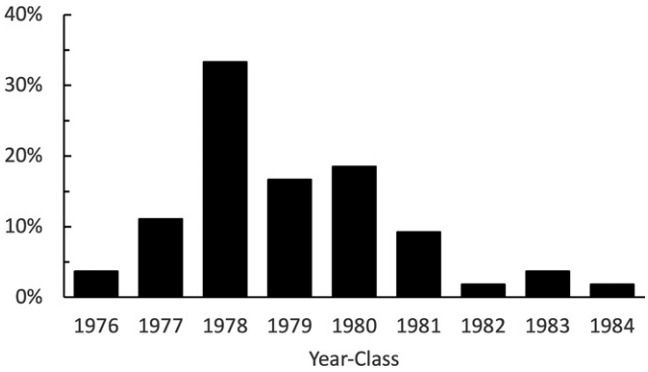

Figure 75. Distribution of *Spisula solidissima* by year-class collected between May 1986 and April 1987 (*n* = 54).

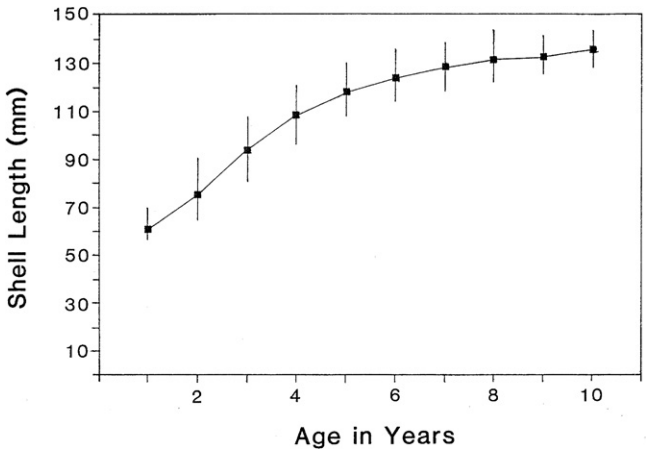

Figure 76. Back-calculated shell length (mean and range) at age of *Spisula solidissima* collected between May 1986 and April 1987.

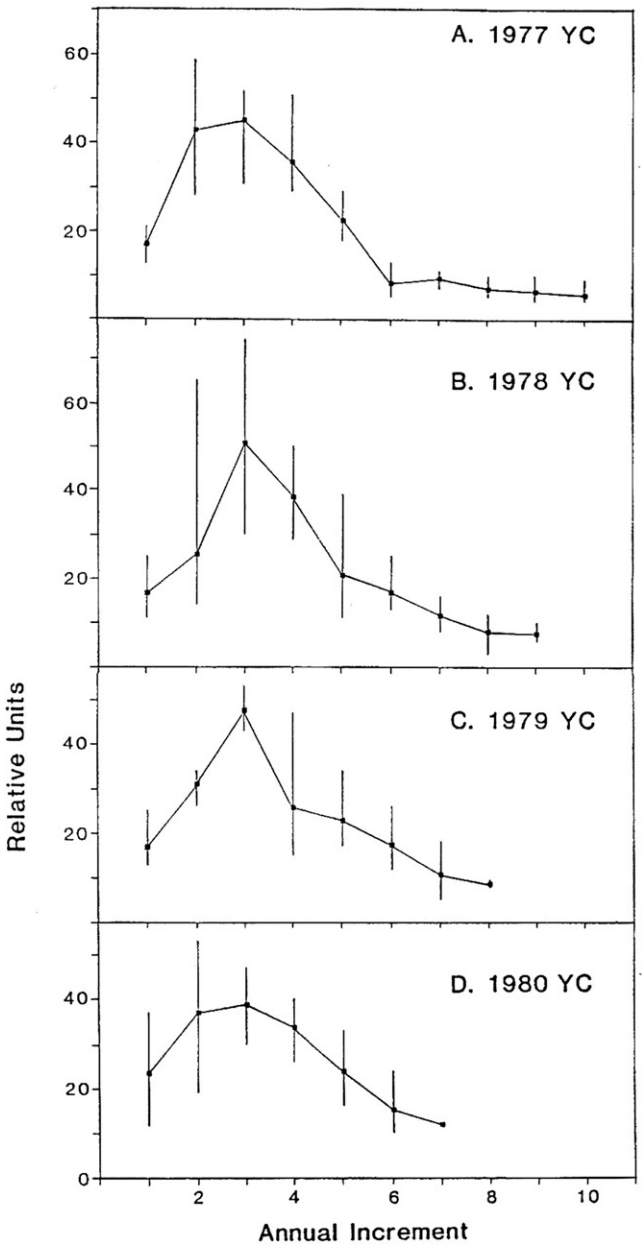

Figure 77. Annual growth increments (mean and range) of the 1977 (A. *n* = 6), 1978 (B. *n* = 18), 1979 (C. *n* = 9), and 1980 (D. *n* = 10) year-classes of *Spisula solidissima* collected in 1986 and 1987.

low dissolved oxygen levels were recorded across wide swaths of the mid-Atlantic Bight in summer-fall 1979 that likely slowed shell growth by *S. solidissima* in these 2 y (Jones 1981, Wagner 1984). Analyses of shell growth records in this manner enables detection of the impacts of an environmental event long after it has occurred.

Analyses of shells of *Spisula solidissima* are useful for reconstructing annual and broad seasonal growth patterns and rates for individuals and groups (e.g., YC). The effects of both chronic and ephemeral environmental disturbances on growth can be evaluated. In an impact assessment study, it would be advisable to focus the analysis of growth history on a single abundant YC of *S. solidissima* to eliminate age as a factor in the response. The lack of periodic shell microstructures deposited on time scales shorter than seasons prohibits the estimation of the date of formation of any particular feature (such as a microgrowth increment or the beginning of an opaque or translucent zone) to any closer than a month. In many cases, this may be sufficient to pinpoint a cause-and-effect relationship. Simple growth measurements from thin chondrophore sections reveal relatively detailed reconstructions of seasonal and annual growth.

CONCLUSIONS

Seasonal changes in the microstructure of the shells of six bivalve species inhabiting fresh, brackish, estuarine, coastal, and continental shelf waters in the mid-Atlantic region are useful for reconstructing individual and population growth histories. Cycles and abrupt changes in the environment or the physiology of the animal, such as seasonal temperature fluctuations, storms, and gametogenesis, were reflected in shell microstructural growth records. Seasonal and annual growth rates and histories can be reconstructed from single samples in time using the annual cycle of shell microstructural deposition. The time of formation of gcm in outer shell layers can be dated relatively accurately in the three species (*Corbicula fluminea, Geukensia demissa*, and *Mytilus edulis*[3]) that form microgrowth increments at known periodicities (e.g., one per tidal immersion or per solar day). This can be done by counting increments from a region of known formation time, such as the shell margin (=date of collection).

The biomineralization of barite by Corbicula fluminea (Fritz et al. 1990a) apparently resulted from Maurice River waters being enriched in soluble barium from the numerous glass factories in the watershed. The clams concentrate barium from solution and presumably excrete it into the extrapallial space where it crystallizes, along with sulfate (which is abundant in freshwaters), as barite along the inner shell depositional surface. Golden clams in this and other rivers could serve as bio-monitors for heavy metal enrichment in surface waters. It is not known whether other freshwater, estuarine or marine bivalves can also biomineralize barite, or whether other minerals can also be deposited. The relatively plastic mineralogical deposition exhibited by *C. fluminea* suggests that investigation and monitoring of bivalve shell mineralogy could also be an important tool, along with growth pattern analysis, for environmental biomonitoring.

In four of the six species analyzed (*Corbicula fluminea*—three sites; *Geukensia demissa*—four sites; *Mya arenaria*—two sites; and *Mytilus edulis*—three sites), growth rates and shell microstructural changes varied by collection site, reflecting different environmental conditions. These changes included (1) greater number of prismatic and granular sublayers in the inner shell layers of *C. fluminea* and *G. demissa* with increases in environmental variability (e.g., temperature and salinity) and (2) increased angle of deposition of outer layer prisms by *M. edulis* as the severity and number of disturbances increased. The documented microstructural changes can be used to quantitatively assess the effects of a particular disturbance, and the time of formation of the resultant gcm can be accurately dated. Thus, for each species, shell micro and macrostructural growth patterns can be used as sublethal, environmental biomonitoring tools.

As with all biological systems, there is both individual variability in the expression of environmental changes in shell microstructure, but also changes with age. In all bivalve

TABLE 5.

Advantages and disadvantages of the use of the shell microstructural growth patterns of six bivalve species in New Jersey for environmental biomonitoring studies.

Species	Advantages	Disadvantages
Corbicula fluminea	Ubiquitous in freshwater habitats	Tolerant
	Daily outer layer microgrowth increments	Short life span (up to 4 y)
	Barite biomineralization	Slow growth in summer when brooding larvae
	Does well in cage studies	–
	Forms recognizable inner and outer layer gcm	–
	Tolerant	–
Rangia cuneata	Only consistent inhabitant of oligohaline zone	–
	Medium life span (up to 6 y)	Restricted to seasonal and annual growth rate analyzes
	Forms recognizable inner and outer layer gcm	–
	Tolerant	–
Geukensia demissa	Intertidal; ubiquitous in meso- and polyhaline-estuarine habitats	Tolerant
	Long life span (up to 18 y)	Formation of seasonal inner layer sublayers is patchy along inner shell surface
	Tidal outer layer microgrowth increments (?)	Epifaunal; aerial exposure effects possible
	Alternates microstructural morphs seasonally in the inner layer for age determination	–
	Forms recognizable inner and outer layer gcm	–
	Tolerant	–
Mya arenaria	Intertidal, infaunal, common in mesohaline estuarine habitats	–
	Forms recognizable inner and outer layer gcm	Restricted to seasonal and annual growth rate analyzes
	Resumes growth in early spring	Reduced shell growth rates in summer and fall
	Medium life span (over 5 y)	–
Mytilus edulis	Intertidal and subtidal; common in polyhaline estuarine habitats	Availability of recent recruits (fast growers) is limited in some systems
	Forms recognizable inner and outer layer gcm	In some habitats, summer/fall growth rates slow at relatively young ages (4–6 y)
	Resumes growth in early spring	–
	Does well in cage studies	–
	Tidal outer layer microgrowth increments (?)	–
	Angle of outer layer prism deposition reflects changes in growth rate	–
Spisula solidissima	Continental shelf; infauna; common	Limited site-specific knowledge if obtained via commercial samples
	Wide depth distribution	Restricted to seasonal and annual growth rate analyses
	Clear seasonal growth bands in chondrophore	–
	Fast growth rate and medium life span (20+ y)	–

GCM, growth cessation mark.

species studied, shell growth rates decline with age, and this is also reflected in seasonal microstructural growth band formation. Generally, as age increased, summer and fall growth rates declined and the only season remaining with relatively fast growth rates was spring. This resulted in the lack of distinct summer and fall growth bands within shell microstructure with increasing age in *Rangia cuneata*, *Geukensia demissa*, *Mytilus edulis*, and *Spisula solidissima*. Generally, opaque (thin section) or light bands (acetate peels) were produced during periods of relatively fast shell growth rates, whereas translucent (thin section) or dark bands (acetate peels) were formed during periods of relatively slow shell growth rates. These differences in optical properties reflect differences in shell microstructural organization, with opaque bands being poorly organized and composed

of larger elements than the highly organized translucent bands composed of smaller elements. Differences in seasonal growth rates and band deposition must be taken into account when using bivalve species for environmental monitoring, because the specific effects of disturbances during slow-growth seasons may not be distinguishable within the shell microstructure. For instance, *Mya arenaria* and *M. edulis* resumed growth in spring earlier than the other species studied, whereas *C\orbicula fluminea*, *R. cuneata*, and *G. demissa* continued to grow through the summer, though at reduced rates.

Advantages and disadvantages associated with the shell growth patterns of each species in environmental monitoring studies are listed in Table 5. In some cases, certain characteristics are listed as both advantages and disadvantages. For instance, species that are tolerant to environmental change are likely to survive a relatively small disturbance (an advantage) but show little if any show any effect (potentially a disadvantage). All species have the disadvantage that growth rates are slow to nonexistent in the winter. All species are recommended for use in environmental monitoring studies, which could consist of periodic samples from the natural population or from groups of caged specimens in specific locations. The former would be more useful for determination of the effects of a wide-ranging disturbance after it had occurred or for investigations of chronic or slow deteriorations in the water quality of a river or estuary. The latter would be more useful in sublethal environmental impact assessment at particular locations, such as in a gradient exposure from an effluent discharge. In either case, the basic knowledge of natural seasonal shell growth patterns and how they are affected by age and habitat enable the effects of a known disturbance to be revealed and understood.

ACKNOWLEDGMENTS

This work began in 1985 and was originally finalized as reports to the New Jersey Department of Environmental Protection who funded it as part of baseline studies to document molluscan shell growth patterns for use in environmental impact assessment. Many people at Haskin Shellfish Research Laboratory and throughout New Jersey assisted in the collection of specimens and supported this project, and we specifically want to acknowledge the contributions of Carolyn Albert, Bruce Barber, Walter Canzonier, Keith Cooper, Merrill Cottrell, Angela Cristini, Stephen Fegley, Antonio Figueras, S. Cynthia Fuller, Richard Gustafson, Timothy Jacobsen, Bruce James, Donald Kunkle, Tim Littlewood, Bruce MacDonald, Dan O'Connor, Jack Parsons, Hu Ya-Ping, Bruce Ruppel, Margaret Schenk, Eric Wagner, Robert Wargo, and the anonymous crews of fishing vessels who saved surf clams for us. We also thank John Grazul, Richard Triemer, and Allan Pooley for their assistance with scanning electron microscopy and energy dispersive X-ray fluorescence; Beverly Webster, Janice Laws, and Wilma Williams for their attention to the financial and regulatory details; and John Kraeuter, Hal Haskin, and Susan Ford for their leadership.

LITERATURE CITED

Abbott, R. T. 1974. American seashells, 2nd edition. New York, NY: Van Nostrand Reinhold. 663 pp.

Ansell, A. D. 1968. The rate of growth of the hard clam (*Mercenaria mercenaria* (L)) throughout the geographical range. *J. Cons. Perm. Int. Explor. Mer.* 31:364–409.

Araujo, R. & A. V. Korniushin. 1998. Microsculpture of *Pisidium casertanum* (Poli, 1791) and some related species forms (Bivalvia: Sphaeriidae). *Malakologische Abhandlungen* 19:59–69.

Araujo, R., D. Moreno & M. A. Ramos. 1993. The Asiatic clam *Corbicula fluminea* (Müller, 1774) (Bivalvia: Corbiculidae) in Europe. *Bull. Amer. Malacol. Union* 10:39–49.

Araujo, R., M. A. Ramos & J. Bedoya. 1994. Microtubules in the shell of the invasive bivalve *Corbicula fluminea* (Müller, 1774) (Bivalvia: Heterodonta). *J. Molluscan Stud.* 60:406–413.

Arrhenius, G. & E. Bonatti. 1965. Neptunism and vulcanism in the oceans. In: Sears, M., editor. Progress in oceanography, vol. 3. New York, NY: Pergamon Press. pp. 7–22.

Barber, B. J. 1990. Seasonal prevalence and intensity and disease progression of neoplasia in soft shell clams, *Mya arenaria*, from the Shrewsbury River, New Jersey. In: Perkins, F. O. & T. C. Cheng, editors. Pathology in marine science. San Diego, CA: Academic Press. pp. 377–386.

Barker, R. M. 1964. Microtextural variation in pelecypod shells. *Malacologia* 2:69–86.

Bauersfeld, W. R., E. W. Moshinsky, E. A. Pustay & W. D. Jones. 1987. Water resources data New Jersey, water year 1986. US Geol. Surv. Water-Data Rep. NJ-86-2.

Bauersfeld, W. R., E. W. Moshinsky, E. A. Pustay & W. D. Jones. 1988. Water resources data New Jersey, water year 1987. US Geol. Surv. Water-Data Rep. NJ-87-2.

Bauersfeld, W. R., E. W. Moshinsky, E. A. Pustay & W. D. Jones. 1990. Water resources data New Jersey, water year 1989. US Geol. Surv. Water-Data Rep. NJ-89-2.

Berry, W. B. N. & R. M. Barker. 1968. Fossil bivalve shells indicate longer month and year in Cretaceous than present. *Nature* 217:938–939.

Berry, W. B. N. & R. M. Barker. 1975. Growth increments in fossil and modern bivalves. In: Rosenberg, G. D. & S. K. Runcorn, editors. Growth rhythms and the history of the earth's rotation. London: John Wiley & Sons. pp. 9–25.

Beverton, R. J. H. 1954. Notes on the use of theoretical models in the study of the dynamics of exploited fish populations. Miscellaneous contributions (U.S. Fishery Laboratory) no. 2. 159 pp.

Blackwell, J. F., L. F. Gainey, Jr. & M. J. Greenberg. 1977. Shell ultrastructure in two subspecies of the ribbed mussel, *Geukensia demissa* (Dillwyn). *Biol. Bull.* 152:1–11.

Britton, J. C. & B. Morton. 1979. *Corbicula* in North America: the evidence reviewed and evaluated. In: Proceedings of the First International Corbicula Symposium. Fort Worth, Christian University Research Foundation Texas, TX. pp. 249–287.

Britton, J. C. & B. Morton. 1982. A dissecting guide, field and laboratory manual for the introduced bivalve *Corbicula fluminea. Malacol. Rev.* 3(Suppl. 3):1–82.

Brousseau, D. J. 1987. A comparative study of the reproductive cycle of the soft-shell clam, *Mya arenaria,* in Long Island Sound. *J. Shellfish Res.* 6:7–15.

Brousseau, D. J. & J. A. Baglivo. 1987. A comparative study of age and growth in *Mya arenaria* (soft-shell clam) from three populations in Long Island Sound. *J. Shellfish Res.* 6:17–24.

Carell, B., S. Forberg, E. Grundelius, L. Henrikson, A. Johnels, U. Lindh, H. Mutvei, M. Olsson, K. Svärdström & T. Westermark. 1987. Can mussel shells reveal environmental history? *Ambio* 16:2–10.

Carriker, M. R., R. E. Palmer, L. V. Sick & C. C. Johnson. 1980. Interaction of mineral elements in sea water and shell of oysters [*Crassostrea virginica* (Gmelin)] cultured in controlled and natural systems. *J. Exp. Mar. Biol. Ecol.* 46:279–296.

Carter, J. G. 1980. Environmental and biological controls of bivalve shell mineralogy and microstructure. In: Rhoads, D. C. & R. A. Lutz, editors. Skeletal growth of aquatic organisms. New York and London: Plenum Press. pp. 69–113.

Clark, G. R., II. 1979. Seasonal growth variations in the shells of recent and prehistoric specimens of *Mercenaria mercenaria* from St. Catherine's Island, Georgia. *Am. Mus. Nat. Hist. Anthropol. Pap.* 56:161–179.

Clark, G. R., II. 1980. Study of molluscan shell structure and growth lines using thin sections. In: Rhoads, D. C. & R. A. Lutz, editors. Skeletal growth of aquatic organisms. New York and London: Plenum Press. pp. 603–606.

Collins, T. W. 1967. Oxygen-uptake, shell morphology and desiccation of the fingernail clam, *Sphaerium occidentale* (Prime). PhD diss., University of Minnesota, Minneapolis, MN. 164 pp.

Cooper, K. R., F. G. Doherty, L. W. Fritz & L. M. Ragone. 1987. Evaluation of biological effects on fish and shellfish potentially impacted by the Ciba-Geigy effluent. Final Technical Report to *Off. Sci. Res.*, New Jersey Department of Environmental Protection, Trenton, NJ. 118 pp.

Counts, C. L., III. 1980. *Rangia cuneata* in an industrial water system (Bivalvia: Mactridae). *Nautilus* 94:1–2.

Counts, C. L., III & R. S. Prezant. 1982. Shell microstructure of *Corbicula fluminea* (Bivalvia: Corbiculidae). *Nautilus* 96:25–30.

Crenshaw, M. A. & J. M. Neff. 1969. Decalcification at the mantle-shell interface in molluscs. *Am. Zool.* 9:881–885.

Deith, M. R. 1985. The composition of tidally deposited growth lines in the shell of the edible cockle, *Cerastoderma edule. J. Mar. Biol. Ass. U.K.* 65:573–581.

Dodd, J. R. 1965. Environmental control of strontium and magnesium in *Mytilus. Geochim. Cosmochim. Acta* 29:385–398.

Dugal, L. P. 1939. The use of calcareous shell to buffer the products of anaerobic glycolysis in *Venus mercenaria. J. Cell. Comp. Physiol.* 13:235–251.

Evans, J. W. 1972. Tidal growth increments in the cockle *Clinocardium nuttalli. Science* 176:416–417.

Fairbanks, L. D. 1963. Biodemographic studies on the clam *Rangia cuneata* gray. *Tulane Stud. Zool.* 10:3–47.

Farrow, G. E. 1971. Periodicity structures in the bivalve shell: experiments to establish growth controls in *Cerastoderma edule* from the Thames estuary. *Paleontology* 14:571–588.

Ferrell, R. E., T. E. Garville & J. D. Martinez. 1973. Trace metals in oyster shells. *Environ. Lett.* 4:311–316.

Fritz, L. W. 1982. Annulus formation in hard clam (*Mercenaria mercenaria*) shells. MA Thesis, Coll. William & Mary, VA *Inst. Mar. Sci.,* Gloucester Point, VA. 160 pp.

Fritz, L. W. 1984. Studies of age and growth history of surf clams near the Ciba-Geigy Tom's River plant, Ortley Beach, NJ. Report to *Off. Sci. Res.,* New Jersey Department of Environmental Protection, Trenton, NJ. 19 pp.

Fritz, L. W. 2001. Shell structure and age determination. In: Kraeuter, J. N. & M. Castagna, editors. Biology of the Hard Clam. Developments in Aquaculture and Fisheries Science 31. Amsterdam: Elsevier. pp. 53–76.

Fritz, L. W., G. Ferrence & T. R. Jacobsen. 1992. Induction of barite mineralization in the Asiatic clam *Corbicula fluminea. Limnol. Oceanogr.* 37:442–448.

Fritz, L. W. & D. S. Haven. 1983. Hard clam, *Mercenaria*: shell growth patterns in Chesapeake Bay. *U.S. Fish. Bull* 81:697–708.

Fritz, L. W. & R. A. Lutz. 1986. Environmental perturbations reflected in internal shell growth patterns of *Corbicula fluminea* (Mollusca: Bivalvia). *Veliger* 28:401–417.

Fritz, L. W., L. M. Ragone & R. A. Lutz. 1990a. Microstructure of the outer shell layer of *Rangia cuneata* (Sowerby, 1831) from the Delaware River: applications in studies of population dynamics. *J. Shellfish Res.* 9:205–213.

Fritz, L. W., L. M. Ragone & R. A. Lutz. 1991. Seasonal changes in outer shell layer microstructure of *Mytilus edulis* in New Jersey, USA. *Veliger* 34:222–228.

Fritz, L. W., L. M. Ragone, R. A. Lutz & S. Swapp. 1990b. Biomineralization of barite in the shell of the freshwater Asiatic clam *Corbicula fluminea* (Mollusca: Bivalvia). *Limnol. Oceanogr.* 35:756–762.

Gallagher, J. L. & H. W. Wells. 1969. Northern range extension and winter mortality of *Rangia cuneata. Nautilus* 83:22–25.

Gordon, J. & M. R. Carriker. 1978. Growth lines in a bivalve mollusc: subdaily patterns and dissolution of the shell. *Science* 202:519–521.

Hilbish, T. J. 1986. Response of aquatic and aerial metabolic rates in the ribbed mussel *Geukensia demissa* (Dillwyn) to acute and prolonged changes in temperature. *J. Exp. Mar. Biol. Ecol.* 105:207–218.

Isaji, S. 1995. Defensive strategies against shell dissolution in bivalves inhabiting acidic environments: the case of *Geloina* (Corbiculidae) in mangrove swamps. *Veliger* 38:235–246.

Jacobsen, T. R. 1987. Impact of the 29 September 1985 Delaware River oil spill on the New Jersey oyster seed beds: monitoring the fate of polyaromatic hydrocarbons (PAH) in sediments and oyster tissue. Final Report to *Off. Sci. Res.,* New Jersey Department of Environmental Protection, Trenton, NJ. 28 pp.

Jones, D. S. 1980a. Annual cycle of shell growth and reproduction in the bivalves *Spisula solidissima* and *Arctica islandica. J. World Maric. Soc.* 12:196–205.

Jones, D. S. 1980b. Annual cycle of shell growth increment formation in two continental shelf bivalves and its paleoecological significance. *Paleobiology* 6:331–340.

Jones, D. S. 1981. Annual growth increments in shells of *Spisula solidissima* record marine temperature variability. *Science* 211:165–167.

Jones, D. S., I. Thompson & W. Ambrose. 1978. Age and growth rate determinations for the Atlantic surf clam *Spisula solidissima* (Bivalvia: Mactracea) based on internal growth lines in shell cross-sections. *Mar. Biol.* 47:63–70.

Jones, D. S., D. F. Williams & M. A. Arthur. 1983. Growth history and ecology of the Atlantic surf clam, *Spisula solidissima* (Dillwyn) as revealed by stable isotopes and annual shell increments. *J. Exp. Mar. Biol. Ecol.* 73:225–242.

Kennedy, W. J., J. D. Taylor & A. Hall. 1969. Environmental and biological controls on bivalve shell mineralogy. *Biol. Rev. Camb. Philos. Soc.* 44:499–529.

Kennish, M. J. 1980. Shell microgrowth analysis: *Mercenaria mercenaria* as a type example for research in population dynamics. In: Rhoads, D. C. & R. A. Lutz, editors. Skeletal growth of aquatic organisms. New York and London: Plenum Press. pp. 255–294.

Kennish, M. J. & R. K. Olsson. 1975. Effects of thermal discharges on the microstructural growth of *Mercenaria mercenaria. Environ. Geol* 1:41–64.

Kennish, M. J., R. A. Lutz & D. C. Rhoads. 1980. Preparation of acetate peels and fractured sections for observations of growth patterns within the bivalve shell. In: Rhoads, D. C. & R. A. Lutz, editors. Skeletal growth of aquatic organisms. New York and London: Plenum Press. pp. 597–601.

Koike, H. 1975. The use of daily and annual growth lines of the clam *Meretrix lusoria* in estimating seasons of Jomon period shell gathering. In: Suggate, R. P. & M. M. Cresswell, editors. Quaternary studies. Wellington: Royal Society of New Zealand. pp. 189–193.

Lent, C. M. 1969. Adaptations of the ribbed mussel, *Modiolus demissus* (Dillwyn), to the intertidal habitat. *Am. Zool.* 9:283–292.

Lutz, R. A. 1976. Annual growth patterns in the inner shell layer of *Mytilus edulis* L. *J. Mar. Biol. Ass. U.K.* 56:723–731.

Lutz, R. A. 1977. Annual structural changes in the inner shell layer of *Geukensia (=Modiolus) demissa. Proc. Natl. Shellfish. Assoc.* 67:120.

Lutz, R. A. & M. Castagna. 1980. Age composition and growth rate of a mussel (*Geukensia demissa*) population in a Virginia salt marsh. *J. Molluscan Stud.* 46:106–115.

Lutz, R. A. & G. R. Clark, II. 1984. Seasonal and geographic variation in the shell microstructure of a salt-marsh bivalve (*Geukensia demissa* (Dillwyn)). *J. Mar. Res.* 42:943–956.

Lutz, R. A. & D. C. Rhoads. 1977. Anaerobiosis and a theory of growth line formation. *Science* 198:1222–1227.

Lutz, R. A. & D. C. Rhoads. 1978. Shell structure of the Atlantic ribbed mussel, *Geukensia dernissa* (Dillwyn): a reevaluation. *Bull. Am. Malacol. Union* 1978:13–17.

Lutz, R. A. & D. C. Rhoads. 1980. Growth patterns within the molluscan shell: an overview. In: Rhoads, D. C. & R. A. Lutz, editors. Skeletal growth of aquatic organisms. New York and London: Plenum Press. pp. 203–254.

MacDonald, B. A. & M. L. H. Thomas. 1982. Growth reduction in the soft-shell clam *Mya arenaria* from a heavily oiled lagoon in Chedabucto Bay, Nova Scotia. *Mar. Environ. Res.* 6:145–156.

Malchus, N. 2006. Amended description of the arcoid bivalve *Philobrya brattstromi* Soot-Ryen, 1957, from Chile. *Nautilus* 120:8–14.

Malchus, N. 2010. Shell tubules in Condylocardiinae (Bivalvia: Carditoidea). *J. Molluscan Stud.* 76:401–403.

Masuda, F. 1981. Chemical composition in marine carbonates as an indicator of paleoenvironment. Report, *Grant-in-Aid, Sci. Res*. (C), Project No. 454262. 46 pp.

Masuda, F. & M. Hirano. 1980. Chemical composition of some modern marine pelecypod shells. *Sci. Rep., Inst. Geosci. Univ. Tsukuba* 1:163–177.

McMahon, R. F. & C. J. Williams. 1984. A unique respiratory adaptation to emersion in the introduced Asian freshwater clam *Corbicula fluminea* (Müller) (Lamellibranchia: Corbiculacea). *Physiol. Zool.* 57:274–279.

Morris, P. A. 1975. Shells of the Atlantic (Peterson field guide). Boston, MA: Houghton Mifflin Co. 330 pp.

National Academy of Sciences. 1977. Drinking water and health. Safe Drinking Water Committee, National Research Council, (ISBN 0-309-02619-9).

Nelson, D. J. 1962. Clams as indicators of strontium-90. *Science* 137:38–39.

Oberling, J. J. 1964. Observations on some structural features of the pelecypod shell. *Mitt. Naturforsch. Ges. Bern* 20:1–63.

Pannella, G. 1975. Palaeontological clocks and the history of the earth's rotation. In: Rosenberg, G. D. & S. K. Runcorn, editors. Growth rhythms and the history of the earth's rotation. London: John Wiley & Sons. pp. 253–284.

Pannella, G. 1976. Tidal growth patterns in recent and fossil mollusc bivalve shells: a tool for the reconstruction of paleotides. *Naturwissenschaften* 63:539–543.

Pannella, G. & C. MacClintock. 1968. Biological and environmental rhythms reflected in molluscan shell growth. *J. Paleontol.* 42:64–80.

Pannella, G., C. MacClintock & M. N. Thompson. 1968. Paleontological evidence of variations in length of synodic month since late Cambrian. *Science* 162:792–796.

Pfitzenmeyer, H. T. & K. G. Drobeck. 1964. The occurrence of the brackish water clam, *Rangia cuneata* in the Potomac River, Maryland. *Chesap. Sci.* 5:209–212.

Prezant, R. S. & K. Chalermwat. 1984. Flotation of the bivalve *Corbicula fluminea* as a means of dispersal. *Science* 225:1491–1493.

Prezant, R. S. & A. Tan-Tiu. 1985. Comparative shell microstructure of North American *Corbicula* (Bivalvia: Sphaeriacea). *Veliger* 27:312–319.

Rhoads, D. C. & R. A. Lutz. 1980. Skeletal growth of aquatic organisms: biological records of environmental change. New York and London: Plenum Press. 750 pp.

Rhoads, D. C. & G. Pannella. 1970. The use of molluscan shell growth patterns in ecology and paleoecology. *Lethaia* 4:413–428.

Richardson, C. A., D. J. Crisp & N. W. Runham. 1979. Tidally deposited growth bands in the shell of the common cockle, *Cerastoderma edule* (L.). *Malacologia* 18:277–290.

Ricker, W. E. 1975. Computation and interpretation of biological statistics of fish populations. *Bull. Fish. Res. Board Canada* No. 191. 382 pp.

Riley, J. P. & R. Chester. 1971. Introduction to Marine Chemistry. London and New York: Academic Press. 465 pp.

Rodgers, J. H., Jr., D. S. Cherry, K. L. Dickson & J. Cairns. 1979. Invasion, population dynamics, and elemental accumulation of *Corbicula fluminea* in the New River, VA. In: Proceedings, First International *Corbicula* Symposium, Christian University Research Foundation Texas, TX. pp. 99–110.

Saloman, C. H. & J. L. Taylor. 1969. Age and growth of large southern quahogs from a Florida estuary. *Proc. Natl. Shellfish. Assoc.* 59:46–51.

Sokal, R. R. & F. J. Rohlf. 1969. Biometry. San Francisco, CA: W. H. Freeman and Co. 776 pp.

Stewart, W. N. & T. N. Taylor. 1965. The peel technique. In: Kummel, B. & D. Raup, editors. Handbook of paleontological techniques. San Francisco, CA: W. H. Freeman and Co. pp. 224–232.

Tan-Tiu, A. 1987. Influence of environment on shell microstructure of *Corbicula fluminea* and *Polymesoda caroliniana* (Bivalvia: Heterodonta). PhD diss., University of South Mississippi, Hattiesburg, MS Thesis. 148 pp.

Tan-Tiu, A. & R. S. Prezant. 1989. Temporal variation in microstructure of the inner shell surface in *Corbicula fluminea* (Bivalvia: Heterodonta). *Bull. Am. Malacol. Union* 7:65–71.

Taylor, J. D., W. J. Kennedy & A. Hall. 1969. The shell structure and mineralogy of the Bivalvia: introduction, Nuculacea-Trigoacea. *Bull. Br. Mus. (Nat. Hist.) Zool*., Suppl. 3. 125 pp.

Taylor, J. D., W. J. Kennedy & A. Hall. 1973. The shell structure and mineralogy of the Bivalvia. II. Lucinacea-Clavagellacea: conclusions. *Bull. Br. Mus. (Nat. Hist.)*. 22:253–294.

Trama, F. B. 1982. Occurrence of the Asiatic clam *Corbicula fluminea* in the Raritan River, New Jersey. *Nautilus* 96:6–8.

Wada, K. 1961. Crystal growth of molluscan shells. *Bull. Nat. Pearl Res. Lab* 7:703–828.

Wada, K. 1972. Nucleation and growth of aragonite crystals in the nacre of some bivalve molluscs. *Biomineralisation* 6:141–159.

Wagner, E. 1984. Growth rate and annual shell structure patterns in a single year class of surf clams *Spisula solidissima* off Atlantic City, New Jersey. MA Thesis, Rutgers Univ., New Brunswick, NJ. 161 pp.

Walford, L. A. 1946. A new graphic method of describing the growth of animals. *Biol. Bull.* 90:141–147.

Waller, T. R. 1980. Scanning electron microscopy of shell and mantle in the order Arcoida (Mollusca: Bivalvia). *Smithson. Contrib. Zool.* 313:1–58.

Watabe, N. 1956. Dahllite identified as a constituent of the prodissoconch of *Pinctada martensii* (Dünker). *Science* 124:630.

Wilbur, K. M. 1964. Shell formation and regeneration. In: Wilbur, K. M. & C. M. Yonge, editors. Physiology of Mollusca, vol. 1. New York, NY: Academic Press. pp. 243–282.

Wilbur, K. M. 1972. Shell formation in molluscs. In: Florkin, M. & B. Scheer, editors. Chemical zoology. VII. Molluscs. New York, NY: Academic Press. pp. 103–145.

Wilbur, K. M. & N. Watabe. 1963. Experimental studies on calcification in molluscs and the alga *Coccolithus huxleyi. Ann. N. Y. Acad. Sci.* 109:82–112.

Wise, S. W. 1971. Shell ultrastructure of the taxodont pelecypod *Anadara notabilis* (Röding). *Eclogae Geol. Helv.* 64:1–28.

Wolfe, D. A. & E. N. Petteway. 1968. Growth of *Rangia cuneata* Gray. *Chesap. Sci.* 9:99–102.

NOTES

[1]The thin section enlargements in Figures 65 and 66 are "negative" images of *Mya arenaria* shells. Opaque zones are dark in cross-sections, but light in these images of thin sections under transmitted light made essentially using the thin section as a negative to make a contact print. Conversely, translucent zones are light in cross-sections, but dark in these images because they transmit more light than opaque zones.

[2]The thin section enlargements in Figure 73 are "negative" images of *Spisula solidissima* shell chondrophores. Opaque zones are dark in cross-sections, but light in these images of thin sections under transmitted light made essentially using the thin section as a negative to make a contact print. Conversely, translucent zones are light in cross-sections, but dark in these images because they transmit more light than opaque zones.

[3]*Mercenaria mercenaria* can also be added to this list (Ansell 1968, Kennish 1980, Fritz 2001).